Advanced Microwave Scanning Radiometer For EOS (AMSR-E)

Science Data Validation Plan

Version 2

July 2000

SCIENCE DATA VALIDATION PLAN
Version 2

1 INTRODUCTION

1.1 Purpose

This Science Data Validation Plan describes the plans for validating the products generated with the team retrieval algorithms and the activities that lead to gathering these validation data.

1.2 Scope

This document includes a description of the algorithm validation approach and the measurements required for validation including the experiments and campaigns that will collect these data.

1.3 Documents

ATBDs:

Ocean Parameter Suite: F. Wentz
Rainfall: C. Kummerow, T. Wilheit and R. Ferraro
Sea Ice: D. Cavalieri and J. Comiso
Snow Water Equivalent: A. Chang
Land Surface: E. Njoku

2 MEASUREMENT AND SCIENCE OBJECTIVE

In support of the Earth Science Enterprise goals, the Advanced Microwave Scanning Radiometer for EOS (AMSR-E) will fly on NASA's Earth Observing System (EOS) Aqua Satellite planned for launch in December 2000. AMSR-E is a passive microwave instrument modified from the AMSR designed and built by Mitsubishi Electronics Corporation for deployment on the Japanese Advanced Earth Observing Satellite-II (ADEOS-II). Atmospheric and surface parameters retrieved are: precipitation, sea surface temperatures, ice concentrations, snow depth and water content, land surface wetness, sea surface wind speed, atmospheric cloud water over the ocean, and water vapor over the ocean.

2.1 The Instrument

The AMSR-E is a twelve channel, six frequency total power passive microwave radiometer system. It measures brightness temperatures at 6.925, 10.65, 18.7, 23.8, 36.5, and 89.0 GHz. Vertically and horizontally polarized measurements are taken for all frequencies.

The instrument consists of an offset parabolic reflector 1.6 meters in diameter, fed by an array of six feedhorns. The reflector and feedhorn arrays are mounted on a drum, which contains the radiometers, digital data subsystem, mechanical scanning subsystem, and power subsystem. The reflector/feed/drum assembly is rotated about the axis of the drum by a coaxially mounted bearing and power transfer assembly. All data, commands, timing and telemetry signals, and power pass through the assembly on slip ring connectors to the rotating assembly.

A cold load reflector and a warm load are mounted on the transfer assembly shaft and do not rotate with the drum assembly. They are positioned off axis such that they pass between the feedhorn array and the parabolic reflector, occulting it once each scan. The cold load reflector reflects cold sky radiation into the feedhorn array thus serving, along with the warm load, as calibration references for the AMSR-E. Calibration of the radiometers is essential for collection of useful data. Corrections for spillover and antenna pattern effects are incorporated in the Level 1 data processing algorithms.

The instrument rotates continuously about an axis parallel to the local spacecraft vertical at 40 rpm. At an altitude of 705 km, it measures the upwelling scene brightness temperatures over an angular sector of +/- 61 degrees about the sub-satellite track, resulting in a swath width of 1445 km.

During a period of 1.5 seconds the spacecraft sub-satellite point travels 10 km. Even though the instantaneous field-of-view for each channel is different, active scene measurements are recorded at equal intervals of 10 km (5 km for the 89 GHz channels) along the scan. The half cone angle at which the reflector is fixed is 47.4 degrees which results in an Earth incidence angle of 55.0 degrees. Table 2.1.1 lists the pertinent performance characteristics.

Table 2.1.1 AMSR-E PERFORMANCE CHARACTERISTICS

Center Frequencies (GHz)	6.925	10.65	18.7	23.8	36.5	89.0
Bandwidth (MHz)	350	100	200	400	1000	3000
Sensitivity (K)	0.3	0.6	0.6	0.6	0.6	1.1
IFOV (Km x Km)	75x43	48x27	27x16	31x18	14x8	6x4
Sampling Rate (Km x Km)	10x10	10x10	10x10	10x10	10x10	5x5
Integration Time (msec)	2.6	2.6	2.6	2.6	2.6	1.3
Main Beam Efficiency (%)	95.3	95.0	96.3	96.4	95.3	96.0
Beamwidth (Degrees)	2.2	1.4	0.8	0.9	0.4	0.18

2.2 Science Objectives

The geophysical standard products retrieved from AMSR-E data will primarily be used in climate change research. Over the ocean these products include rainfall, sea surface temperature (SST), surface wind speed, integrated water vapor and cloud water contents, and sea ice parameters. Over land, the standard products include soil moisture, rainfall, and snow cover water content. This wide variety of products will enable an equally wide variety of science investigations, especially those dealing with the atmospheric and surface hydrologic and energy cycles. Because some investigations will compare the relationships between the various parameters (e.g. the variability of tropical average surface winds with SST) it is important to reduce retrieval algorithm cross-talk between parameters, e.g. so that variations in wind speed are not misdiagnosed as being SST variability, and *vice versa*. Another possibility would be the misdiagnosis of temperature variability as a change in one of the retrieved parameters. Reduction of algorithm cross talk is essential to the useful exploitation of these products.

The AMSR-E's monitoring of the interannual variability in the standard product parameters will provide much insight into the climate system, helping to improve physical processes and parameterizations in climate models. These improvements, in turn, will enable more accurate predictions of global and regional climate changes associated with both natural and anthropogenic influences.

2.3 Science Data Products

The AMSR-E Science team members are developing all the retrieval algorithms. The individual development takes place on each member's science computing facility (SCF); before delivery to the Team Leader SCF (TLSCF) they are responsible for stand-alone testing of their software on the TLSCF. The generation of science data products can be divided into three groups: Level 1 - brightness temperatures (Tbs), Level 2 and higher - the EOS agreed standard

data products, and special data products - research products whose retrieval algorithms are not yet proven. The generation flow of all the products is shown in Figure 2.1.1.

Level 1 data will be processed at NASDA's Earth Observation Center (EOC). It is customary to have the sensor manufacturer do the Level 1 processing because it involves instrument data taken during the ground calibration/qualification testing.

Level 2A data, are spatially consistent T_b data sets at 5 different footprint sizes corresponding to the 6.9, 10.7, 18.7, 36.5 and 89 GHz footprints.

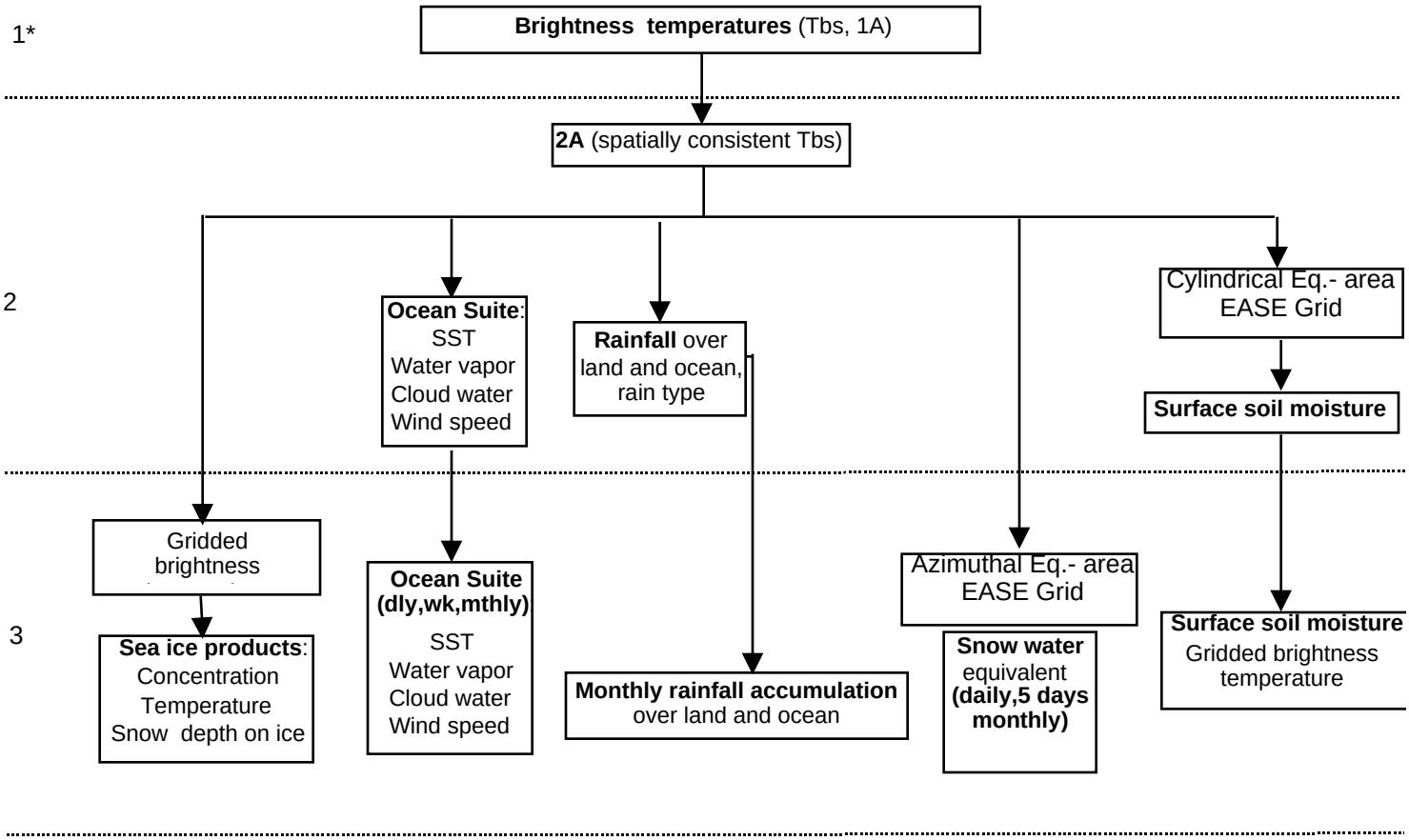

Figure 2.1.1 AMSR-E products

2.4 Standard Data Products Accuracy and Resolution

a) Level 2 standard products

PRODUCT	ACCURACY	SPATIAL RESOLUTION (KM)
Brightness Temperature	0.2 – 0.7 K	5 - 56
Ocean: Sea Surface Temperature	0.5 K	56
Columnar Water Vapor	0.6 mm	25
Columnar Cloud Water	0.02 mm	25
Wind Speed	0.9 m/s	25
Rainfall: Over oceans	1 mm/hr or 20%	12
Over land	2 mm/hr or 20%	12
Type		
Land: Surface soil moisture	0.06 g/cm^3	56

b) Level 3 standard products

PRODUCT	ACCURACY	GRID RESOLUTION (KM)	TEMPORAL RESOLUTION
Ocean: Sea Surface Temperature	0.5 K	_ x _ degrees	daily asc and dsc weekly, monthly
Columnar Water Vapor	0.6 mm	_ x _ degrees	daily asc and dsc weekly, monthly
Columnar Cloud Water	0.02 mm	_ x _ degrees	daily asc and dsc weekly, monthly
Wind Speed	0.9 m/s	_ x _ degrees	daily asc and dsc weekly, monthly
Rainfall: Over oceans	20%	5 x 5 degrees	monthly
Over land	30%	5 x 5 degrees	monthly
Sea Ice: Concentration	≤5%	12.5, 25	daily asc and dsc
Temperature	≤4 K	25	daily asc and dsc
Snow depth on ice	≤5 cm	12.5	5 days
Gridded brightness temp	0.3 – 0.6 K	6.25, 12.5, 25	daily
Land: Surface soil moisture	0.06 g/cm^3	25	daily
Gridded brightness temps	0.3 - 0.6 K	25	daily
Snow: Water equivalent	10 mm or 20%	25 (EASE grid)	Daily, 5 days, monthly

3 Validation/Algorithm Development Activities

The AMSR-E validation program has two distinct phases: Pre-launch, where both the software stability and algorithm capability to retrieve valid products (by comparing them to ground truth data) are implemented, and Post-launch, where the latter is continued for 1 to 2 years after launch.

The **pre-launch** activities are:

1) Demonstrate the stability of the software by using TRMM TMI (and to a smaller extent SSM/I) data for the algorithms that do not require the lower frequency channels.

2) Demonstrate the validity of the retrieved products with ground truth data, where possible.

The algorithms using the lowest frequency (6.9 GHz) channel have to be calibrated post-launch.

Post-launch: the activities started before launch will continue and add, wherever possible, new campaigns and field truth data.

3.1 Ocean Parameters (submitted by F. Wentz)

There are four primary ocean parameters that require validation: sea-surface temperature (SST) T_S (C°), near-surface wind speed W (m/s), columnar water vapor V (mm), and columnar cloud water L (mm). These parameters will be validated through intercomparison with other satellite and in-situ data products as described below. The intercomparisons will probably reveal some differences between the AMSR-E products and the validation data sets. When these differences indicate a problem with the AMSR-E products, physical coefficients in the AMSR-E radiative transfer model will be adjusted so as to make the AMSR-E products agree with the validation data set. Care will be taken to ensure that the validation data set is sufficiently accurate to warrant a change in the AMSR-E model. In addition we expect that small offsets will need to be applied to each of the AMSR-E channels to remove absolute biases in the radiometer calibration and/or in the radiative transfer model.

These calibration/validation methods are currently being applied to the SSM/I and the TRMM TMI. In this way, our cal/val methods can be developed and tested before launch, and the AMSR-E retrieval algorithm and radiative transfer model can be improved based on current radiometer missions. These methods will also be used for the ADEOS-II AMSR whose launch is planned in 2001.

3.1.1 Validation Criteria and Method

Computer simulations discussed at length in the AMSR-E Ocean ATBD indicate the rms accuracies given in Table 3.1.1 should be achieved by AMSR-E. These accuracies are for a 60-km spatial resolution for T_S and 25 km for the other three parameters. In view of the high accuracies, it will be necessary to carefully quality control the various validation data sets. The calibration and validation of the first 3 ocean products (T_S, W, and V) will be based on intercomparison of buoy and radiosonde observations and on SST and wind retrievals coming from other satellite sensors. Because there are no reliable ancillary data sets for calibration or validation of cloud liquid water, we will rely on a histogram analysis similar to that done by *Wentz* [1997]. The following sections more fully explain each of the calibration data sources.

Table 3.1.1. Predicted Accuracy for AMSR-E Ocean Products

Ocean Parameter	Calibration methods	Rms. Error
Sea-Surface Temperature (T_S)	Satellite, Buoy	0.5 C
Wind Speed (W)	Satellite, Buoy, GCM	0.9 m/s
Columnar Water Vapor (V)	Radiosonde	0.6 mm
Columnar Cloud Water (L)	Histogram	0.02 mm

In validating the ocean parameters, the spatial-temporal mismatch between the calibration source (i.e., in situ observation or other satellite product) and the AMSR-E product must be considered. In addition, errors in the calibration source need to be accounted for. For example, the true wind speed averaged over a 25 km AMSR-E footprint will, in general, not equal the wind speed measured by a buoy because the buoy wind is a point observation taken at a different time and contains measurement error. Similar problems exists for the SST and vapor intercomparison.

Thus in the intercomparison statistics, we will first compute the rms difference between the AMSR-E product and the calibration source. For this difference we will then subtract (in a root-mean-squared sense) the spatial-temporal mismatch error and the calibration source measurement error. The residual will then be the indicator of the accuracy of the AMSR-E retrieval. Our validation criterion is that this computed accuracy meets or exceeds the accuracy given in Table 3.1.1.

The spatial and temporal mismatch error depends on the size of the collocation window, which is defined as the maximum allowable space-time difference between the AMSR-E observation and the *in situ* observation. To minimize the spatial-temporal mismatch error, the collocation criteria must be carefully selected. Table 3.1.2 gives the spatial and temporal windows we plan to use for the different types of *in situ* validations. The buoy collocation window for wind is smaller than that for SST because wind has a higher spatial-temporal variability. Ideally, we would like to have the collocation window for the vapor versus radiosonde intercomparisons as small as the collocation window used for wind. However, since the radiosonde observations come from islands, a larger spatial window is required to capture the adjacent AMSR-E ocean observations. In addition, a larger temporal window is required because radiosonde flights only occur every 12 hours, as compared to the hourly buoy observations. Thus the vapor collocation window is larger than that for wind.

Table 3.1.2. Collocation Windows for In Situ Validation

AMSR-E Product	In Situ Calibration Source	Spatial Collocation Window	Temporal Collocation Window
SST	Ocean buoys	50 km	3 hours
Wind	Ocean buoys	30 km	1 hour
Vapor	Radiosondes	60 km	6 hours

The validation of cloud water is different than that for SST, wind, and vapor. There is no reliable calibration source for the total columnar cloud water, and hence we have to rely on the histogram technique (i.e., an error model) described below. For cloud water, the validation criterion is that the histogram alignment meets or exceeds the accuracy given in Table 3.1.1.

Geophysical parameters generated as part of the Level 2B data set (i.e., sea surface temperature, wind, vapor, and cloud) will be temporally averaged by day, week, and month, and gridded as part of the Level 3 data sets. The spatial resolution of the gridded data sets will be _ degree, resulting in data volumes of approximately 2 Megabyte for each data set, or a total of 8 Megabytes per time period for the entire suite of ocean parameters.

The accuracy of each of the temporally averaged data sets will be better than that of the corresponding instantaneous Level 2B measurements, although the amount of improvement attained through temporal averaging will differ by parameter and time period. Because the AMSR-E instrument will not view the entire Earth within a single day, some Earth locations will not be measured even once in the daily averaged products, while a few locations will have the benefit of more than one observation. Thus, the primary purpose of the daily Level 3 product will

be to arrange the observations on a common Earth grid rather than to average them. In contrast, weekly and monthly averages will generally enjoy a substantial temporal averaging benefit.

3.1.2 Operational Surface Networks

The two operational surface networks that will be used are the moored ocean buoys and island radiosonde stations. Moored buoys will be used to validate sea-surface temperature (SST), and wind speed, and the radiosondes will be used to validate the columnar water vapor. The moored buoy data are available as hourly data and are described below. The radiosonde stations are part of the World Meteorological Organization (WMO) and daily radiosonde reports can be obtained from National Center for Atmospheric Research (NCAR).

Buoys are frequently used to validate satellite SST measurements even though satellites measure the ocean skin temperature (temperature of the first millimeter for microwaves and the first several microns for the infrared) while buoys measure the ocean bulk temperature. Moored buoys typically measure T_S at a depth of one meter. The buoy data are obtained from the National Data Buoy Center (NDBC) and the Pacific Marine Environmental Laboratory (PMEL). NDBC maintains a network of buoys in coastal regions around the continental United States, Alaska and Hawaii. Currently, approximately 35 of the buoys are distanced greater than 30 km from shore and hence can be used for AMSR validation. (AMSR cannot retrieve ocean parameters too close to shore because of land contamination in the antenna pattern.) PMEL maintains the 70-buoy Tropical Atmosphere-Ocean (TAO/TRITON) network in the equatorial Pacific and also provides data from the Pilot Research Moored Array in the Tropical Atlantic (PIRATA). NDBC hourly measurements are available by anonymous ftp from NDBC in near real time whereas the hourly TAO and PIRATA data are only available after buoy servicing or recovery, a process that occurs approximately once per year for each buoy. Fortunately, daily averages of the hourly TAO and PIRATA data are available in near real time.

Wind observations from moored buoys in the open ocean will be used to validate the AMSR-E wind speed product. The buoys measure barometric pressure, wind direction, wind speed, wind gust, air and sea temperature, and wave energy spectra (i.e., significant wave height, dominant wave period, and average wave period). NDBC wind speed and direction is measured during an 8-minute period prior to the hour of report. Exactly when the data is collected prior to report and the height of the anemometer depends on the type of payload on the moored buoy. Table 3.1.3 outlines the location of the NBDC moored buoys in service as of June 2000. These locations are mapped in Figure 3.1.1.

The TAO array covers the tropical Pacific Ocean at intervals of approximately 10 to 15 degree longitude, and 2° to 3° degree latitude. They measure air temperature, relative humidity, surface winds, T_S, and subsurface temperature to 500 meters. Wind measurements are made at a height of 4 m for 6 minutes centered on the hour and are vector averaged to derive the hourly value reported. The TAO/TRITON buoys measure T_S at 1-meter depth. These T_S samples are taken every ten minutes and averaged at the end of each hour. To conserve battery power, hourly data is transmitted only 8 hours each day, 0600 to 1000 and 1200 to 1600 buoy local time. Three to four hours of T_S and wind data are available in near-real time from the GTS. These data are considered preliminary until the buoy is serviced and the stored hourly data is processed. Figure 3.1.1 includes the TAO/TRITON buoy network.

The PIRATA moored buoy array in the Atlantic Ocean operates in a similar manner as the Pacific TAO/TRITON buoy array but is much smaller. Currently 13 buoys are deployed and measure air temperature, relative humidity, surface winds, T_S, and subsurface temperature to 500 meters. The wind measurements are made at 4m for 6 minutes like the TAO/TRITON array. Surface SST measurements are at 1 m. Figure 3.1.1 also includes the PIRATA buoys.

Anemometer height z for the buoys vary. The NDBC moored buoys in general have z equaling 5 or 10 m, the TAO/TRITON and PIRATA anemometers are at 4 m above the sea surface. All buoy winds W_B will be normalized to an equivalent anemometer height of 10-m (1000-cm) assuming a logarithmic wind profile.

$$W_{B,10M} = [\ln(1000/h_0)/\ln(h/h_0)]\, W_{B,Z} \quad (1)$$

Table 3.1.3. NDBC Moored Buoy Open Water Locations as of June 2000

NUMBER	LATITUDE	LONGITUDE
41001	34.7	287.4
41002	32.3	284.8
41004	32.5	280.9
41009	28.5	279.8
41010	28.9	281.5
42001	25.9	270.3
42002	25.9	266.4
42003	25.9	274.1
42019	27.9	265.0
42020	27.0	263.5
42036	28.5	275.5
42039	28.8	274.0
42040	29.2	271.7
42041	27.2	269.6
42053	29.6	271.5
44004	38.5	289.3
44005	42.9	291.1
44008	40.5	290.6
44011	41.1	293.4
44014	36.6	285.2
44025	40.3	286.8
46001	56.3	211.8
46002	42.5	229.7
46003	51.9	204.1
46005	46.1	229.0
46006	40.9	222.5
46035	57.0	182.3
46042	36.8	237.6
46047	32.4	240.5
46050	44.6	235.5
46059	38.0	230.0
51001	23.4	197.7
51002	17.2	202.2
51003	19.1	199.2
51004	17.4	207.5
51028	0.0	206.1

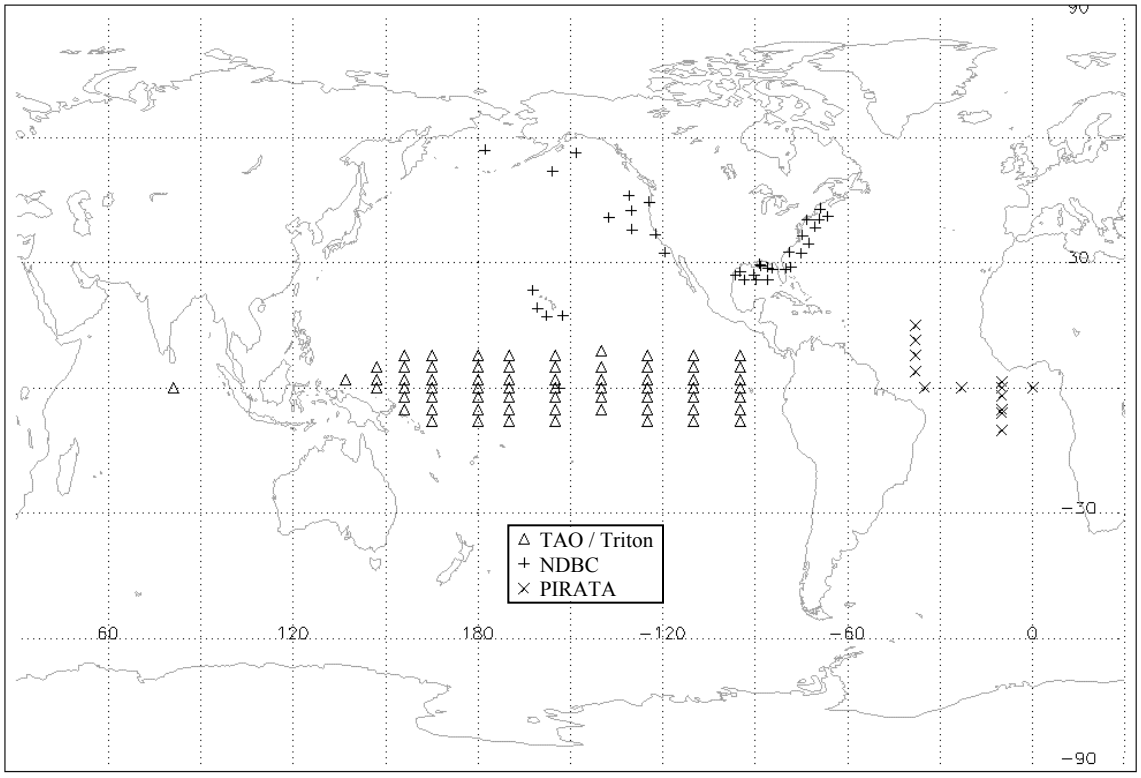

Fig. 3.1.1. Locations of operating moored data buoys as of June 2000

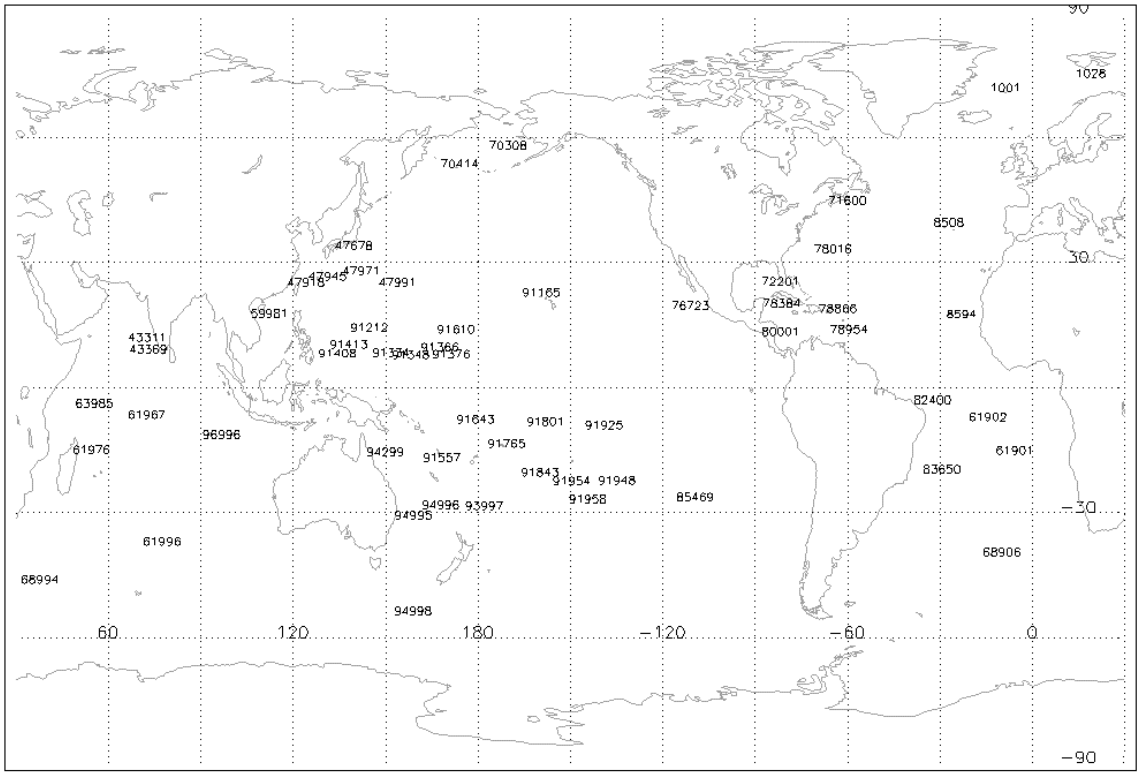

Fig. 3.1.2. Small island radiosonde stations operating as of June 2000

where h_0 is the surface roughness length, which equals 1.52×10^{-2} cm assuming a drag coefficient of 1.3×10^{-3} [*Peixoto and Oort*, 1992].

The buoy data sets will undergo quality check procedures, including checks for missing data, repeated data, blank fields, and out-of-bounds data. A time interpretive collocation program will calculate the wind speed at the time of the nearest satellite overpass, as is described in *Wentz* [1997].

Radiosondes measure temperature, pressure, and humidity as a helium balloon carries them aloft. The international radiosonde network will be the primary data source used to validate the AMSR-E water vapor product, and such data are available from several sources, including NCEP, NCDC, and NCAR. In many locations throughout the world radiosondes are launched twice each day (00Z and 12Z). To compare water vapor over ocean regions, only stations on small islands or ships are used. A preliminary list of 57 radiosonde stations currently operating on small islands is listed in Table 3.1.4 and is displayed in Figure 3.1.2.

Quality control measures will include discarding incomplete or inconsistent soundings, soundings without a surface level report, soundings with fewer than a minimal number of levels, and those with spikes in the temperature or water vapor pressure profiles. These measures will reduce the size of the available data set. In addition, corrections or normalizations among the various types of sensors and sensor configurations will be required since the radiosonde data are from different stations, countries and vendors. A collocation program will be used to find the AMSR-E measurements within a specific space and time of each radiosonde sounding. Alishouse et al. [1990] and Wentz [1997] give the details of collocating radiosondes with satellite observation and the associated quality control procedures.

3.1.3 Satellite Data

Observations from other satellite sensors play a vital role in our AMSR-E calibration/validation activity. In the pre-launch calibration/validation phase, the SSM/I and TMI microwave radiometers have been essential in our algorithm development work. And, after the launch of AMSR-E, two major satellite intercomparison projects will be done: 1) intercomparison of microwave and infrared SST retrievals and 2) intercomparison of microwave passive and active wind retrievals. We first discuss how satellite data has been used during the pre-launch phase of our investigation, and then the two post-launch satellite intercomparison studies will be discussed.

Pre-launch algorithm testing and development has been primarily based on SSM/I and TMI observations collocated with existing buoy and radiosonde observations. Figure 3.1.3 shows the four basic steps in developing and testing the AMSR-E ocean algorithm. In the first phase of development, the Pre-Launch Version 0 algorithm was written. This first algorithm was primarily based on the SSM/I observations and radiative transfer theory. One shortcoming of the Version 0 algorithm was that there was some uncertainty about the wind component of the radiative transfer model (RTM) at 6.9 and 10.7 GHz. At these frequencies, we used SeaSat SMMR T_B's collocated with SeaSat scatterometer winds to specify the wind component of the RTM [*Wentz et al.*, 1986]. The SeaSat SMMR suffered from calibration problems, and we were concerned about the accuracy of the surface component of the RTM at 6.9 and 10.7 GHz.

More recently, using observations from the new TRMM microwave radiometer (TMI), we completed the next phase of algorithm development. TMI is providing well-calibrated 10.7 GHz ocean observations. We collocated these observations with wind vector measurements from ocean buoys and NCEP's global circulation model and with AVHRR SST retrievals. The combined T_B, wind, SST data set provided the means to update the sea-surface emissivity model at 10.7 GHz. The updated algorithm, called Pre-launch Version 1, has been delivered to the AMSR-E Science Computing Facility.

Table 3.1.4. Island Radiosonde Locations as of June 2000

WMO No.	Name	Latitude	East Long.	Area (km^2)
1001	Jan Mayen	70.93	351.33	373
1028	Bjornoya	74.52	19.02	179
8508	Lajes / Janta Rita	38.75	332.93	
8594	Sal	16.73	337.05	
43311	Amini	11.12	72.73	
43369	Minicoy	8.30	73.00	
47678	Hachija Jima	33.12	139.78	70
47918	Ishigaki Jima	24.33	124.17	215
47945	Minamidaito Jima	25.83	131.23	47
47971	Chichi Jima	27.08	142.18	25
47991	Marcus Is.	24.30	153.97	3
59981	Xisha Is.	16.83	112.33	
61901	St. Helena	-15.96	354.30	122
61902	Ascension Is.	-7.97	345.96	88
61967	Diego Garcia	-7.35	72.48	152
61976	Serge-Frolow / Tromelin	-15.88	54.52	
61996	I. N. Amsterdam	-37.80	77.53	62
63985	Seychelles Intl	-4.67	55.52	23
68906	Gough Is.	-40.35	350.12	83
68994	Marion Is	-46.88	37.87	388
70308	St. Paul Is.	57.15	189.79	91
70414	Shemya Is.	52.72	174.10	21
71600	Sable Is.	43.93	299.98	8
72201	Key West	24.57	278.32	
76723	Socorro Island	18.72	249.05	
78016	Kindley Field	32.37	295.32	53
78384	Roberts Fld.	19.30	278.63	183
78866	San Maarten	18.05	296.89	85
78954	Barbados	13.07	300.50	431
80001	Isla San Andreas	12.58	278.30	21
82400	Fernando de Noronha	-3.85	327.58	4
83650	Trindade Is.	-20.50	330.68	10
85469	Easter Is.	-27.17	250.57	117
91165	Kauai	21.98	200.65	
91212	Guam	13.48	144.80	
91334	Truk	7.47	151.85	118
91348	Ponape/Caroline Is.	6.96	158.22	68
91366	Kwajalein	8.72	167.73	16
91376	Majuro	7.03	171.38	10
91408	Koror	7.33	134.48	8
91413	Yap	9.48	138.08	54
91557	Efate	-17.70	168.30	
91610	Tarawa	13.05	172.92	23
91643	Funafuti	-8.52	179.22	3
91765	Pago Pago	-14.33	189.29	135
91801	Penrhyn	-9.00	201.95	10
91843	Cook Isles	-21.20	200.19	218
91925	Atuona	-9.82	220.99	200
91948	Rikitea	-23.13	225.04	31
91954	Tubuai Island	-23.35	210.52	36
91958	Austral Is.	-27.61	215.67	47
93997	Kermadec Is	-29.25	182.09	34
94299	Willis Is.	-16.30	149.98	
94996	Norfolk Is.	-29.03	167.93	34
94995	Lord Howe Is.	-31.53	159.07	2
94998	Macquarie Is.	-54.48	158.93	109
96996	Cocos Is.	-12.18	96.82	14

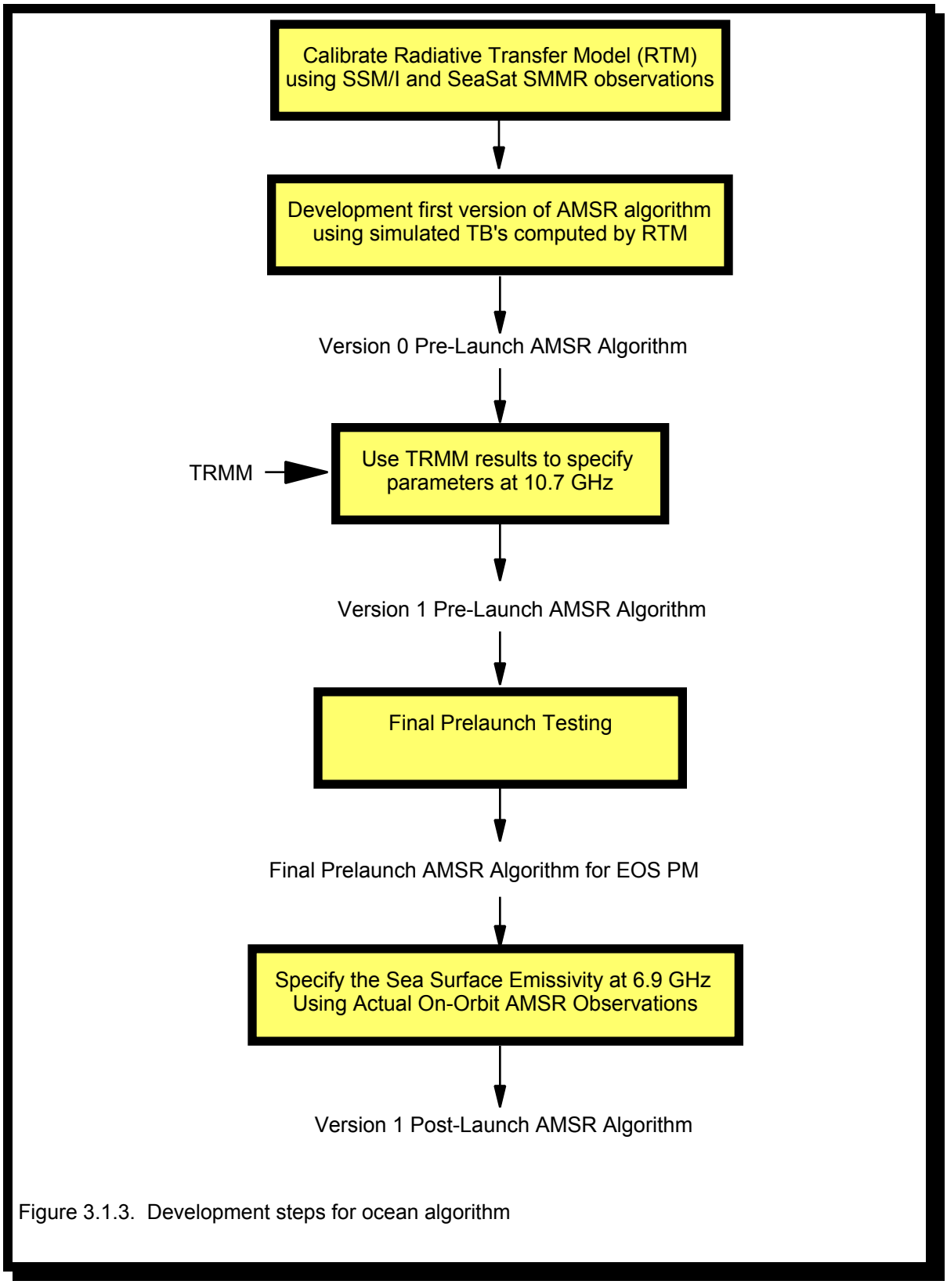

Figure 3.1.3. Development steps for ocean algorithm

The Version 1 algorithm has been tested using the TMI observations as input. The primary focus of these tests was the SST retrieval. In spite of the impressive TMI SST results as illustrated by Figure 3.1.4. [Wentz et al., 2000], there is still room for improvement. The TMI analysis shows that the largest error in the SST retrieval is due to wind direction (not withstanding sensor calibration problems). At higher wind speeds, T_B can vary by several degrees with changing wind direction [Wentz, 1992]. Figure 3.1.5 shows the effect of wind direction on the SST retrieval. If not accounted for, wind direction variations can produce significant errors in the SST retrieval. For TMI, we use NCEP wind directions in an attempt to remove this error, but this approach is certainly less than desirable. (Figure 3.1.4 utilizes the NCEP wind direction correction.) . It should be noted that the addition of the 6.9 GHz channels for AMSR-E (TMI does not have these channels) reduces the wind direction error relative to that shown in Figure 3.1.5. However, the SST error due to wind direction is still a problem and will be a primary concern during the post-launch calibration/validation for AMSR-E.

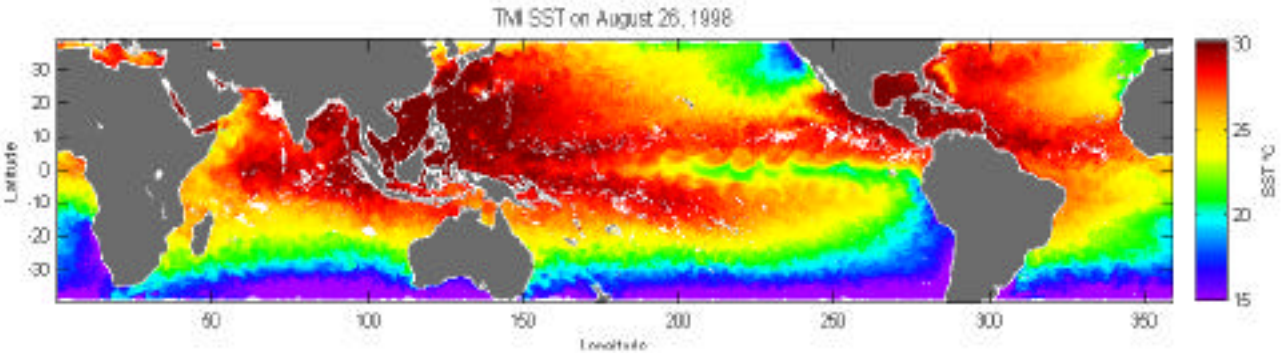

Fig. 3.1.4 TMI through-clouds microwave SST retrievals for August 25-27, 1998. Cool water directly East of Florida is cold upwelling due to the passage of Hurricane Bonnie. Tropical instability waves are propagating along both north and south of the Equator in the Pacific Ocean

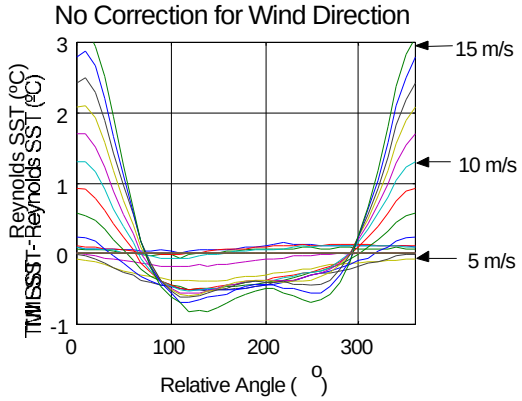

Fig. 3.1.5 Effect of wind direction on SST retrievals. Reynolds SST, which should have no wind direction dependence, is subtracted from TMI SST. No correction for wind direction has been applied to the TMI SST. This difference is binned according to wind speed and is plotted versus the relative wind direction, which is the satellite's azimuthal viewing angle minus wind direction (from NCEP). The colored curves show the results for each wind speed bin from 0 to 15 m/s, in 1 m/s steps. At low wind speeds (< 5m/s) there is no appreciable error. Above 5 m/s the peak-to-peak amplitude of the error increases to a maximum of 4ºC when winds are 15 m/s.

After AMSR-E is launched, we will begin the two satellite intercomparison studies. The first study involves comparing the microwave SST retrieval with infrared SST retrievals from a number of satellite sensors. The Advanced Very High Resolution Radiometers (AVHRR) have a two-decade heritage of retrieving T_S. They have a proven capability of measuring T_S in the absence

of clouds. We will use these T_S retrievals in cloud-free areas to calibrate the AMSR-E T_S retrievals. Once calibrated in the cloud-free areas, the AMSR-E T_S retrievals should also be valid in cloudy areas because non-raining clouds are nearly transparent at 6.9 GHz. In addition to AVHRR, we will collaborate with the Aqua AIRS and MODIS Teams to do further SST intercomparison studies. The final component of the satellite SST study involves the European Along Track Scanning Radiometer (ATSR). According to some, ATSR's multiple look design currently provides the most accurate infrared SST retrievals. We are having discussions with the ATSR Team about collaborating on an AMSR-ATSR SST intercomparison.

Our baseline SST for these intercomparisons will be the blended AVHRR-buoy SST data set produced by R. Reynolds using optimum interpolation (OI). This product is routinely generated on a weekly, one-degree grid, as is shown in Figure 3.1.6. The advantage of this product is that it is routinely available and has global uninterrupted coverage. This makes intercomparison with the AMSR-E observations a relatively simple task. Furthermore, a very large database of intercomparison statistics can be generated in a short time, which is ideal for a quick validation study shortly after launch. The disadvantage of the data set is its low spatial and temporal resolution and questionable accuracy in some parts of the ocean. To address these concerns, we will be doing more detailed intercomparisons with the AVHRR Pathfinder SST produced by the JPL PO-DAAC and with the AIRS, MODIS, and possibly ATSR high resolution infrared SST products.

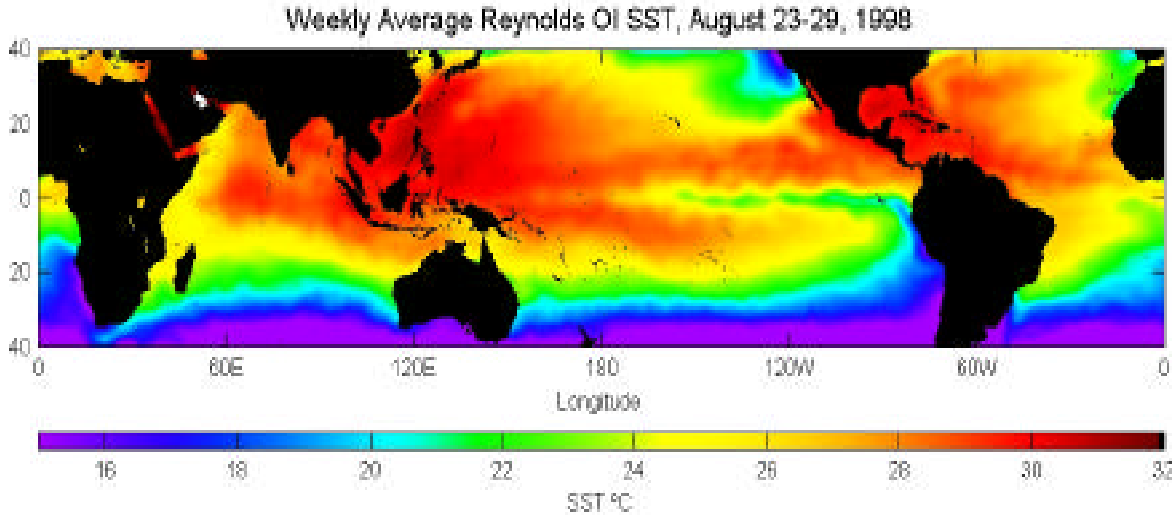

Fig. 3.1.6. An example of the Reynolds OI SST product that will be used for SST validation.

The second satellite intercomparison study is the AMSR-SeaWinds project, as illustrated in Figure 3.1.7. The ADEOS-II platform flies both the microwave radiometer AMSR and the microwave scatterometer SeaWinds. With this combined active/passive sensor package, we expect that the SST error due to wind direction can be virtually eliminated. Simulations show that by combining AMSR and SeaWinds the SST rms accuracy for a 3-day, 60-km product will be 0.2°C. Given this accuracy, investigators will be able to study the interaction between wind and SST in greater detail and with more confidence than ever before. The early TMI results are rich with examples of wind-SST interactions: upwellings off of the continents, cold water wakes from storms and hurricanes, and remarkably tight correlations between the tropical instability waves and the surface wind (see Figure 3.1.4). A highly accurate, combined vector wind - SST data set (through clouds) will be of enormous value to oceanography and climate research.

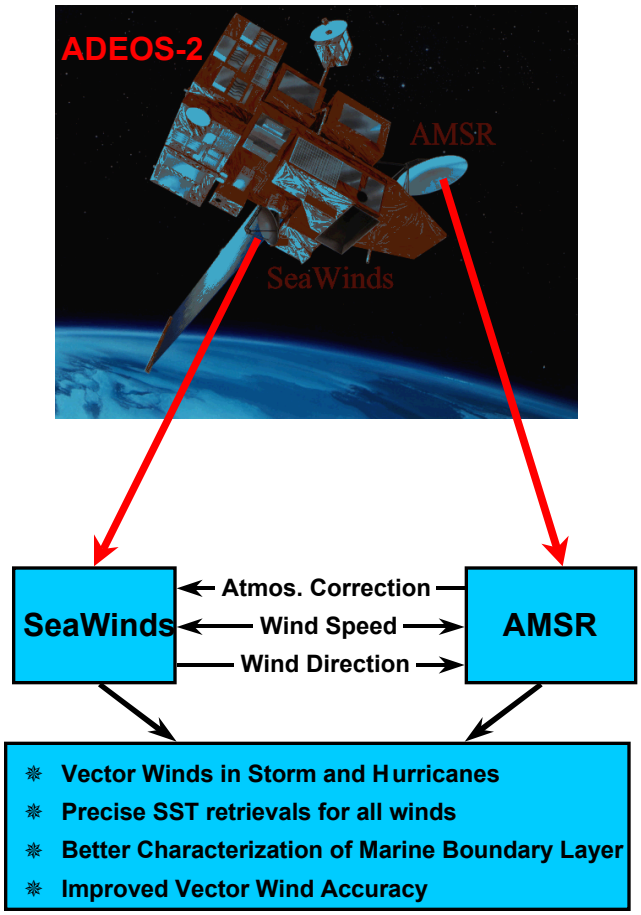

Fig. 3.1.7. Benefits derived from combining SeaWinds and AMSR

In addition to improving the SST accuracy, the scatterometer data will contribute greatly to our wind validation study. The microwave scatterometer provides highly accurate wind vector retrievals at a spatial resolution of 25 km. The QuikScat scatterometer (SeaWinds' precursor) is now in operation and should still be functioning when AMSR-E is launched. SeaWinds will then be launched in 2001 on ADEOS-II, and it is most probable that two scatterometers will be in operation during the AMSR-E and ADEOS-II AMSR time frame.

Inter-comparisons of the AMSR-E and scatterometer wind speed will be done on a global basis and any systematic differences will be identified. Early studies comparing SSM/I wind retrievals with scatterometer retrievals did reveal curious systematic differences in areas of upwelling. The top frame of Figure 3.1.8 shows the SSM/I wind minus the QuikScat wind, and the bottom frame shows the SSM/I minus the NSCAT wind. The blue areas (SSM/I low relative to the scatterometer) seem to be correlated with areas of upwelling. This hypothesis is further reinforced by the fact that during the NSCAT period, the upwelling off of South America's West Coast had shut down due to the El Nino episode, and this absence of upwelling is evident in the SSM/I minus scatterometer imagery (i.e., blue area west of Peru is not present for the NSCAT period). We will attempt to relate these systematic differences to physical phenomena like sea

surface temperature and roughness, atmospheric stability, atmospheric attenuation, and wind fetch.

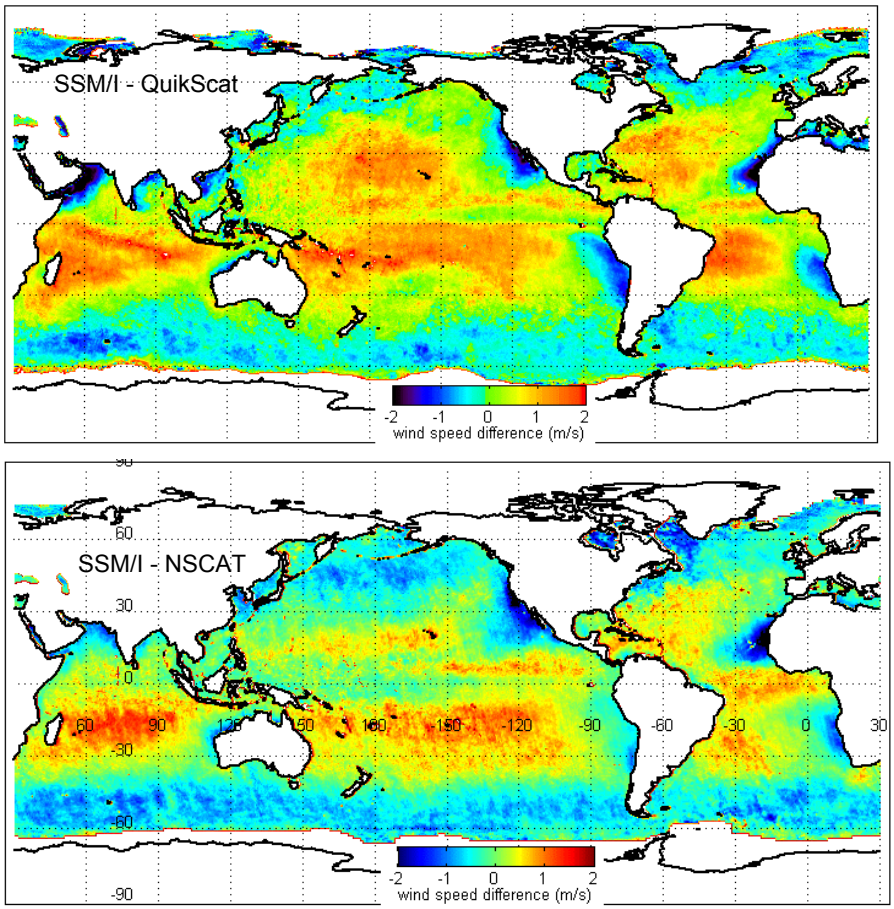

Figure 3.1.8. Systematic differences between wind speed retrievals from microwave radiometers and scatterometers.

Collocated microwave T_B's and scatterometer wind vectors provide one of the best means to study wind direction effects on the T_B's and ocean products. For example, the difference between the AMSR-E and scatterometer wind speed will be plotted versus wind direction to determine if the AMSR-E wind speeds contain any systematic error related to wind direction. Likewise, the effect of wind direction on SST retrievals can be studied, as discussed above.

Finally, we point out that the QuikScat/SeaWinds Science Team will be conducting its own wind validation activity. We plan to incorporate the validation data sets and field experiments coming from the scatterometer team into our AMSR-E wind validation activity.

3.1.4 Validation of Wind Speed using GCM

In addition to the buoy and scatterometer intercomparisons, we will also compare the AMSR-E winds to those coming from global circulation models (GCM). Two GCM will be used: NCEP and ECMWF (if ECMEF is made available to us). The GCM comparisons have the advantage of providing global winds for every AMSR-E cell. Thus a very large database of intercomparison statistics can be quickly

accumulated. The disadvantage is that the GCM winds are an analysis product rather than a direct measurement of the ocean wind field. Our approach will be to use the GCM for the initial validation period, and then as the AMSR-buoy and AMSR-scatterometer database grows with time, more emphasis will be placed on the buoy and scatterometer observations as the eventual calibration reference.

3.1.5 Histogram Validation of Cloud Water Product

Microwave radiometry is probably the most accurate technology for measuring the vertically integrated cloud liquid water L. In the 18 to 37 GHz band, clouds are semi-transparent and the absorption by the entire column of liquid water can be measured. Apart from using upward-looking radiometers to calibrate downward-looking radiometers (or vise versa), there are no other calibration sources for L. Several nations (e.g., The Netherlands) maintain upward looking radiometers or routinely make aircraft flights (e.g., Australia) to measure L in support of their meteorological operations. These data sets are increasingly made available to the scientific community over the Internet. However, comparison of the L inferred from upward looking radiometers with that inferred from downward looking satellite radiometers has limited utility. The great spatial and temporal variability of clouds makes such comparisons difficult. Also, the major problem in calibrating L is in obtaining accurate retrievals over the full range of global conditions. There are not enough upward looking radiometers to do this. Finally, when differences arise, it will be difficult to determine which radiometer system is at fault.

We prefer to use the statistical histogram method described by *Wentz* [1997]. This technique is illustrated in Figure 3.1.9. We assume the probability density function (pdf) for the true cloud water observed by AMSR-E has a maximum at L = 0 and rapidly decays similar to an exponential pdf as L increases. The pdf for the retrieved L will look similar, but retrieval error will tend to smear out the sharp peak at L = 0. Simulations in which Gaussian noise is added to a random deviate having an exponential pdf show that the left-side, half-power point of the pdf for the noise-add L is located at L = 0. Thus we require that histograms of the L retrievals are aligned such that the half-power point of the left-side is at L = 0. Furthermore, we require this condition be met for all T_S, W, and V.

For example, the top plot in Figure 3.1.9 shows 6 histograms of L retrieved from SSM/I. The 6 histograms correspond to 6 different ranges of T_S (i.e., 0-5 C, 5-10 C, ..., 25-30 C). The middle and bottom plots show analogous results for wind and water vapor groupings. The peak of the pdf's is near L = 0.025 mm. At L = 0, all histograms are about half the peak value. The misalignment among the 6 histograms is about $\pm$0.005 mm. We use the width of this half power point (i.e., 0.025 mm) as an indicator of the rms error in L.

This procedure effectively eliminates the bias and crosstalk error in the L retrieval, and we consider it the best available way to validate the cloud water retrieval

3.1.6 Field Experiments

No field experiments are specifically planned for validation of the AMSR-E ocean algorithms. However, we do plan to make use of field experiments scheduled for the AIRS and MODIS SST validation and the Quikscat/SeaWinds wind validation. These field experiments will provide useful data for the AMSR-E validation that will supplement the *in situ* and satellite observations discussed above.

3.1.7 Calibration and Validation Time Line

The AMSR-E calibration and validation plan is shown above in Figure 3.1.3. We have completed the calibration and validation of the 10.7-GHz components of the model and retrieval algorithm using the TRMM TMI observations. This was the last step of the pre-launch calibration and validation phase. This pre-launch ocean algorithm for AMSR-E has benefited from two separate calibration and validation activities: SSM/I and TMI.

We originally planed to use the AMSR aboard the ADEOS-II spacecraft to further develop and test the AMSR-E ocean algorithm. Now that the ADEOS-II launch date has slipped to 2001,

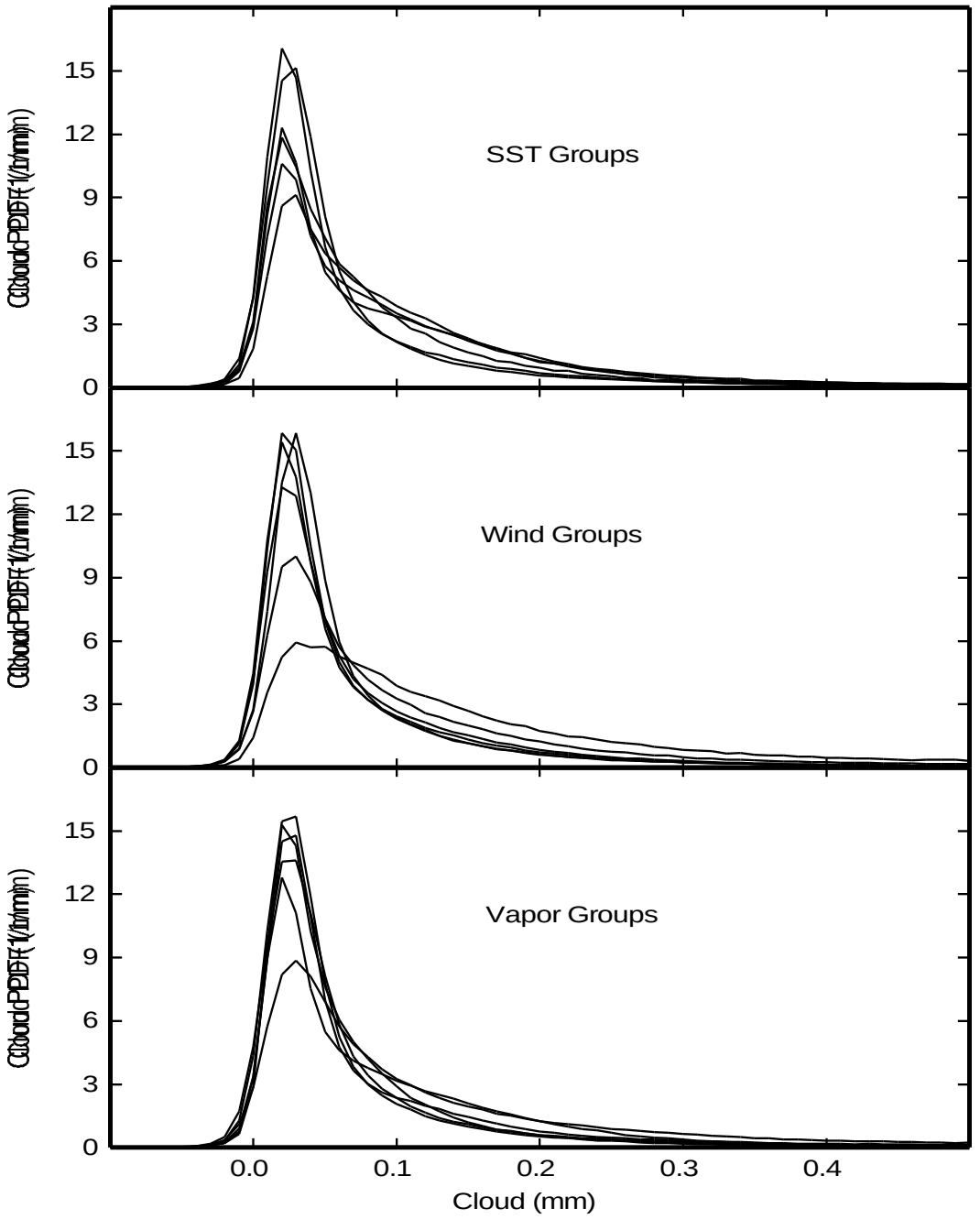

Figure 3.1.9. Probability density functions (pdf) for liquid cloud water. The cloud pdf's are stratified according to sea-surface temperature, wind speed, and water vapor. Each curve shows the pdf for a particular stratification.

this is no longer possible. Therefore, the final specification of the 6.9-GHz emissivity will need to be done after the AMSR-E launch using actual on-orbit AMSR-E observations. Given the AMSR-E 6.9-GHz observations, the dependence of the sea-surface emissivity on temperature, wind speed, and wind direction can be precisely determined. Calibration data for the sea-surface temperature will be obtained from buoys and cloud-free IR temperature retrievals. Buoy and scatterometer winds will be used to calibrate the wind component of the RTM at 6.9 GHz. We expect that the 6.9-GHz emissivity can be adequately specified 3 to 6 month after we begin receiving the AMSR observations.

Another post-launch activity that needs to be done as soon as possible after launch is the determination of absolute biases for each of the AMSR channels. With current technology, it is not possible to absolutely calibrate satellite microwave radiometers to better than 1 to 2 K. Also the RTM probably has an absolute bias due to uncertainty in specifying the dielectric constant of sea water and the oxygen/vapor absorption. Thus we expect that there will probably be a relative bias of 1 to 2 K between the AMSR-E observations and the RTM. Such offsets occurred for both SSM/I and TMI. These T_B offsets need to be derived after launch. This activity will run in parallel with the determination of the 6.9-GHz emissivity and will be complete 3 to 6 month after we begin receiving the AMSR observations.

We will also be looking for possible Level-1 problems during this initial cal/val period, including possible geolocation errors and sensor calibration problems. In addition, we anticipate that some unexpected problems will occur (they always do). Given the very demanding workload during this initial period coupled with the fact that this will be the first AMSR to fly, it will probably take the full 6 months to complete the initial cal/val. Once the initial cal/val is completed, the first release of AMSR-E ocean products (Version 1) will be provided to the user community.

The second phase of the AMSR-E validation will then begin. This will be a more thorough 1-year investigation in which a comprehensive set of *in situ* and satellite observations are used to calibrate and validate the AMSR ocean products. A precise T_B calibration will be done, and the retrieval algorithm and associated RTM will be fine-tuned. The updated algorithm coming from this activity will represent the Version 2 post-launch AMSR-E algorithm and we anticipate that it will be used to process data for several years. Once the Version-2 software is implemented, we will begin several research activities aimed towards extracting the maximum information content from the AMSR observations. Our AMSR-E investigation will conclude with an optimal algorithm for retrospective processing of the AMSR-E data.

3.2 Rainfall (submitted by C. Kummerow, T. Wilheit and R. Ferraro)

3.2.1 Approach Philosophy

There are two paradigms for validation. In the conventional paradigm, some "truth data", are collected and compared with the product to be validated. We will refer to this paradigm as "GT" {Ground Truth}. The key to GT is some truth data in which you have more confidence than you have in the product being validated. Historically, both ground based radar and raingauge data have been used as “truth data” for precipitation. The GT approach has been dominant in remote sensing because it has not been common for a remote sensing technique to provide the best estimate of anything. Advances in spaceborne technology and algorithms, however, may require a shift in paradigms. The TRMM radar, for instance, has demonstrated quite clearly that its stability is such that it can be used to verify the calibration of ground-based radars. There is now ample evidence [Anagnostou et al, 2000] that the “truth” in this case, resides with the space borne sensors.

Another approach is to develop an error model of the measurement process and to determine the uncertainties of the important elements in the error model. This will be referred to as "PV" {Physical Validation} The key here is that the product being validated be derived on a physical basis with empirically testable assumptions. The largest component of this effort is to observe and build reliable rainfall models or statistics for those quantities (e.g. sub-pixel inhomogeneity), which affect the retrieved rainfall, but cannot be directly measured by the sensor.

In the case of rainfall, there is in addition to GT and PV, the opportunity to compare results to concurrent sensors such as TRMM (in the tropics) and SMM/Is which have been flying continuously since 1987. While these comparisons do not represent ‘truth’, these datasets have been studied extensively. In the case of TRMM, there is a large validation effort underway also. Large discrepancies with these existing data sets could therefore point at software errors and provide a straightforward opportunity to check the overall performance of the algorithm immediately following launch.

In validating the AMSR rainfall products, all forms of validation will be used. Comparisons with existing data will provide the first assessment of the products and will be used to determine if the algorithms are working as intended. We intend to release the rainfall products once we are convinced that the algorithms are indeed performing as intended and there are no large discrepancies with previous sensors that cannot be explained based upon uncertainties in our physical assumptions. Given the historical difficulties with the GT approach for rainfall, we will then turn our attention to a carefully selected set of measurements intended to simultaneously serve GT and PV purposes. The key to this approach is to make enough ancillary measurements such that any discrepancies in the GT approach can immediately be traced to uncertainties in the physical assumption of both satellite and ground based measurements. This is the only way the team feels that progress is possible.

Finally, the team feels that the tropical regions were studied extensively by TRMM, which should still be flying by the time of the Aqua launch. The TRMM Microwave Imager (TMI) has very similar characteristics to AMSR and TRMM spend vast resources establishing unique validation resources such as the Kwajalein radar site. This resource should be picked up by the AMSR team after TRMM’s demise. Until that time, however, the tropics are taken care of by the TRMM program. The team therefore feels that AMSR’s unique contribution to the validation and improvement of global rainfall should concentrate on the extra-tropics. The implementation plan reflects this thinking.

3.2.2 Validation Approach

Over land, the high and variable emissivity of the land surface at microwave frequencies masks any useful signal from the liquid hydrometeors. We are reduced to using the scattering from the ice phase to estimate the rainfall intensity. Unfortunately, the ice phase is not uniquely connected to the rain rate. A further complication related to the land algorithm is the potential false signal connected to cold and snow covered surfaces, which have Tb depressions that can easily be mistaken for rain signals.

There are a great deal of reasonably good rainfall data from the US WSR-88 network or the Japanese AMeDAS network. These data can be used to validate the rain discrimination portion of the algorithm without too much difficulty. These operational radar networks, however, are less reliable when it comes to generating climate quality rainfall maps. This shortcoming will be corrected by adding a layer of quality control and radar/rain gauge comparisons to the operational processing. The process is labor intensive but Climate Quality radar rainfall products can be produced. The AMSR team will take advantage of this framework. The WSR-88 radar at Eureka, California was selected by the AMSR team as a key validation site. The selection of Eureka was based on a number of factors: Microwave retrieval algorithms have historically had problems on the West coast of the United States; Eureka has minimal beam blockage related to the local topography; Eureka has good coverage over the oceans as well as land; and the staff at the Eureka Office have been very supportive and willing to cooperate with the team for improving the local infrastructure. The infrastructure consists in additional triple-gauge clusters (needed to have complete confidence in the gauge rainfall) and disdrometers. While the AMSR team can supply this equipment, the team must relay on the local support for continuous maintenance. While more radar locations are certainly desirable, the AMSR team felt that it should concentrate its resources on a single site and insure that useful products could be derived from it before expanding the number of sites.

In contrast to the land situation, the ocean background is ideal for the passive measurement of rainfall. We are able to infer the rain rate from the emission by the hydrometeors in the centimeter wavelength range. Ocean backgrounds, however, have virtually no ground based radar or rain gauges available. We expect that monthly rain totals over 5 degree squares will have accuracies of the order of 20% for the rainiest parts of the globe. This is a very challenging level of accuracy to validate given the poor ground based observations. Experience with six major intercomparison projects has convinced us that the GT approach will be inadequate by itself. A combination of GT and PV methods will therefore be used over oceans.

The ideal experiment is one in which a ground based radar is available to observe not only the surface rainfall but the key parameters affecting rainfall retrievals from AMSR as well. We will call this class of experiments the GT/PV combined approach. It is useful because it both compares and tries to explain any discrepancies between the sensors. Of course, ground based radars themselves need validating and this requires a careful investment in support equipment such as rain gauges and disdrometers as well as tools to keep the radar calibrated and the signal free of spurious echoes. If some confidence can be established in the radar rainfall product, comparisons can be made with the satellite products. If the proper data is collected, the same ground based radar can also be used to define the assumptions inherent in passive microwave algorithms. The parameters not observed by the ground-based network can typically be observed through aircraft penetration of the storms. In so doing, we then pursue the PV approach and check that any differences between satellite and ground based radars are indeed accounted for by physical makeup of the particular rain scenes.

The dominant sources of uncertainty in the AMSR rainfall algorithm are identified next. If one considers climatological products (rainfall totals over a space-time volume) then sampling is a major source of error. AMSR observations are limited to two observations per day at best. We simply do not see all the rain and must infer the occurrence of rainfall between the observations.

In practice, this will always the dominant source of error. If additional observation capability is added the users will immediately demand finer space-time resolution, so that the sampling error remains at the maximum tolerable level. While the uncertainty cannot be reduced, it can be quantified.

We plan two approaches for estimating the sampling error. First the data taken for the GT approach will be sub-sampled to coincide with the satellite sampling observations. The rainfall totals derived from this sub-total will be compared with totals from the complete data set. Adjustments will have to be made for the areal coverage of the radar not coinciding with that of the satellite, but these will not prove difficult. The second approach, that can be applied globally, is to make two separate satellite derived estimates based on alternate days. (e.g. odd and even days of the year) If the area covered by each estimate is doubled, the sampling will remain constant. This approach will estimate all random sources of error rather than just the sampling error. The impact of the other random sources of error can be estimated by comparing with the sampling error estimates derived from the radar data. Thus the sampling error estimated at a few radar locations can be applied globally.

In addition to sampling errors, there are three major sources of uncertainty in rainfall retrievals over water. In order of importance, these are the beam-filling error (sub-pixel inhomogeneity in the rainfall field), uncertainty in the vertical distribution of hydrometeors, and errors in the freezing level retrieval.

The beam filling correction can be done either from ground based radar statistics or by simulation and is incorporated into the Brightness Temperature - Rain Rate (TR) relationships either directly (in the Level 2 algorithm) or as a multiplicative factor (in the Level 3 algorithm). To date this work has been based on limited data sets from ground- and airborne radar or hydrodynamic Cloud Resolving Models (henceforth "CRM's") of which Tao's model is a well-known example [Tao and Simpson, 1999]. The relative advantages and disadvantages of each approach are fairly obvious. It is not practical to get enough airborne radar data to cover the range of possibilities adequately. Ground based radars overcome the data volume issue, but are limited to coastal regions at best. The CRM could be run for as many situations as we chose, but we have less confidence that the length scales are really correct. . In no case do we have a sufficiently wide range of conditions to be comfortable with the corrections or even estimates of the uncertainty of the corrections. What is needed is to get reliable statistics derived from radar data for a few dozen locations in the tropics and extratropics in various seasons. TRMM is actively seeking these statistics in the tropics. A concerted effort to sample a number of different locations in the extra tropics is therefore a key priority. We further recommend that these observations be coupled with sounding such that CRMs can be initialized and their properties compared to the observations. The CRM's may need to be refined to achieve the same results over the range of conditions. Having models in which we have confidence is critical not only for advances in beam filling corrections, but latent heating inferences as well.

The vertical distribution of hydrometeors is a particularly difficult parameter to observe. CRM's are a good source of information but they still give widely disparate pictures of the liquid content in the mixed phase region just above the freezing level. This, in turn, gives widely varying effects of scattering in this region. The bright band region is of special interest. In the bright band region, the region just below the freezing level where the snow melts to form raindrops, the radiometer and radar communities model the attenuation differently. The radiometer community, on the basis of limited evidence, treats the attenuation as being the same as in the rain area below whereas the radar community treats the bright band as having twice the attenuation of the rain below. Aircraft penetrations with simultaneous radar and radiometer observations are the best way to settle the questions. Cloud particle imaging systems (e.g. PMS probes) provide phase and density information. Upward viewing microwave radiometers provide integrated measurements of the attenuation above the aircraft. Once again, having soundings to go with the measurements will allow the running of CRM's to compare with the observations and allow the

refinement of these models so they can be used to cover a wider range of conditions than is accessible with a reasonable number of aircraft hours.

If the Aqua satellite had a radar, it would be straightforward to validate the freezing level retrieval, and by implication, the thermodynamic assumptions of the RT models. With TRMM data, the retrieved freezing levels are being compared with freezing levels inferred from the bright band in the radar data. This will nearly suffice for the AMSR freezing levels in the tropics. It will be important to extend this validation to higher latitudes (lower freezing levels). The ground-based radar at Eureka and the planned field experiments, when scanned appropriately for this purpose, can partially achieve this goal by making careful measurements of the bright band height. An airborne radar in rain underflying the Aqua spacecraft, and direct aircraft penetrations of convective systems may be needed to obtain the freezing level when no bright band is present.

Summary of Physical Validation Needs (Ocean)

Source of uncertainty: Sampling
Applicable Sfc: Land & Water
Severity of problem: Greater than 100% depending upon rainfall characteristics
Remarks: None. Uncertainty is easily quantifiable based upon local radars and satellite data itself. Uncertainty cannot be overcome except by increasing the number of satellites.

Source of uncertainty: Beam filling
Applicable Sfc: Water
Severity of problem: ~40% low bias if uncorrected
Remarks: Both the global mean variability (needed to generate unbiased retrievals), and variability about that mean (to estimate uncertainty) are needed. Level 3 algorithm can incorporate mean value directly. Level 2 algorithm needs to match observations to cloud models.

Source of uncertainty: Misidentification of freezing height
Applicable Sfc: Water
Severity of problem: Bias directly proportional to error as a function of liquid water column (e.g. 20% for 500m bias in 2.5 km freezing level).
Remarks: Can make immediate use of information to improve freezing height detection scheme or estimate uncertainty.

Source of uncertainty: Misidentification land surface background
Applicable Sfc: Land
Severity of problem: Dominates signal in cold/snow & ice covered Sfcs.
Remarks: Operational ground based radar networks will provide significant information. Some questions will remain that require a spaceborne radar to solve.

Source of uncertainty: Convective/Stratiform nature of rainfall
Applicable Sfc: Land & Water
Severity of problem: ~10% bias in rainfall if climatological variations are not accounted for. Larger impact for fine scale rainfall estimates. Also has a large impact upon latent heating uncertainty
Remarks: Is only used in Level 2 algorithm.

Source of uncertainty: Hydrometeor characterizations (phase, size, shape, cloud water)
Applicable Sfc: Land & Water
Severity of problem: Minor for rain. Serious to disabling for snow. Serious for coincident radar observations when used for validation.
Remarks: Not enough data can be collected from a few aircraft flights. Information must thus be coupled with dense radiosonde network to allow for improvements cloud dynamical models.

Source of uncertainty: Errors in spectroscopy
Applicable Sfc: Water
Severity of problem: 2-3% errors at best
Remarks: We will monitor progress in this area but there are no specific plans to address this topic.

3.2.3 Implementation Plan

Based upon our Validation Approach, we have derive the following more specific validation activities intended to better understand and quantify the sources of uncertainty described in the previous section. In addition, the team wanted to maximize the use of existing infrastructure and our participation in ongoing experiments. Because of the latter requirement, the details of the implementation plan must remain flexible. We feel that a one-year lead-time is necessary but changes can be incorporated into the experiments planned beyond that as opportunities arise. In FY02, for example, the team felt that a joint experiment with NASDA in the Sea of Japan was useful to quantify uncertainties in very cold rainfall conditions, including snow over the ocean. The partnership brings a lot of assets to bear on this experiment. If NASDA decides not to go forward with the experiment, however, the AMSR team would certainly look for a location with similar meteorological conditions but with easier access.

1. Initial Validation and Data Release

As noted at the outset of this document, we will make the initial algorithm assessment based upon comparisons with existing satellite rainfall products. While not truly a 'validation' exercise, we feel that enough effort has gone into existing satellite product verification that they are probably correct to first order. No simple methods exist to improve upon these products immediately after launch and we will therefore use this as a benchmark for releasing the data and products to the public. Sensor differences as well as diurnal sampling issues will be taken into account for these initial comparisons.

2. Comparison with ground based radar data (GT)

The WSR-88 radar at Eureka, CA will be the key ASMR contribution to climatological validation of rainfall products at mid-latitudes. This will be supplemented by the TRMM assets (Kwajalein Atoll; Darwin Australia; Melbourne, FL and Houston, TX) in the tropics. The radar will be used both for climatological rainfall validation as well as obtaining statistics on sampling, sub-pixel rainfall inhomogeneity, freezing level heights, and mean rainfall vertical structure.

Processing of the radar data will be combined with the current effort underway for TRMM. It is important in these efforts to process data from different locations as uniformly as possible to match the AMSR algorithm that does not change with location. While this may not always produce the best results at any given location, it does insure that results can be intercompared. The TRMM procedure consists of an initial quality control of radar reflectivities to remove ground clutter, anomalous propagation and second trip echo effects. Rainfall is obtained by applying an initial Z-R relation to the radar data and then bias adjusting the results to match quality controlled raingauge data. To make this second step more robust, the team is installing 2 clusters of 3 gauges each (within 1 m. of each other) in order to have sites in which we can have absolute confidence that the gauges are working properly. We intend to keep adding gauge clusters and a disdrometer that can be used to independently verify the Drop Size Distribution inferred from the gauge-adjustment procedure. Long-term statistics are needed for all the applications described above. We plan to keep the radar data processing going for the duration of the AMSR mission.

3. Flight Campaigns

Flight campaigns are necessary to obtain in-situ verification of the remotely sensed parameters. We require a plane capable of measuring the in-cloud microphysics (the UND Citation or the U. of Washington Convair 580 are possible options), and a plane capable of overflying precipitation to simulate the AMSR instrument with high spatial resolution. The NASA DC-8, or ER-2 are possible options. Radiosonde launches are also needed to initialize the CRMs. Eight week campaign should be base lined in order to maximize the chances that observations of rainfall can be made coincident with AMSR overpasses. The missions will be designed to verify (assign uncertainties) to:

- Rainfall variability
- Drop Size Distributions & particle habitat
- Freezing level height derived from ground based radar via in-cloud observation
- Specific relationship between radar and radiometer properties of bright band
- Relationship between high-resolution radiometric observations to AMSR
- End to end modeling of rainfall and uncertainties
- Provide sounding data to allow for CRM initial state description.

4. Schedule

FY 99

Objective #1: Test NOAA ETL X-band radar operations and data processing to routinely generate the following products:

i) High resolution 3-D reflectivity for beam filling statistics
ii) Freezing level height for satellite validation
iii) DSD statistics for satellite algorithm as well as validation against gauges

Experiment: Automate scanning and generate data for 30 day period from NOAA ETL X-band polarimetric radar. The radar should be deployed initially (before launch) in logistically simple locations. We recommended Colorado (to avoid travel) in summer of 1999. This is a good test of its capabilities and while we don't need the statistics, there as much as in other places, it allowed us to verify the experimental setup at a minimum cost.

Results: Only one rain event. Learned about mutual requirements and developed routine data processing strategy for future experiments. Examined scan strategy used in CO and developed better alternatives for next Field Experiment; 3-D data were delivery within 4 months of experiment completion. Turn-around should be faster next time. Freezing level height data is straightforward to obtain from raw data but automated software needs to be developed. DSD data needs attention to insure quality data.

FY 00

Objective #1: Begin routine validation from Eureka WSR-88 radar. Installing AMSR gauge clusters at two locations. Train analyst to perform routine radar QC activities.
Experiment: Generate routine validation products as with TRMM ground validation sites.
Expected Results: Smooth data flow by the end of the year.

Objective #2: refurbish upward looking aircraft radiometer for FY02 deployment. Will need to examine bright band issues in radiometry as well as cloud microphysical models.
Experiment: None. Preparation only
Expected Results: Refurbished radiometer

FY01

Objective #1: Routine Validation from Eureka WSR-88 radar
Experiment: Generate routine validation products consisting of:
i) Surface rainfall maps
ii) High resolution 3-D reflectivity for beam filling statistics
iii) Freezing level height for satellite validation
Results: Not available yet.

Objective #2: Complement West coast observation with East coast observations. Add 3-Dimensional drop size distributions to observation suite. Insure that NASA NPOL radar is suitable for future operations. Establish DSD accuracy achievable from dual polarization radars.
Experiment: 2 Multiparameter radars at Wallops observing 3-D structure, freezing level and DSD. NOAA ETL will be shipped to Wallops during March-April, 2001 and will operate next to new NASA NPOL radar (scheduled for completion around 12/00). NPOL radar is more suitable for AMSR validation, but X-Pol has experience. Both radars will compare to extensive network of gauges and disdrometers available at Wallops for TRMM research.
Expected Results: ASCII data set of physical parameters needed by AMSR algorithm team will be delivered by PIs and posted on AMSR Web site for research by other interested PIs. Dataset will follow formats developed during test phase in FY99. Statistics on 3-D inhomogeneity and DSD will be accumulated and used to refine algorithm assumptions. Freezing level over ocean is assumed by both level 2 & level 3 and will be compared to AMSR observations directly. SSM/I can be used as proxy for AMSR if satellite is not in orbit yet.

FY02

Objective #1: Continue routine validation from Eureka WSR-88 radar

Objective#2: Assess ability to retrieve frozen precipitation over oceans (and land). Snow will create scattering signature at high frequencies but there are serious issues with regards to it quantitative interpretation. Detailed in-situ with coincident radiometric observations are needed to make progress. Without them, little progress can be made in the interpretation of different precipitation types.
Experiment: Currently in early planning phases for a joint experiment with NASDA in Sea of Japan in Jan/Feb 2002. Plan (pending approval) is to use the NASA NPOL radar in addition to the NASA DC8 aircraft carrying a radar and radiometer. Japan to contribute existing radar network, in-situ microphysics aircraft as well as ground support. If NASDA can supply high altitude aircraft for radiometric measurements, a NASA supplied in-situ aircraft can also be considered.
Results: A description of snow characteristics in the cloud, coupled with ground radar and airborne radiometer measurements will allow correlations between snow intensity & type with the corresponding radiometric observations. Information will be used to build (if possible), regression based snowfall retrievals similar to the currently implemented land scheme. Physical retrievals will be examined in the current rainfall retrieval framework, but results cannot be guaranteed at this time.

FY03

Objective #1: Continue routine validation from Eureka WSR-88 radar

Objective #2: Obtain high latitude rainfall statistics to drive the uncertainty models. Uncertainties are needed for the rainfall inhomogeneity; random error in AMSR-E derived freezing level; random error in Conv/stratiform separation over land & ocean; mean vertical structure of hydrometeors. Long-term statistics are needed.

Experiment: Currently planned for 1 year of observations at Wallops using NPOL. Meteorology is not ideal but location is. Long-term duration is seen as more important than detailed short-term measurements. Will continue to explore possibilities about better site but this will involve partners.
Results: Long-term statistics about beam filling, freezing height, and 3-D hydrometeor distributions.

FY04

Objective #1: Continue routine validation from Eureka WSR-88 radar

Objective #2: Obtain high latitude West Coast rainfall statistics to drive the uncertainty models. Uncertainties are needed for the rainfall inhomogeneity; random error in AMSR-E derived freezing level; random error in Conv/stratiform separation over land & ocean; mean vertical structure of hydrometeors. Long-term statistics are needed.
Experiment: Currently planned for deployment from Seattle with emphasis on area covered by Eureka radar. In addition to existing assets, need multiparameter radar and in-situ aircraft for 60 days to verify interpretation. Will continue to explore cost sharing possibilities but this will involve partners.
Results: Long-term statistics about beam filling, freezing height, and 3-D hydrometeor distributions.

FY05

Objective #1: Continue routine validation from Eureka WSR-88 radar

Objective #2: Fill in any uncertainties in the AMSR retrievals.

3.3 Sea Ice (submitted by D. Cavalieri and J. Comiso)

The standard sea ice products to be derived from AMSR-E are (a) sea ice concentration, (b) ice temperature and (c) snow cover thickness. The validation of these products will be the focus of the sea ice validation effort of the AMSR-E team. Other sea ice validation efforts, such as those supported by the validation project under the NASA Research Announcement (NRA-00-OES-03) and those of the MODIS team for sea ice, will be closely coordinated with our team activities.

All of the sea ice standard products will be Level 3 products. They will be mapped to a polar stereographic projection similar to the grid used for SSM/I data in which data are projected to a plane at 70 degrees latitude in both hemispheres (NSIDC, 1996). In addition to the sea ice products, AMSR-E brightness temperatures (TBs) will also be mapped to the SSM/I grid. The rationale for mapping both the sea ice products and TBs to the SSM/I grid is to provide the sea ice research community consistency and continuity with the existing 20-year Nimbus 7 SMMR and DMSP SSM/I TB and sea ice concentration products currently archived and distributed by the National Snow and Ice Data Center (NSIDC, 1996). The grid resolution for each Level 3 product will be as follows:

a) TBs for all AMSR-E channels: 25-km resolution
b) TBs for the 18, 23, 36, and 89 GHz channels: 12.5-km resolution
c) TBs for the 89 GHz channels: 6.25-km resolution
d) Sea ice concentration: 12.5-km, 25-km resolutions
e) Sea ice temperature: 25-km resolution
f) Snow depth on sea ice: 12.5-km resolution.

Our accuracy goal for each of the sea ice products is based on extensive experience with satellite multichannel passive microwave radiometer data. These goals are provided below for each standard product.

Sea ice concentration: Based on our experience with the SSM/I, the anticipated accuracy of AMSR-E sea ice concentrations will range from 4% to 10%, while that of sea ice concentrations from high resolution satellite and aircraft sensors can be significantly better. For example, the accuracy of sea ice concentrations derived from cloud free Landsat MSS imagery is estimated to be in the range of 2-4% (Steffen and Schweiger, 1991). Biases relative to the validation data can be reduced through the adjustment of the algorithm tie-points. Our accuracy goal for sea ice concentration ranges from 4% during the dry winter months to 10% during late spring and summer when surface wetness and meltponding make the emissivity of sea ice highly variable both spatially and temporally.

Sea ice temperature: The expected accuracy of sea ice temperatures derived from AMSR-E is estimated to be about 4K based on our experience with the Nimbus 7 SMMR. This estimate is largely dependent on the variability of the sea ice emissivity at 6 GHz. This product represents the physical temperature of the radiating portion of the ice that provides the observed microwave signal. Generally, for first-year ice, the radiating portion is the snow-ice interface, whereas, for multiyear ice, the radiating portion is a weighted mean of the freeboard layer of the ice. The validation data set will be derived using a combination of satellite infrared data, field measurements including buoy data, and an ice thermodynamics model. Our accuracy goal for sea ice temperature is 4 K or better.

Snow depth on sea ice: The algorithm uses regression coefficients to derive snow depth on sea ice in seasonal sea ice regions to an estimated accuracy of about 4-cm based on our experience with the SSM/I (Markus and Cavalieri, 1998). A comparison of snow depth distributions from ship measurements and from SSM/I snow depth retrievals in the Southern Ocean suggests that the SSM/I retrievals underestimate the insitu measurements by 3.5 cm and that the rms difference is

about 4 cm. Temporal information is used to filter retrievals that have been affected by freeze-thaw processes using a threshold of 5 cm per day. Thus, our accuracy goal for snow depth on sea ice is 5 cm. Under winter conditions, the accuracy may be better.

3.3.1 Validation Criteria and Method

The validation criterion is that the derived AMSR-E sea ice products agree on average with the corresponding validation data set to within the estimated accuracy of the validation data set. The validation data sets will be derived from any one or a combination of field, aircraft, submarine, and high-resolution visible and infrared satellite data and are expected to provide a more accurate measure of the standard sea ice products than the AMSR-E retrieved products. The underlying philosophy of this approach is that confidence in the sea ice products derived from the AMSR-E will be achieved by showing consistency of such products with independently derived data that are spatially and temporally coincident (Comiso and Sullivan, 1986; Cavalieri, 1991; Cavalieri et al., 1991; Steffen and Schweiger, 1991; Grenfell et al., 1994). The following is a summary of validation methods for each standard product.

Sea Ice Concentration: Sea ice concentration is defined as the areal percentage of sea ice observed within the field of view of the satellite sensor. The primary approach for the validation of retrieved AMSR-E ice concentrations is to utilized data from dedicated aircraft campaigns in conjunction with high resolution satellite data, including those from Landsat 7, Terra and Aqua MODIS, NOAA AVHRR, DMSP-OLS, and RADARSAT. The aircraft data will provide the means to assess the absolute accuracy of the retrieval at some places and seasons, while the use of satellite data provides for better spatial and temporal coverage. The focus of the aircraft campaigns will be on those seasons and regions that exhibit large retrieval errors based on past studies. High-resolution active microwave satellite systems, such as RADARSAT, are most useful during persistent cloud cover and during darkness. Data from microwave scatterometers, such as those from QuickSCAT, will be utilized for identifying areas of divergence and ice drift. However, data from active systems are more difficult to interpret than those from passive and visible systems, because of unpredictable backscatter from different ice types, from open water within the ice pack, and from wind-roughened seas.

The aircraft campaign will provide high resolution passive microwave and ancillary data that will be used to test how effectively the mixing algorithm performs for different sea ice regions. These data will also be used to evaluate sources of errors and how the errors vary from one ice regime to another. The strategy is to apply the algorithm on co-registered and coincident aircraft and spacecraft data and evaluate how the results match each other quantitatively and how they compare with similar analyses from high resolution visible and infrared data.

A complementary approach will make use of time series of images to check AMSR-E retrievals for temporal consistency. This effort will minimize errors associated with extreme environmental conditions and bad data records.

The validation program will also take into consideration the changes in physical and radiative characteristics of sea ice as a function of time and space. As the sea ice cover undergoes its annual cycle of growth and decay, changes in its radiative signature affect the accuracy of the retrieval. Thus, although the ice cover is most extensive in winter, there is also a strong need to obtain validation data during ice growth in fall, during onset of melt in spring, and meltponding period in the summer, to assess the known changes in the emissivity of the surface. The signature of the perennial sea ice cover also changes with season and possibly from one year to another.

One important aspect of the sea ice concentration validation that is not covered in this validation plan is the effect of weather on the sea ice concentration retrievals. This is particularly

important for those retrievals derived from the enhanced NASA Team algorithm which makes use of the AMSR-E 89 GHz channels. It would be highly desirable to have an aircraft outfitted with meteorological sensors to measure cloud liquid water and atmospheric water vapor between the satellite and surface over several AMSR-E footprints. This would be important especially in marginal ice zones where weather effects are largest.

Sea Ice Temperature: For first-year sea ice, the ice temperature derived from the vertically polarized 6.9 GHz channel represents the temperature of the sea ice surface at the snow/ice interface, because at this frequency the snow cover is transparent to the radiation. For multiyear ice, the derived sea ice temperature represents a weighted-average of the freeboard portion of the ice. During previous field campaigns snow measurements usually included temperature profiles down to the snow-ice interface. These data were taken during the Weddell Sea Cruises of 1982, 1983, and 1986, and the series of MIZEX experiments in the Arctic region. We have made use of these data to obtain empirical relationships between the ice temperature and snow surface temperature. The primary technique for the validation of AMSR-E ice temperature is to make use of this empirical relationship together with aircraft and satellite (i.e., MODIS and AVHRR) thermal infrared data. The aircraft data will be compared with ship measurements to assess errors associated with the use of empirical parameters. Further refinements of the empirical parameters will be made as more field data become available and through the use of a thermodynamic model of sea ice and snow.

The retrieved ice temperatures will be further validated using surface temperature data from buoys and other platforms. While these are only point measurements, arrays of buoys exist and they provide continuous measurements that can be used to check the temporal consistency of the derived AMSR-E temperature data. The temperature algorithm was developed through the use of 6.6 GHz data that were observed by the Nimbus-7 SMMR and historical buoy and field data. The SMMR data, however, have limited value for testing the effectiveness of the AMSR-E algorithm because of very large footprint and instrumental problems associated with polarization mixing.

Snow Depth on Sea Ice: Because snow depth observations over sea ice are so sparse and because surface measurements are so costly to acquire, the validation strategy is to develop an airborne sensor to measure snow depth on sea ice. It is extremely important that this airborne sensor be developed. It is the only way to adequately validate snow depths measured by AMSR-E. Once it is developed it will become part of our aircraft program. In addition, available snow depth measurements made from ships such as those compiled by Markus and Cavalieri (1998) will be used to help validate the AMSR-E snow depth retrievals. Qualitative checks will also be made through comparisons with SSM/I ice type maps and with AVHRR images.

3.3.2 Arctic Aircraft Validation Program

There are three planned aircraft experiments for the Arctic. The first is a pre-launch mission during June/July 2000 to address the issue of melt ponds. The second is a post-launch mission in March 2002 to address the problems associated with various ice types and surface conditions in seasonal sea ice zones. The third will focus on the validation of snow depth on sea ice.

3.3.2.1 Summer Arctic: June/July 2000

Rationale and Issues

Currently, the largest single source of error in the determination of Arctic sea ice concentrations with satellite passive microwave sensors is the presence of summer melt ponds.

This has been the case since the launch of the single-channel Nimbus 5 ESMR in 1972 (Crane et al., 1982; Carsey 1985), continued with the multichannel Nimbus 7 SMMR (Cavalieri et al., 1990), and today with the DMSP SSM/I sensors (Comiso and Kwok, 1996). Typically, in the central Arctic there is a gradual increase in radiometric brightness temperatures from the end of March until mid June following the seasonal march of surface air temperatures. In mid June there is a sudden increase in brightness as a result of the onset of melt. In July and August there is large variability in the brightness temperatures presumably reflecting variations in surface wetness, the formation of melt ponds, freezing and thawing of the surface, and other changes in surface characteristics. From mid August and September with the beginning of freeze up, the observed variability decreases and the brightness temperatures return to their winter signatures. We need to quantify retrieval errors resulting from surface melt and to develop techniques to reduce these errors.

Objectives and Strategy

The prime objective of this campaign is to estimate the errors incurred by the standard AMSR-E sea ice algorithms resulting from the presence of melt ponds. A secondary objective is to develop a microwave capability to discriminate between the presence of melt ponds and open water.

The SSM/I and AMSR-E sensors do not operate at sufficiently low frequencies to discriminate between melt-ponded areas and areas of true open water (sea water). Thus, our strategy will be to use radiometer systems that cover the AMSR-E frequencies and polarizations, and a cross-track scanning L-band (1.4 GHz) airborne radiometer. At L-band the potential exists for the discrimination between melt ponds and sea water. It is this capability that we want to exploit in this Arctic aircraft mission. This would enable us to map the distribution of melt ponds over an area sufficiently large to compare with our DMSP SSM/I retrieved sea ice concentrations using the AMSR-E algorithms. The data obtained from the aircraft and high-resolution satellite imagery will permit an association between the degree of surface melt (from a frozen surface to a melt-ponded surface) and the errors in the SSM/I sea ice concentration retrievals. As discussed below, the P-3 flights will be coordinated with surface measurements of melt ponds from a Canadian ice camp. A Navy Air Warfare Command P-3 aircraft will make 6 data flights with these radiometers over a two week period from about June 25 through July 7. The P-3 will also have video cameras with which to map the distribution of melt ponds and an IR scanner. Weather permitting, we will also make use of high-resolution visible sensors such as Landsat 7 ETM and Terra MODIS to aid in the characterization of the sea-ice surface overflown by the aircraft. RADARSAT coverage will be particularly useful under cloudy conditions.

Flight Program and Aircraft Instrumentation

Our planned flight program is make 6 flights from Thule, Greenland over Baffin Bay, the western Canadian Arctic Ocean, and in the vicinity of the Canadian ice camp. We will fly mosaic patterns over ponded as well as pond-free sea ice areas covering as many SSM/I footprints as possible. The specific areas to be overflown will depend on surface and weather conditions at the time of the mission, and on coordination with Canadian scientists at the ice camp near Resolute, Canada. Near real-time DMSP SSM/I and NOAA AVHRR imagery will guide the flight planning sessions before each flight.

The Navy P-3 will be equipped with the following suite of instruments:

- Polarimetric Scanning Microwave Radiometer

The primary tool for aircraft validation will be two NOAA/ETL Polarimetric Scanning Radiometer (PSR) systems, PSR-A and PSR-C. The PSR-A radiometers operate at 10, 19, 37, and 85 GHz and the PSR-C radiometer at 6.7 GHz. These sensors have radiometer accuracies of 2K or better and footprints of about 700 m at the cruising altitude of about 25,000 ft. However,

in the present format, the 6 GHz radiometer will share the same positioner as so cannot be used concurrently with the PSR-A radiometers.

- Scanning Low Frequency Microwave Radiometer

Another NOAA/ETL sensor that will be part of the Arctic program during the summer of 2000 is the scanning low-frequency microwave radiometer (SLFMR) that operates at 1.4 GHz. This instrument will be used primarily to test the capability of estimating the fraction of melt ponded areas during the summer from salinity differences between melt ponds and sea water.

- Scanning Infrared Radiometers

The PSR IR sensors are 9.6-11 um, with 50 msec integration time, unpolarized, and co-boresited with the scanning PSR antennas. There is one each within each PSR scanhead. Thus, conical scanned IR imagery is produced along with the microwave imagery. The absolute accuracy is believed to be within 1 degree C, and the brightness resolution is ~0.2 degrees C.

- Aerial Cameras

Video and digital camera coverage will be acquired during the aircraft flights. These data will be invaluable in determining actual open water areas within the footprint of the radiometers and can be used to identify melt ponds and other surface characteristics. Such data will be coincident in time and space with the other measurements and will be useful for improving interpretation of other validation tools such as Landsat, SAR, and MODIS.

The following describes anticipated flight scenarios. Some adjustments may be necessary during the campaign (e.g., different flight days and different location sites), due to unpredictable weather conditions. It is anticipated that altogether, the campaign will take about two weeks and will start on or about June 25, 2000.

Transit flight: From the Patuxent Naval Air Test Center, Maryland to Thule, Greenland

Flight Sites

A typical site would be located west of the Canadian Archipelago at about 80^{o}N 110^{o}W. The reason for this general location is that this is an area of multiyear ice and melt ponds over multiyear ice are composed of fresh or at least very low salinity water. It is the contrast between low-salinity melt pond water and saline sea water we wish to discriminate. Actual sites will be determined the day before a flight based on surface and weather conditions. We will be using near realtime DMSP SSM/I imagery and imagery from weather satellites to determine the flight plan for a given day. A typical flight plan would consist of a transit flight from Thule to a predetermined location (e.g., 80^{o}N 110^{o}W), followed by 4 or 6 (depending on length) parallel flight lines at either high or low altitude, and then a flight returning to Thule. We are currently planning a combination of 6 high and low altitude flights over a two week period.

6/25 transit from Pax River to Thule (8 hours)
6/26 data flight preparation at Thule
6/27 data flight with PSR/A & SLFMR (8 hours)
6/28 data flight with PSR/C & SLFMR ((8 hours)
6/29 rest day/data analysis
6/30 data flight with PSR-A & SLFMR ((8hours)
7/1 rest day/data analysis
7/2 rest day/data analysis
7/3 data flight with PSR/C & SLFMR ((8 hours)
7/4 data flight with PSR/A & SLFMR ((8 hours)
7/5 rest day/data analysis

7/6 data flight with PSR/C & SLFMR ((8 hours)
7/7 transit from Thule to Pax River (8 hours)

Coordination with other Programs

There will be coordination with a Canadian ice camp operated as part of the Collaborative-Interdisciplinary Cryospheric Experiment (C-ICE) under the direction of Dr. David Barber of the University of Manitoba, Canada. The camp is located near Resolute, Canada approximately 400 Nautical Miles from Thule. Dr. Barber and his team will be making physical, chemical, radiometric, and morphological measurements of melt ponds (Barber and Yackel, 2000). These surface measurements will be coordinated with our P-3 overflights. Plans have been made to enable communication between the camp site and flight planning operations in Thule to ensure greatest possible coordination.

3.3.2.2 Winter Arctic: February-March 2002

Rationale and Issues

The largest errors in winter Arctic sea ice concentration retrievals occur in the seasonal sea ice zones (SSIZs). These very dynamic regions consist of various unresolved ice types and sea ice surface conditions. A comparison of the NASA Team and Bootstrap algorithms also shows that these regions are where the algorithm Arctic retrievals differ the most (Comiso et al., 1997). Thus, the rationale for making a series of aircraft flights over SSIZs is based on the need to quantify the errors incurred in the retrieval of sea ice concentration from the standard AMSR-E algorithms and to acquire the observations needed to make future improvements in the algorithms.

Objectives and Strategy

The prime objective of this mission is to underfly the EOS Aqua AMSR-E and validate the standard sea ice concentration algorithms under wintertime conditions. The Bering, Beaufort and Chukchi seas provide very different sea ice conditions. The Bering Sea is highly divergent and provides an opportunity to test the algorithms in areas of thin ice. The St. Lawrence Island polynya is particularly active in March and is an ideal site for testing the algorithms. A transect from the Chukchi Sea where sea ice temperatures are relatively warm to north of the Canadian Archipeligo in the Beaufort Sea where sea ice temperatures are their coldest will provide an opportunity to test the sensitivity of the algorithms to changing sea ice temperatures. The Chukchi and Beaufort seas are also areas where there are mixtures of first-year and multiyear ice types which have very different microwave signatures, thus providing additional sites for testing the algorithms.

Flight Program and Aircraft Instrumentation

Our tentative flight program is to fly 6 flights with the NASA DC-8 from Fairbanks, AK over the Bering, Beaufort and Chukchi seas. The plan is to fly mosaic patterns over these areas while covering as many AMSR-E footprints as possible. The specific areas to be overflown will depend on surface conditions and weather at the time of the mission. Near real-time AMSR-E or DMSP SSM/I imagery will guide the flight planning sessions before each flight. The suite of aircraft instruments will be the same as for the summer 2000 campaign with the exception of not having the SLFMR.

The following describes anticipated flight scenarios. Some adjustments may be necessary just prior or during the compaign (e.g., different flight days and different location sites),

resulting from unpredictable sea ice and weather conditions. It is anticipated that the compaign will take about two weeks and will start in late February or early March 2002.

Transit flight:
From: Dryden Flight Facility, CA 34.9 °N, 117.9oW
To: Fairbanks, AK 64.8 °N, 147.9oW

Flight Sites

Beaufort Sea Site #1: Mosaic pattern centered at 79°N, 126°W
Beaufort Sea Site #2: Mosaic pattern centered at 75°N, 150°W
Bering Sea Site #1: Mosaic pattern centered at 64°N, 170°W
Bering Sea Site #2: Mosaic pattern centered at 61°N, 172°W
Chukchi Sea Site #1: Mosaic pattern centered at 70°N, 170°W
Chukchi Sea Site #2: Mosaic pattern centered at 71°N, 160°W

Day 1: Transit Dryden Flight Facility, CA to Fairbanks, AK 2138 Nautical Miles---5.0 Hours
Day 2: Flight preparation
Day 3: Data Flight to Beaufort Sea Site #1----------8.0 Hours
Day 4: Rest Day/preliminary analysis of Day 3 data
Day 5: Data Flight to Beaufort Sea Site #2----------8.0 Hours
Day 6: Rest Day/preliminary analysis of Day 5 data
Day 7: Data Flight to Bering Sea Site #1----------8.0 Hours
Day 8: Rest Day/Preliminary analysis of Day 6 data
Day 9: Data Flight to Bering Sea Site #2----------8.0 Hours
Day 10: Rest Day/Preliminary Analysis of Day 8 data
Day 11:Data Flight to Chukchi Sea Site #1----------8.0 Hours
Day 12:Rest Day/Preliminary Analysis of Day 10 data
Day 13:Data Flight to Chukchi Sea Site #1----------8.0 Hours
Day 14:Rest Day/Preliminary Analysis of Day 10 data
Day 15: Transit Fairbanks, AK to Dryden Flight Facility, CA 2138 Nautical Miles---5.0 Hours
Total: 58 Hours

Coordination with other Programs

During the February and March 2002 time frame, we will coordinate and share the use of the NASA DC-8 aircraft with both the AMSR-E Team snow and precipitation validation activities. The sea ice, snow, and precipitation efforts will utilize the same complement of passive microwave sensors including the PSR-A and PSR-C radiometers. The aircraft will make flights out of Seattle, WA for precipitation, whereas for the sea ice and snow, the flights will be made out of Fairbanks, AK.

3.3.2.3 Winter Arctic: March 2003

Rationale and Issues

The issue is how best to validate snow depth on sea ice, a sea-ice parameter that is highly variable both in space and time. Traditional methods of measuring snow depth on sea ice by ship depend on visual observations of snow thickness on ice floes forced on their side as the ship breaks through the sea ice pack. This method does not provide the requisite spatial and temporal coincidence needed, and is highly dependent on observer skill. Thus, a method is needed to objectively measure snow depth over areas as large as AMSR-E footprints and coincident in time with AMSR-E observations. The only way to do this is to develop a capability to remotely sense snow depth with an airborne sensor capable of providing the required spatial and temporal coverage. Thus, it is critical that this capability be developed. There is no other

way to adequately validate snow depth on sea ice. The accuracy of the airborne sensor would have to be better than 5 cm, the accuracy goal of the AMSR-E snow depth algorithm.

Objectives and Strategy

The objectives and strategy presume the development of an airborne sensor to map snow depth on sea ice. The main objective then will be to validate areas with very different snow depths in seasonal sea ice zones. The Bering Sea is a particularly good target, because of a persistent polynya south of St. Lawrence Island providing a gradient of snow depths from 0 cm on new ice to 10-15 cm on first-year ice downwind of the polynya. North of the island is an area of ridged ice generally containing much deeper snow.

Flight Program and Aircraft Instrumentation

We want to fly 5 flights from Fairbanks, AK over the Bering, Beaufort and Chukchi seas. The plan is to fly mosaic patterns over these areas while covering as many AMSR-E footprints as possible. The specific areas to be overflown will depend on surface conditions and weather at the time of the mission. Near real-time EOS Aqua AMSR-E imagery will guide the flight planning sessions before each flight.

The aircraft instrumentation includes not only the snow-depth sensor to be developed, but also the complement of PSR radiometers and the IR scanners as planned for the two previous Arctic missions.

The following describes anticipated flight scenarios. Some adjustments may be necessary just prior or during the campaign (e.g., different flight days and different location sites), resulting from unpredictable sea ice and weather conditions. It is anticipated that altogether, the campaign will take about two weeks and will start in early March 2003.

Transit flight:
From: Wallops Flight Facility, VA 37^{o}N, 118^{o}W
To: Fairbanks, AK 65^{o}N, 148^{o}W

Flight Sites

Beaufort Sea Site #1: Mosaic pattern centered at 79^{o}N, 126^{o}W
Bering Sea Site #1: Mosaic pattern centered at 64^{o}N, 170^{o}W
Bering Sea Site #2: Mosaic pattern centered at 61^{o}N, 172^{o}W
Chukchi Sea Site #1: Mosaic pattern centered at 70^{o}N, 170^{o}W
Chukchi Sea Site #2: Mosaic pattern centered at 71^{o}N, 160^{o}W

Day 1: Transit Wallops Flight Facility, VA to Fairbanks, AK 2027 Nautical Miles---6.5 Hours
Day 2: Flight preparation
Day 3: Data Flight to Bering Sea Site #1----------8.0 Hours
Day 4: Rest Day/preliminary analysis of Day 3 data
Day 5: Data Flight to Bering Sea Site #2----------8.0 Hours
Day 6: Rest Day/preliminary analysis of Day 5 data
Day 7: Data Flight to Chukchi Sea Site #1----------8.0 Hours
Day 8: Rest Day/Preliminary analysis of Day 6 data
Day 9: Data Flight to Chukchi Sea Site #2----------8.0 Hours
Day 10: Rest Day/Preliminary Analysis of Day 8 data
Day 11: Data Flight to Beaufort Sea Site #1……8.0 Hours
Day 12:Rest Day/Preliminary Analysis of Day 11 data
Day 13: Transit Fairbanks, AK to Dryden Flight Facility, CA
2138 Nautical Miles---6.5 Hours
Total: 53 Hours

3.3.3 Antarctic Aircraft Validation Program

The Antarctic sea ice cover is different from that of the Arctic in that there are no outer land boundaries that limit the growth and advance of sea ice. In winter, the ice cover expands until atmospheric and oceanic forces limit its northward advance, while in the spring and summer, the ice retreats rapidly because of its vulnerability to wave action and oceanic heat. As a result, the Antarctic sea ice cover exhibits a much greater seasonal variability than the Arctic sea ice cover. It is thus not surprising that the signature of sea ice in the Antarctic is quite different from that of the Arctic (Gloersen et al., 1992). But although the ice cover is mainly that of seasonal ice, the microwave emissivity of the surface has been observed to be spatially very variable (Comiso et al., 1989; Comiso et al., 1992; Grenfell et al., 1994). Such variations in emissivity should be studied in detail since it is important to know how they affect the performance of the sea ice algorithms. Since the advent of microwave remote sensing, there have been numerous remote sensing aircraft overflights over sea ice in the Arctic. However, we don't know of any passive microwave sea ice flight program that has been implemented over the Antarctic. This flight experiment is aimed at providing the much needed aircraft remote sensing data set in the region. The aircraft data is needed for validation because they provide intermediate resolution and spatial coverage that enables accurate interpretation of AMSR-E data. The strategy is to obtain such passive microwave data in conjunction with simultaneous visible, infrared, and ship data to assess the real physical characteristics of the ice cover. The data set is in turn used to quantify the effectiveness of the mixing algorithms that are used to estimate ice concentrations and other data products.

3.3.3.1 Antarctic Winter Experiment (August 2001)

Rationale and Issues

The winter sea ice in the Antarctic covers an area of about 20 million square kilometers which is more extensive than that of the Arctic. An Antarctic validation program is needed to ensure that the retrieved sea ice products from such a big region are accurate. Also, because of apparently changing climate in many parts of the region, the sea ice cover needs to be quantified as accurately as possible. The main issue is that sea ice algorithms that have been developed for SSMI and SMMR data have been shown to provide results that differ from each other by as large as 35% in large areas of the Antarctic (Comiso et al., 1997). Such discrepancies need to be resolved and the reasons for such discrepancies need to be evaluated before the data can be used for heat fluxes, climate, and other scientific studies.

Objectives and Strategy

There are three major objectives of the validation program. The first is to provide the means to assess quantitatively the performance of the AMSR-E sea ice algorithms in the Antarctic region. In particular, the accuracy of the standard sea ice products (sea ice concentration, ice temperature, and depth of the snow cover) derived from AMSR-E, will be estimated through comparative analysis with those derived from the validation data set. The second objective is to determine the optimum values to be used by the algorithm as reference brightness temperatures for 100% ice cover and open water. This will help optimize the performance of the AMSR-E ice algorithms. Finally, the spatial variability of the emissivity and temperature of sea ice will be evaluated to assess how such variability affects the accuracy of the algorithm products. With aircraft data, this is made possible by the utilization of intermediate resolution radiometer data that enables identification of the different types of surfaces within each footprint of the satellite. Other channels of AMSR-E not present in currently available satellite

data will be utilized to minimize the error due to the existence of different surface types and improve the performance of the algorithm.

In essence, the long term objective is to obtain as accurate characterization of the sea ice cover as possible. High accuracy is needed to be able to quantify the small percentage of open water that can have a very strong effect on heat fluxes between the ocean and the atmosphere. Such accuracy is also required to gain insight into the changing climate conditions in the polar regions.

Flight Program and Aircraft Instrumentation

The strategy is to perform flight experiments after the launch of EOS/PM in December 2000 so aircraft data can be compared directly to spacecraft data. The first of two missions will be a winter program (set for August 2001) over selected sites in the Weddell Sea and Bellingshausen/ Amundsen/Ross Seas. The approximate location of the sites for the winter program are given below and are regions where significant discrepancies have been observed, as described by Comiso et al. (1997) and by Markus and Cavalieri (2000). The flight program will enable a high-resolution characterization of the ice cover, provide accurate estimates of the sea ice parameters, and help establish causes of the discrepancies in these regions. The flights along the coastal areas are expected to validate quantitatively the extent of open water and thin ice in this region. The uncertainties in this region are usually affected by the contamination of the sea ice data by data from the continent and unusually cold temperatures in the region. It is very important that retrievals in these regions are validated since these areas are regarded as ice factories and key sources of global bottom water. During each flight, the exact location of the ice edges will also be quantified to assess how accurately the AMSR-E algorithm identify the 15% ice edge. The exact location of the ice edge is key to the calculation of the ice extent, which is an important climate parameter.

It is anticipated that the campaign will take about three weeks (from USA and back) and will start in early August. The days of flight may have to be adjusted, as necessary, because of unpredictable weather conditions. Times of flight will also be coordinated such that the chances of having coincident EOS AQUA AMSR-E overpass data are optimized. Mosaic patterns will be made within the pack to cover as many AMSR-E footprints as possible. The patterns are based on the following range of the P3:

Approximate range for P-3: 330 knots*10 = 3300 Nautical Miles = 5,940 km
Approximate range required for the Weddell overflights = 5,900 km
Approximate range required for the Bellingshausen/Amundsen Sea overflights = 5,900 km

The aircraft campaign is successful only if equipped with the right set of sensors and instrumentation. The following are the instruments that will be installed in the P-3 for the Antarctic mission and the rationale for using them:

- Scanning Microwave Radiometer

The primary tool for validation will be the Polarimetric Scanning Radiometer (PSR) which will be used to obtain brightness temperatures at AMSR-E frequencies but at a much higher resolution. During the Antarctic mission, two positioners will be used to obtain simultaneous passive microwave coverage at all AMSR-E frequencies except the 23 GHz channels. These sensors are imaging radiometers with accuracies of 2K or better and footprints of about 700 m at the usual P-3 flying altitude of about 6,000 m. Occasionally, the operating altitude will be about 1000 m for a footprint size of about 115 m which is good enough to image leads and pancakes. One positioner will also have a scanning 11.5 μm infrared radiometer to obtain high-resolution surface temperature data for comparison with ice temperature retrievals. High-resolution passive microwave radiometer data are useful for validation since they provide the means to assess the spatial variability in the emissivity of sea ice in the consolidated ice regions. They also are needed to identify important information that may be lost in the low-resolution satellite system.

- Window Microwave Radiometer

Non-scanning microwave radiometers will be installed at some aircraft windows to provide a means to obtain radiometer data independently of the PSR. These radiometers have higher performance rating than the scanning radiometers and can be used to validate the calibration of the PSR as well as provide supplementary data that can be used to better interpret the PSR data. Current plans involve the installation of dual polarized radiometers at 6, 18, and 37 GHz which are the basic channels used in the algorithms.

- Ranging Lidar

A scanning ranging laser instrument called the Airborne Topographic Mapper (ATM) has been developed for the Greenland ice sheet project. The predecessor of this Lidar has been used in the Arctic on board a P3 while overflying a nuclear submarine equipped with an upward looking sonar that measures the thickness of the ice. The results from the study show that the thickness distribution of sea ice inferred from the submarine sonar data can be reproduced from the freeboard thickness distribution of the ice as observed by the Lidar (Comiso et al., 1991). Among the key issues in validation studies is how the emissivity of Antarctic ice changes with ice type and thickness. In addition to thickness determination, the Lidar can also be used for obtaining ice type, rafting and ridging statistics. The Lidar will thus serve as a good validation tool and with its imaging capability, the data can be co-registered with PSR data for detailed comparison to evaluate the effects of thickness, ice type, surface roughness, and ridging on the ice parameter retrievals.

- Digital Camera

The digital camera provides the best resolution data that can be acquired from the aircraft mission. The data will be invaluable in determining actual open water areas within the footprint of the radiometers and can be used to identify new ice and evaluate effects of significant ridging, rafting, and flooding. Such data will be coincident in time and space with the other measurements and will be useful for improving interpretation of other validation tools such as Landsat, SAR, and MODIS. A zoom lens will be used for this purpose to enable flexibility in spatial coverage and resolution.

- Multifrequency Radar (if available)

Snow Radar thickness remains one of the most difficult to quantify on a large scale. The most dependable thickness measurements are from ships on the ground but data sampling is a problem because the snow cover in the ship's vicinity do not necessarily represent average snow thickness within the footprint of the satellite. When the ship tracts are primarily in newly frozen lead areas, which are the most likely path for multi-disciplinary cruises that requires the shortest possible time to get to the next destination, such data may not even be useful for validation. To complement sparsely available ship measurements, an aircraft sensor that measures snow depth will be highly valuable. A multifrequency radar designed to measure snow thickness is under development and will be used for this mission if it becomes operational before flight time.

The following describes anticipated flight scenarios. Some adjustments may be necessary during the campaign (e.g., different flight days and different location sites), due to unpredictable weather conditions. It is anticipated that altogether, the campaign will take about three weeks (from the USA and back) and will start in early August 2001. Staging and refueling sites:

Wallops , VA	37^{o}N, 118^{o}W
San Jose, Costa Rica	9.98^{o}N, 84.07^{o}W
Punta Arenas, Chile	53.15^{o}N, 70.92^{o}W

Flight Sites

Bel/Amundsen Sea, Site #1: Mosaic pattern centered at 70°S,80°W
Bel/Amundsen Sea, Site #2: Mosaic pattern centered at 70°S, 90°W
Bel/Amundsen Coastal Polynyas Areas, Site #3, starting at the western Antarctic Peninsula
Weddell Sea Site #4:Mosaic pattern centered at 65°S,35°W
Weddell Sea Site #5: Mosaic pattern centered at 68°S,50°W
Weddell Coastal Polynya Areas, Site #6: starting at the eastern Antarctic Peninsula

Day 1 and 2: Outbound Transit

Wallops to San Jose, Costa Rica 2629 Nautical Miles----------5.8 hours
San Jose to Punta Arenas, Chile 3847 Nautical Miles ----------8.5 hours
Chalk Time----------1.0 hour
Total ----------15.3 hours
Day 3: Rest/Flight preparation
Day 4: Data Flight to Bellingshausen/Amundsen Seas, Site #1 ----------10.0 Hours
Day 5: Rest Day/preliminary analysis of Day 4 data.
Day 6: Data Flight to Bellingshausen/Amundsen Seas, Site # 2----------10.0 Hours
Day 7: Rest Day/Preliminary analysis of Day 6 data.
Day 8: Data Flight to the Bel/Amundsen Seas coastal areas, Site #3---------10.0 Hours
Day 9: Rest Day/Preliminary Analysis of Day 8 data.
Day 10: Data Flight to the Weddell Sea, Site #4----------10.0 Hours
Day 11: Rest Day/Preliminary Analysis of Day 10 data.
Day 12: Data Flight to the Weddell Sea, Site #5----------10.0 Hours
Day 13: Rest Day/Preliminary Analysis of Day 12 data
Day 14: Data Flight to the Weddell Coastal Polynyas, Site #6---------- 10.0 Hours
Day 15: Rest Day/Preliminary Analysis of Day 14 data
Days 16&17: Homebound transit----------15.3 Hours
Total: ---------- 90.6 hours

Approximate Range for P-3: 330 knots*10 = 3300 Nautical Miles = 5,940 km
Approximate range required for the Weddell overflights = 5,900 km
Approximate range required for the Bellingshausen/Amundsen Sea overflights = 5,900 km

Coordination with other Programs

Fortuitously, the Antarctic winter aircraft project will occur at the same time that a big Antarctic field program called, the GLOBEC (Global Ocean Ecosystem Dynamics) project, will be in progress. The funding for the latter program has recently been approved by the National Science Foundation and is scheduled to go on almost continuously for two years. It will also have an international component with participations expected from the United Kingdom, Germany, Korea, Argentina, and Japan. The focus of the program is the Bellingshausen Sea region and deep into the ice during winter. This will provides an ideal opportunity to obtain physical and radiative characterization of the ice cover for all seasons in the region. Data from the aircraft mission will be supplemented by data from high-resolution satellites during the program. Special arrangements have been made to coordinate the aircraft flight program with scientists who will be doing the cruises during the period. The key contacts are Dr. Eileen Hofmann, who is the chief scientist and Drs. Ray Smith, Doug Martinson, and Don Perovich who are funded to do the sea ice component of the project.

Two ships (the R.V. Nathaniel Palmer and R.V. Gould) are scheduled to be in the study region from July 17 through August 25, 2001. This schedule is very compatible with the aforementioned aircraft schedule. Ship based in situ measurements that will be made during the cruises will include: temperature profile from the surface of the snow through the ice, thickness of the snow and ice cover, layering in both snow and ice cover, wetness of snow, snow-ice

component of the ice, and flooding frequency and statistics. Dr. Koni Steffen is also planning to participate as part of the aircraft program and will bring microwave radiometers with him for high resolution measurements and improved determination of sea ice emissivities. The latter will be useful for establishing the accuracy of the emissivities derived from aircraft measurements.

3.3.3.2 Antarctic Spring Experiment

Rationale and Issues

A second Antarctic aircraft program is planned for the spring of 2002. This program is required to enable accurate assessment of the accuracy of inferred sea ice parameters during the transition period from the cold and dry surfaces during winter and early spring, to the warm and wet surfaces during the late spring and summer. The transition from dry to wet surface causes large changes in the emissivity of sea ice that may affect the accuracy of the retrieval. Good accuracy of the ice parameters during spring and summer is important since the sensitivity in the response of the ice cover to changes in surface temperature is highest during this period. Thus, in a global change scenario, accurate quantification of ice parameters during this time period is critical.

Objectives and Strategy

As with the winter program, a key objective for the spring program is to provide the means to assess quantitatively the performance of the AMSR-E sea ice algorithm in the Antarctic region. This project will ensure that the algorithm has been tested as truly seasonal algorithm. A second objective is to determine quantitatively the magnitude of the change in the emissivity of sea ice from winter to spring and make sure that this is accounted for by the algorithm. The results will thus provide the reference values needed to optimize the accuracy of the retrievals. Finally, the spatial variability of the emissivity and temperature of sea ice during spring will be evaluated to assess the overall impact of such variability on the accuracy of the algorithm products. With the utilization of intermediate resolution aircraft radiometer data, regional and seasonal emissivities will be quantified. Other channels of AMSR-E not present in currently available satellite data will be utilized to assess how they can be used to minimize the error due to the existence of regional differences and different surface types and thereby improve the performance of the algorithm.

The strategy is to perform the spring aircraft experiment as soon as feasible after the launch of EOS/PM and the completion of the winter aircraft experiment. The plan is to conduct the spring program from mid October 2002 to mid November 2002. The experiment will be conducted in the Ross Sea and Western Pacific Ocean regions to complement the data from the Weddell and Bellingshausen Seas and be able to assess how the emissivity varies from one region of the Antarctic to another. The flights along the coastal areas are expected to validate quantitatively the extent of open water and thin ice in this region. The uncertainties in this region is usually affected by the contamination of the sea ice data by data from the continent and unusually cold temperatures in the region. It is very important that retrievals in these regions are validated since these areas are regarded as ice factories and key sources of global bottom water. Also, during ice retreat, it is important to know the timing when the coastal regions are free of sea ice. During each flights, the exact location of the ice edges will also be quantified to assess how accurately the AMSR-E algorithm identify the 15% ice edge. The exact location of the ice edge is key to the calculation of the ice extent, which is an important climate parameter.

Flight Program and Aircraft Instrumentation

It is anticipated that the campaign will take about three weeks (from USA and back) and will start in mid October 2002. The specific days of flight will depend, as in the winter case, on weather conditions, which at times are generally unpredictable. Times of flight will also be

coordinated such that the chance of coincident EOS AQUA AMSR-E overpass is optimized. The patterns are again based on the range of the P3 as indicated in the section for the winter mission. The instruments aboard the P3 during the spring validation period will be basically the same as those used for the Antarctic winter project. New window-microwave radiometers are being developed and may be used during this mission if available.

The following describes anticipated flight scenarios. Some adjustments may be necessary during the campaign (e.g., different flight days and different location sites), due to unpredictable weather conditions. It is anticipated that altogether, the campaign will take about three weeks (from USA and back) and will start in mid October 2002. It should be mentioned that the P3 has not done a scientific mission from McMurdo before because of the requirement of an alternate airport for landing. Such requirement is now fulfilled. However, in case of unforeseen problems, a backup location would be Punta Arenas in Chile with flight paths similar to the winter mission. The GLOBEC program will still be going on at this time.

Staging and Refueling Sites:

Wallops , VA	37 ^{o}N, 118 ^{o}W
Honolulu, Hawaii	21 ^{o}N, 158 ^{o}W
Christ Church, New Zealand	43 ^{o}S, 172.5 ^{o}E
McMurdo, Antarctica,	78 ^{o}S, 167 ^{o}E

Flight Sites

Ross Sea Site #1:Mosaic pattern centered at 73°S, 180°W
Ross Sea Site #2: Mosaic pattern centered at 75 °S, 170 °W
Coastal Regions Site #3: Coastal regions along the edge of the Ross Sea ice shelf.
West Pacific Ocean Site #4: Mosaic pattern centered at 68 ^{o}S, 165 ^{o}E
West Pacific Ocean Site #5 Mosaic pattern centered at 65 ^{o}S, 150 ^{o}E
Coastal Regions Site #6 Along the Victoria Land coastline up to Cape Adams

Day 1 and 2: Outbound Transit

Wallops to Honolulu, Hawaii via LA, 4,350 Nautical Miles---------- 13 hours
Honolulu to Christ Church, New Zealand via Amer. Samoa, 3,960 Nautical Miles --12 hours
Christ Church to McMurdo, 3814 km, 2,119 Nautical Miles---------- 6.5 hours
Chalk Time----------3.0 hours
Total ---------- 34.5 hours
Day 3: Rest/Flight preparation
Day 4: Data Flight to the Ross Sea Site #1 ----------10.0 Hours
Day 5: Rest Day/preliminary analysis of Day 4 data.
Day 6: Data Flight to Ross Sea Site # 2----------10.0 Hours
Day 7: Rest Day/Preliminary analysis of Day 6 data.
Day 8: Data Flight to the Ross Sea Ice Shelf coastal region, Site #3-10.0 Hours
Day 9: Rest Day/Preliminary Analysis of Day 8 data.
Day 10: Data Flight to the West Pacific Ocean, Site #4 -10.0 Hours
Day 11: Rest Day/Preliminary Analysis of Day 10 data.
Day 12: Data Flight to the West Pacific Ocean, Site #5 -10.0 Hours
Day 13: Rest Day/Preliminary Analysis of Day 12 data
Day 14: Data Flight to the coastal region of the Victoria Land, Site #6 –10.0 Hours
Day 15: Rest Day/Preliminary Analysis of Day 14 data
Days 16&17: Homebound transit----------34.5 Hours
Total: ----------129 Hours
Approximate Range for P-3: 330 knots*10 = 3300 Nautical Miles = 5,940 km
Approximate range required for the Ross Sea underflights = 5,900 km
Approximate range required for the West Pacific Ocean underflights = 5,900 km
Approximate range required for the coastal underflights = 5,900 km

Coordination with other Programs

The timing of the spring underflight program will again take advantage of planned surface field programs in the region during the October to November time period. Two programs are planned in the region during the period: (1) the Antarctic Shelf Slope Project (ANSLOPE), involving the R.V. Nathaniel Palmer in the Ross Sea Area and (2) the CRC Remote Sensing Project, involving the R.V. Aurora Burealis in the West Pacific Area. ANSLOPE is led by Prof. Arnold Gordon and Stan Jacob of Lamont-Doherty Earth Observatory of Columbia University, while the CRC project is headed by Drs. Robert Massom and Ian Allison of the University of Tasmania at Hobart, Australia. The scientists have expressed interest in the NASA aircraft validation program and their desire to do the surface measurements required for the validation of the sea ice parameters. The field measurements will be similar to those of the winter measurements with more emphasis on quantifying the wetness parameter for the snow cover.

3.3.4 Satellite Validation Data Sets

The relatively large footprint of the AMSR-E sensor makes the sea ice products particularly difficult to validate. The validation program for sea ice will therefore rely heavily on the analysis of coincident ice data sets from aircraft and satellite. The AMSR-E validation data set will include both historical data as well as new data that will be acquired during the AMSR-E validation period.

Satellite data sets will include data derived using visible and infrared radiometers, radars, scatterometers and altimeters. Other data sets planned to be used include data sets previously acquired for validation of sea ice parameters derived from the DMSP SSM/I and Nimbus-7 SMMR (Comiso et al., 1991; Cavalieri, 1992; Grenfell et al., 1994). Some of these historical data sets have already been used in a recent sea ice algorithm comparison (Comiso et al., 1997). The primary sources of satellite validation data for AMSR-E ice products include the following:

(a) High-Resolution Visible (Landsat-7, OLS, GLI, AVHRR, MODIS)
(b) High-Resolution Infrared (AVHRR, ATSR, GLI, MODIS, etc.)
(c) High-Resolution SAR (ERS-1, 2, JERS-1, RADARSAT)
(d) Scatterometer/Altimeter Data (QuickSCAT, TOPEX)

High-resolution SAR, scatterometer, and altimeter data are particularly useful in areas of persistent cloudiness and darkness.

Those satellite data, which are approximately coincident in time and space for all seasons and for both the northern and southern hemispheres will be compiled for comparative analyses.

3.3.5 Buoy and Other In Situ Data

Arctic and Antarctic Ocean buoy networks will be used for the validation of sea ice drift retrievals and for checking derived ice temperatures. Weather station and ice station data will also be used for checking ice temperature and snow depth retrievals. We plan to make use as well of historical ground measurements, like those from AIJEX (1975-76), MIZEX (1986-1989), SHEBA (1997-1998), Winter Weddell (1986-1992), and Weddell Flux (1994-1995) experiments to better understand how observed brightness temperatures are affected by different ice surface characteristics and conditions. Data from future field experiments, such as those from the Southern Ocean GLOBEC (2001) and the Lincoln Sea Project (2001) in the Arctic will be utilized in a similar manner and will be especially valuable because they are scheduled to be collected after the expected launch of AMSR-E.

3.3.6 Model Output Data

While model output data cannot be classified as a validation data set, these data are sometimes needed in the interpretation of aircraft, field, and satellite data sets. They are especially useful for evaluating changes during studies of temporal changes in the microwave signatures. The ECMWF and NCEP re-analyses are examples of such data sets.

3.3.7 Validation Schedule

Task / Year	2 0 0 4				2 0 0 4				2 0 0 4				2 0 0 4			
	2 1	0 2	0 3	0 4	2 1	0 2	0 3	1 4	2 1	0 2	0 3	2 4	2 1	0 2	0 3	3 4
Pre-launch Activities																
FIRE III ER2 data analysis				>>>												
Satellite intercomparison								>>>								
Summer Arctic Aircraft Mission			X													
Aircraft Data Analysis								>>>								
Aqua Launch				X												
Post Launch Activities																
Satellite intercomparison																>>>
Winter Antarctic aircraft mission							X									
Aircraft data analysis													>>>			
Winter Arctic aircraft mission									X							
Aircraft data analysis																>>>
Spring Antarctic aircraft mission												X				
Aircraft data analysis																>>>
Snow depth Arctic aircraft mission													X			
Aircraft data analysis																>>>

3.4 Snow (submitted by A. Chang, with contributions from R. Armstrong)

3.4.1 Validation Criterion and Method

The quality of the retrieved snow water equivalent (SWE) values can be confirmed by thorough comparisons of satellite estimates with independent measurements of the SWE with a known accuracy. This is a challenging effort, because there are very limited areal SWE measurements available for validation. There is no single global SWE data set available for comparison with satellite derived SWE estimates. We will have to rely on the snow depth information collected by various meteorological stations and SWE obtained from individual snow courses.

Given the large passive microwave footprint, snow storage within a footprint is seldom uniformly distributed. Therefore, large differences between gauge (point) measurements and satellite estimates (areal) can be expected. In addition, for certain applications, snow measurements or surveys are typically located at sites where significant snow accumulation is expected. Therefore, the in-situ data may be biased towards larger snow amounts than the satellite-derived values that represent the integration across an entire footprint where the snow cover may in fact not be continuous.

Because they were readily available, surface station point measurements were first used as a validation data source. However, after comparing the point measurements with satellite derived areal snow estimates for the last several years, it was found that this approach is far from ideal. It is necessary to re-design a workable strategy on how are we going to carry out the validation of snow water equivalent values.

The number of samples required to accurately representing the SWE value of a large field depend on the spatial variability of SWE within the large field and accuracy requirements. To be 95% confident that the true mean is within plus and minus L of the estimated mean, the number of sample n required is (Snedecor and Cochran, 1967)

$$n = (1.96\,\sigma/L)^2 \sim 4(\sigma/L)^2$$

For σ = 20 mm and L = 10 mm, n = 16. In other words, we need 16 measurements within a footprint with SWE variations of 20 mm accurate to +/- 10 mm. With four measurements the accuracy is +/- 20 mm. If there is only one measurement within the footprint, the expected accuracy is +/- 40 mm (twice the variations within the footprint). If the accuracy requirement of the estimated SWE is 20% (NASA, 1982) 100 measurements are needed.

We extended the comparisons with point measurements to a 2x2 EASE grid (50 x 50 km^2 grid) over the Northern Great Plains. With 2 to 3 measurements per grid box the r^2 for snow depth and brightness temperature is around 0.6. Further extended to a larger area in North Dakota (5x5 EASE grid) where there were 14 measurements within the grid box, we were able to obtain a better temporal and spatial dependence of snow depth and brightness temperature relationships.

During February 1994, in connection with the BOREAS project, microwave radiometers (18, 37 and 92 GHz) were flown on the Twin Otter aircraft over the Canadian boreal forest region. Simultaneous field measurements were acquired. A detail examination of these data found that it is possible to match the SWE derived from aircraft measurement and from satellite measurements in the forested area. Airborne microwave observation, thus, may be used to validate the satellite SWE estimates. However, it is necessary to account for the forest coverage for better SWE estimates (Chang et al. 1996). The physical temperature of the tree followed the air temperature closely (Chang et al., 1997). To better model the forest brightness temperature an estimate of air temperature is needed.

Carroll et al. (1995) reported using a kriging model to incorporate snow gage data to estimate areal SWE. We will use a similar statistical method to provide optimum estimates of snow storage from the areas where sufficient measurements are available from the ground-based network. This statistical information will provide us an opportunity to more objectively assess the quality of retrieved SWE.

Recently, results from a block kriging analysis of the snow water equivalent over the Ob River basin, Russia (Brubaker et al., 2000) show that SSM/I derived SWE and the interpolated snow course SWE are comparable. A 2500 km north to south transect across the Urals was selected for the study. Data from snow courses in the Ob River basin were used to generate an optimally interpolated SWE map. When the SWE derived from SSM/I data and the interpolated station data were compared, the differences were consistently well within two standard deviations of the kriged SWE. Due to the limited snow course observations in the Ob River basin, the standard deviation of SWE estimate is rather large. However, this is the best SWE estimate for this area since there are no other SWE estimates available for comparison.

We are also collaborating with an ongoing NASA-funded projects (NASA Research Grants NAG5-4906 and NAG5-6636) at the University of Colorado (CU) National Snow and Ice Data Center (NSIDC), (Armstrong and Brodzik, 2000) This study involves the comparisons of six different passive microwave snow algorithms. These algorithms represent examples that include both mid- and high-frequency channels, vertical and horizontal polarizations and polarization difference approaches. The following is a summary of the CU/NSIDC project.

While SWE data are much less prevalent than snow depth data, there are numerous SWE data sets available for limited regions and over short periods of time. However, the CU/NSIDC project concentrates on those SWE data sets which are the most spatially and temporally comprehensive. The philosophy of this study is to focus on the robust nature of the larger validation data sets which are expected to provide a full range of snow/climate relationships rather than on smaller data sets that may only represent a "snapshot" in time and space.

In order to compare algorithms over a wide variety of snow cover and land surface types, the current phase of this study focuses on the data set "Former Soviet Union Hydrological Surveys" (FSUHS) which is archived at NSIDC (Haggerty an Armstrong, 1996) and which is the same data set used in the Brubaker et al (2000) study described above. In order to focus the analysis on a region that is as homogeneous as possible over the footprint scale, a subset of these data have been selected. The subset represents an area west of the Ural Mountains (45-60 deg. N. Lat., 25-45 deg. E. Lon) where station density is maximum (approximately one or more stations per 100 km) the terrain is non-complex (grassland steppe with maximum elevation differences of less than 500 m) and most of the region is non-forested.

These data are available during both the SMMR and the SSM/I allowing pre-launch analysis of both the low (6 and 10 GHz) and high frequency channels (85 GHz) comparable to those which will be available on AMSR-E. These station data represent a unique and valuable source for algorithm validation as they include not only SWE values but additional information pertaining to snow structure including density and number and thickness of melt-freeze crusts, extent of snow cover within the surrounding terrain, as well as forest type and percent of forest cover from a 50 km diameter area surrounding the station. The transects are typically 1.0 to 2.0 km in length with measurements every 100 to 200 m and are representative of both open and forested locations. These linear transect data allow the unique opportunity to statistically evaluate the response of an algorithm to a spatial pattern that lies between a single point measurement typical of most reporting networks and the area integration represented by the satellite foot-print. These data have now been compiled and interpolated to the EASE-Grid format for use in this study.

For each station file, the analysis involves the extraction from the NSIDC mass storage of daily brightness temperature files for the observation date and for the previous two days to provide complete spatial coverage. Algorithm output and station measurements are then compared over the complete period of available data using statistics which include average, maximum and minimum differences, root mean square (rms) differences and total number of pixels available for comparison.

Basin-scale Hydrologic Data

Another validation approach is to compare the satellite derived areal SWE values with those derived from a snowmelt runoff model for a river basin. Where the models are known to be accurate, we also can use the models to calculate the areal snow water equivalent that is needed for the basin to produce the observed runoff (Martinec et al. 1983). The Rio Grande basin above Del Norte in the State of Colorado has been selected for this purpose. The basin is about 3419 square km. Based on the amounts of snowmelt runoff recorded at Del Norte, a snowmelt model is employed to infer the amount of snow storage in the basin. The model derived snow storage matches well with the contoured snow water equivalent. Data from 1979 to 1985 were used to derive the regression relationship between SRM snow water equivalent and microwave brightness temperature. When applying this to 1987 data, the predicted SWE was 39.4 cm while the actual value was 43.3 cm, a difference of 9 percent (Rango et al. 1989).

The following is the proposed plan for SWE validation. It is designed to compare the areal snow storage with satellite derived snow storage. We propose three types of validation tasks to validate the snow storage estimates with different spatial scales.

Type 1: Grid scale validation

The SWE products will be evaluated at the 25 km by 25 km EASE-Grid scale (Armstrong and Brodzik, 1995). This represents an area that can be surveyed from aircraft with a reasonably high observation density. Sensors such as the airborne gamma SWE detector and multi-frequency microwave radiometers can provide overflights of several EASE grids that will then be used to provide estimates of the grid scale SWE. Since these sensors require the aircraft to fly at a very low altitude, flat open areas will be selected for this purpose. In addition, aircraft derived SWE values will be compared to ground observations.

Type 2: River basin scale validation

In mountainous regions it is not always feasible to obtain SWE using a small aircraft. One method to evaluate the accuracy of areal SWE estimates in mountainous regions involves comparisons with water balance output from a hydrologic model. We will compare the satellite derived areal SWE values with those derived from a snowmelt runoff model for specific river basins. Where the snowmelt model can predict the runoff accurately, we also can use the model to calculate the areal snow water equivalent that would be required for the basin to produce the observed runoff (Martinec et al. 1983). River basins over different parts of the world with the size of several thousand square km will be selected for this effort.

With respect to the river basin scale approach, we will benefit from a new study at CU/NSIDC (NASA and NSF funded) that involves the development of an integrated near-real time monitoring and historical analysis of the major components of the pan-Arctic hydrologic cycle. Output from the AMSR-E snow algorithm will be compared with river discharge data compiled by this project as well as with modeled values of distributed winter precipitation.

Type 3: Regional scale validation

There are few regional scale SWE validation data sets beyond the FSUHS data sets described above. Unfortunately these data sets are only available through 1990 at this time. In order to obtain surface station measurements of snow depth and water equivalent during the Northern Hemisphere winter of 2000-2001 and beyond, CU/NSIDC is currently negotiating with the All-Russia Research Institute of Hydrometeorological Information, Obninsk, Russia, the Satellite Meteorology Institute, Beijing, China, the Cold and Arid Regions Environmental and Engineering Research Institute, Lanzhou, China and the Canadian IDS team CRYSYS.

We will also evaluate the potential of snow depth information collected by meteorological stations and SWE obtained by snow courses in the U.S. Carroll et al. (1995) reported using a kriging model to incorporate snow gage data to estimate areal SWE with some success. We will use a similar statistical method to provide optimum estimates of snow storage from the areas where sufficient measurements are available from the ground-based network. This statistical information will provide us an opportunity to objectively assess the quality of retrieved SWE for a large area.

3.4.2 Field Experiments

Field experiments were organized to further our understanding of the effect of regional weather conditions on the snowfield characteristics. A joint field experiment with the MODIS land/snow group was conducted in the winter of 1996-1997. ER-2 with Millimeter Imaging Radiometer (MIR) and MODIS Airborne Simulator (MAS) on board flew over several snow test sites over New York, Wisconsin and Wyoming. The purpose of this experiment was to evaluate the capability of high frequency (85 GHz) microwave radiation in determining snow depth. It is known the higher frequency radiation is more sensitive to the scattering of snow crystals. However, it is also more sensitive to the atmospheric water vapor and cloud water contents. Different snow depths, shallow pack in New York, medium pack in Wisconsin and deep snow pack in Wyoming were observed. During the same time period of ER-2 flights, NOAA operational airborne gamma snow water equivalent measurements were also taken over many coincident flight lines. Overpass SSM/I data were also collected for comparisons.

Field experiments over the Red River valley and Colorado River basin continued in the 1997-1998 winter season. These field activities are designed to further our understanding of the evolution of snow grain size and spatial inhomogeneity of snow storage over a large area and to validate the pre-launch algorithm. SSM/I data have been used to test the pre-launch algorithm. Due to several logistical problems, 1999 snowfield experiment was terminated early. For the winter of 2000 there was little snow accumulated in the snow sites, thus the experiment was cancelled.

In developing the snow algorithm it is found that the grain size distribution is a most critical parameter. With a priori snowpack grain size profiles built into the algorithm, snow retrieval accuracy has been improved. Field experiments will be continued to collect the snow grain size distribution and its variation with time. This is a part of the on going effort to create a comprehensive database of snow crystal size profiles with different snow conditions. By collecting different snowpack profiles in different snow conditions, we will be able to improve the model calculation of the brightness temperatures emerging from the snowpack. This is an ongoing effort in conjunction with all visits to snow measurement field sites. In order to spatially characterize the snow grain size within the snow algorithm we will investigate two approaches. First we will evaluate the potential of an empirical method based simply on the history of the snow temperature gradient derived from the air temperature record (Armstrong et al. 1993; Mognard and Josberger, 2000). The second method would involve combining a physical model of the full snow depth structure with a microwave emissions model (Wiesman and Maetzler, 1999).

3.4.3 Operational Surface Networks

Snow water equivalent and depth data are available from the limited snow courses scattered over the snow-covered area. These sites are diminishing fast due to budgetary constraints and limited personnel available for these measurements. There are climatology and co-op stations in the US collecting snow depth data routinely. There are more than 600 automated USDA SnoTel sites in the mountainous regions of the western US providing daily SWE observations. Snow course and SnoTel data will be collected for comparison studies. The FSUHS snow course data described above are available for the years 1966 to 1990 from CU/NSIDC. Currently this data set is also being analyzed at GSFC. It is necessary to interpolate these point data before they can be used for comparisons with areal snow data. Substantial increases in funding would be required in order to speed up such comparison studies.

3.4.3.1 Surface Networks – Lessons Learned from earlier studies (CU/NSIDC Project)

As noted above, the primary data set used in the initial phase of the SWE validation study is the "Former Soviet Union Hydrological Surveys" (FSUHS)(Haggerty & Armstrong, 1996). At this stage we are simply evaluating the ability of the individual algorithms to reproduce the monthly climatology provided by the station data. Subsequent comparisons will explore these relationships for time series covering discrete time periods.

We have developed a specific processing environment and output format to compare the various algorithms with the station SWE data. For each station file this involves the combination of the daily brightness temperature files for the observation date and for the previous two days to provide complete spatial coverage. SWE for all pixels containing at least one transect measurement are compared with the output from the respective algorithms. Figure 1 shows a time series comparison of station data with a single algorithm (19H – 37H example) for the total study area for a twelve-year period. Figure 2 shows a single year comparison of 3 different algorithms. The final step in the analysis involves the computation of rms differences for each set of comparisons.

Results indicate a general tendency for the algorithms tested thus far to underestimate SWE. Underestimates of increase significantly as the forest cover density begins to exceed 30 to 40 percent. Because of the detailed land cover data available for this validation study area, we will apply algorithm adjustments as a function of fractional forest cover using methods based on earlier work by Chang. et al. (1996).

3.4.4 Satellite Data

SSM/I with seven channels (19V, 19H, 22V, 37V, 37H, 85V and 85H) flew on board the DMSP F-8, F-10, F-11, F-12, F-13, F-14 and F-15 satellites. There are over ten years of SSM/I data (since July 1987) available for snow algorithm development and testing. These data are extremely valuable for AMSR algorithm development. The higher frequency channels offer the greatest sensitivity to the accurate detection of snow cover and water equivalent. We are also actively engaged in the NASDA snow algorithm test over 100 selected gage stations using SSM/I data.

The Japanese ADEOS-II with the original AMSR on board will be launched in 2001. The at-launch snow algorithm will be tested on both ADEOS-II AMSR and EOS Aqua AMSR-E. However, there are still issues that need to be resolved. In particular, NASDA wants to infer snow parameters based on the overlapping microwave footprints. Snow retrieval software has been delivered to NASDA.

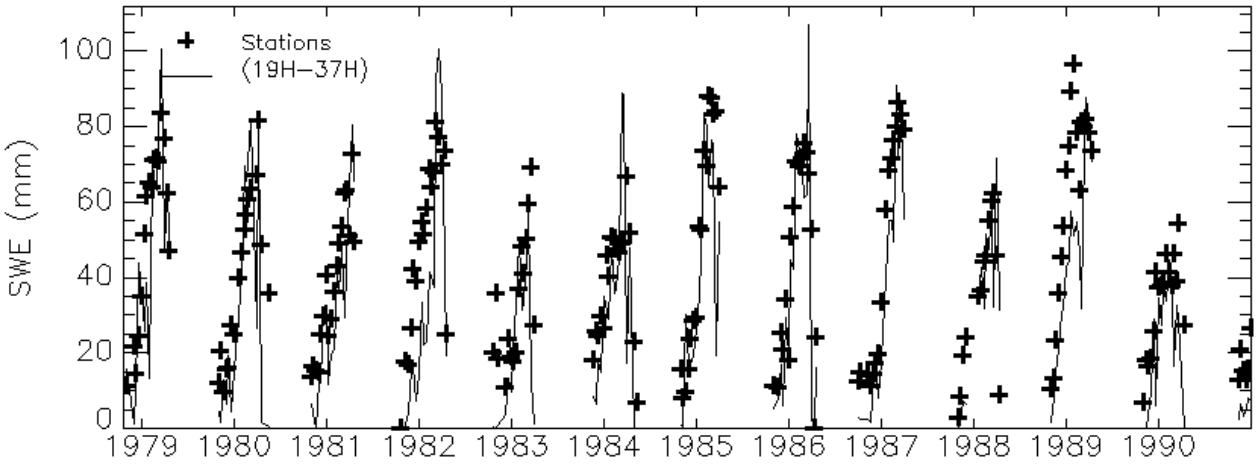

Fig. 3.4.1. Average of total study area (FSUHS subset) snow water equivalent and passive microwave snow water equivalent using horizontally polarized difference algorithm, 1978-1990.

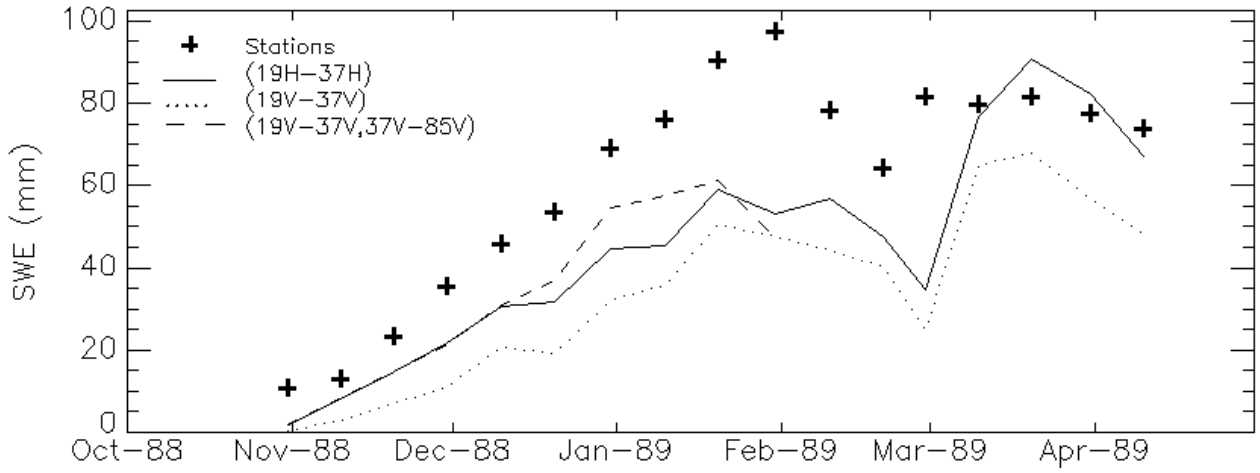

Fig. 3.4.2. Average of total study area (FSUHS subset) snow water equivalent and passive microwave snow water equivalent from three algorithms, 1988-1989.

After the launch of AMSR-E, SSM/I data will still be very useful especially during the period when the snow condition changes rapidly. The overpass time of EOS Aqua satellite (equator crossing times of approximately 1:30 AM/PM) will be different from the DMSP F-13, F-14 and F-15 satellites (and their successors). Frequent monitoring of the snow parameters will help us to understand the snowpack evolution. When the snowpack is not changing rapidly, SWE retrieved from SSM/I data can be used in the SWE comparison studies.

Data from the MODIS instrument on the EOS Terra satellite will provide snow extent maps with a 500m spatial resolution. They will be used to evaluate the ability of the microwave data to determine snow cover area. The CU/NSIDC team will compare the MODIS and AMSR-E products, both of which will be processed in the EASE-Grid and available on a near-real time basis, to determine the accuracy of snow extent as determined by the AMSR-E algorithms. Because one EASE-Grid AMSR-E pixel contains 2,500 MODIS 500 m pixels we will have the

opportunity to evaluate the relationship between actual percent coverage of snow in the AMSR-E pixel and associated microwave signatures and algorithm output.

3.4.4.1 Satellite Data – Lessons Learned from earlier studies (CU/NSIDC Project)

For the validation of snow extent, Armstrong and Brodzik (1998) compared microwave snow maps (SMMR and SSM/I) with the EASE-Grid version of the NOAA Northern Hemisphere weekly snow charts (Robinson et al. 1993). The original NOAA charts were derived from the manual interpretation of AVHRR (Advanced Very High-Resolution Radiometer), GOES (Geostationary Operational Environmental Satellite) and other visible satellite data.

The goal of this study is to determine if the differences between the algorithm output and the validation data are random or systematic. In the case of systematic differences, the patterns are being correlated with the specific effects of land cover type, atmospheric conditions and snow structure. Because we compare algorithm output with continuous records of station data we will be able to identify any seasonal or inter-annual patterns in the accuracy of the algorithms.

For the 22-year study period the passive microwave and visible data show a consistent pattern of inter-annual variability and both indicate maximum extents consistently exceeding 40 million square kilometers (Figure 3). During this same period the trend in mean annual snow extent derived from both visible and microwave satellite data indicates a decrease of approximately 0.2 percent per year.

When the monthly climatologies produced by the two data sources are compared, results clearly indicate those time periods and geographic regions where the two techniques agree and where they tend to consistently disagree. During the early winter season (October through December) the passive microwave algorithms generally indicate less snow covered area than is indicated by the visible data (Figure 4). In both of these situations (shallow and/or wet snow) the microwave algorithms tested thus far are often unable to detect the presence of snow. However, preliminary results indicate that the inclusion of the 85 GHz channel, with the associated enhanced scattering response, improves the accuracy of mapping shallow snow, while algorithms which include the 37 GHz polarization difference improve the detection of wet snow.

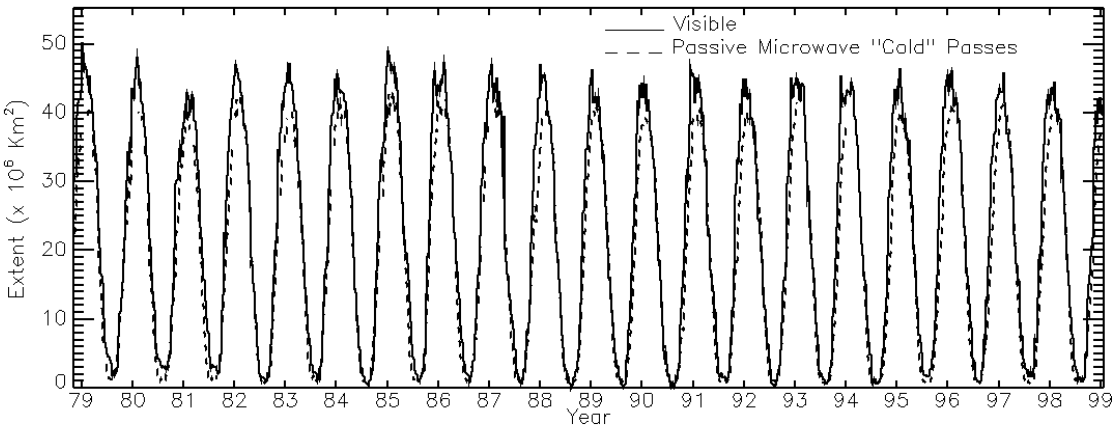

Figure 3.4.3. Northern Hemisphere snow-covered area (x 10^6 km^2) derived from visible (NOAA) and passive microwave (SMMR and SSM/I) satellite data, 1978-1999.

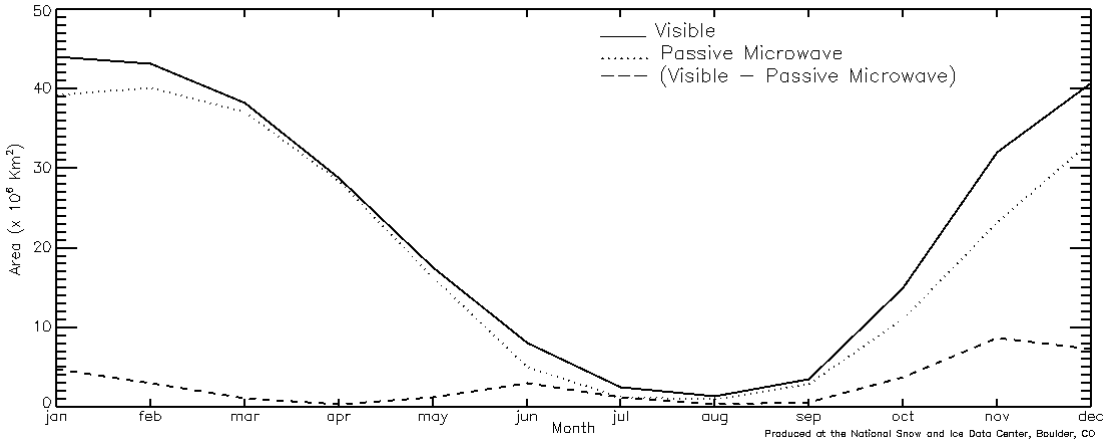

Figure 3.4.4. Northern Hemisphere mean monthly snow-covered area (x 10^6 km^2) derived from visible (NOAA) and passive microwave (SMMR and SSM/I) and the difference between the two (visible minus passive microwave, 1978-1999.

3.4.4.2 Other Data

Brightness Temperatures

The National Snow and Ice Data Center (NSIDC) has produced a 23 year time series of gridded satellite passive microwave data in a common format called the Equal Area Scalable Earth-Grid (EASE-Grid), (Armstrong & Brodzik, 1999). This data set was developed using SMMR (Scanning Multichannel Microwave Radiometer) data for the period 1978 to 1987 and the SSM/I (Special Sensor Microwave Imager) data for 1987 to 2000. These EASE-Grid brightness temperatures provide the standard input to all algorithms being evaluated in this study.

3.4.5 Intercomparisons

Intercomparison studies are critical to consolidate the advancements in snow parameter estimates made by other researchers. The ideal time schedule for intercomparison activity is one year after the launch. This effort will involve assembling satellite and ground truth data sets for comparison. Additional manpower and support funding are required to organize an international inter-comparison study to include additional snow investigators. We will collaborate with the Japanese AMSR team in this endeavor.

We have contacted B. Goodison of the Canadian IDS team CRYSYS on this matter. They showed interest in SWE validation in conjunction with their continued operational SWE program. We will include their SWE product in our comparisons.

3.4.6 Validation Time Line

Post-launch validation:

We have planned many post-launch validation activities for Type 1: grid scale, Type 2: river basin scale, and Type 3: regional scale validation activities in the year 2001, 2002 and 2003. Detailed descriptions of these three types of validation efforts are followed.

Type 1: Grid scale validation

There are several aircraft experiments planned for the next few years. For the airborne microwave mission, we will collaborate with Prof. Hallikainen of the Helsinki Technical University of Finland. For the gamma flights we will collaborate with NOHRSC. Other aircraft experiments will be carried out with the AMSR-E sea ice group and the EOS EX-7 mission study group.

(1) Microwave experiment

This will be a joint effort with Technical University of Helsinki, University of Reading, USDA, USGS and NASA. Technical University of Helsinki will operate the aircraft and remote sensing instruments. The microwave radiometer consists of six frequencies (6.9, 10.7, 19, 23, 37 and 90 GHz). All other groups will contribute to the ground snow observations. Snow depth, density, grain size, underlying soil condition and forest cover distribution will be documented. Currently, two test sites are selected. They are Sodankyla, Finland at 67^{o}N, 26^{o}E and Kuusamo, Finland at 64^{o}N, 27^{o}E. Detailed flight lines will be selected when we visit the sites in August, 2000. The flight lines will cover at least two 50km by 50km areas with different snow cover conditions.

(2) Gamma experiment

Airborne gamma sensors have been used to monitor snow storage in the US for many years. Most of the data lines, of the order of 5 km each, are located in the mid-western part of US. We will cooperate with NOHRSC in this effort. Two test basins Rosael, MN and Black River, WI will be used for this part of validation effort. Gridded flight lines that cover an area 50 km by 50 km of the river basin will be flown in the upcoming winters (2001, 2002, and 2003). The exact day for the gamma flights will be determined in real time based on the snow condition and aircraft schedules. Extensive ground measurements will be conducted during the aircraft flights. USGS, USDA and NASA researchers will participate in coordinating the flights and collecting snow data. These measurements will serve as the calibration points for the areal snow water equivalent values.

(3) Joint airborne experiments

Joint snow and sea ice airborne experiments are planned for regional validation purposes. Cold weather conditions are required for both parameters. Ideally, this experiment is conducted using the NASA DC-8 airborne laboratory. Scanning microwave radiometer and fixed beam radiometers with AMSR-E frequencies will be required. Flight lines over different snow classes over an area of 50 km by 50 km will be selected to evaluate the accuracy of the retrieved snow parameters. Two future experiments are in the active planning stage. The sea ice and snow experiment is currently planned for March 2002. The primary test site for the snow is the Central Alaska and the Brooks Range of Alaska. The representative snow types in Northern Alaska are tundra and taiga snow. Flight lines will be designed to cover several EASE grids on the ground for easy comparison with the AMSR SWE product. Extensive ground snow observations will also be planned during the aircraft mission.

The Canadian EOS CRYSYS IDS team have planned a field campaign for the winter of 2002, most likely during early February, in the Canadian prairies (agricultural land plus boreal forest) for the purpose of satellite microwave validation during the AMSR-E era. Depending on available funding, the plan is to involve flights by a Twin Otter carrying the CRYSYS microwave radiometer (19, 37 and 85 GHz) plus newly acquired low frequency radiometers (1.4 and 6.9 GHz). It is the intention to coordinate these flights with flights of the NWS NOHRSC airborne gamma sensors. Other possible locations for airborne campaigns include southern Ontario, central Quebec and the Mackenzie Basin.

Another mission, EOS EX-7, (Cline, 2000) will most likely take place in Colorado. The

representative snow types will be alpine and prairie. There will be a meeting in the later part of June 2000 at Fort Collins, CO to select the test sites and to plan for the mission. The test site experiment will support the risk reduction effort of the post 2002 EOS EX-7 mission, currently planned for the winter of 2002 or 2003. We will try to coordinate the NOHRSC gamma flights and ground snow observations over the same test sites.

Type 2: River basin scale validation

Six river basins located in north America, Europe and Asia are selected for this portion of the validation effort. They are (1) Rhine, Switzerland 3249 square km, (2) Rhone, Switzerland 3371 square km, (3) Rio Grande, Colorado, US 3419 square km, (4) Kings River, California, US 4000 square km, (5) Beas, Thalot, India 5144 square km and (6) Chatkal, Uzbekistan 6309 square km. Historical snow information, stream runoff data, temperature, precipitation, satellite microwave (SSM/I) data are being compiled. These ancillary data will be used to calibrate the snowmelt runoff model for the particular basin. Once the AMSR-E Level-2A data becomes available we will be ready to validate the satellite SWE estimates. We will conduct the river basin SWE validation for the next several winters.

Type 3: Regional scale validation

Regional scale studies depend on climate stations and co-op networks for snow depth and other weather information. Currently, the US is the only country with enough observations to allow us to pursue this effort. In the Northern Great Plains, the vicinity of the Red River basin of the North (43 – 49 ^{o} N;90 – 105 ^{o}W) will be the major site for validation. These data will be krigged to produce an areal snow map. Due to limited number of stations, the variance of interpolated snow maps will be large. MODIS and SSM/I derived snow products will be used as another sources of snow information for comparisons. We will try to extend the effort to Russia and Canada if we can routinely obtain the station snow data. The Ob River basin of Russia (60 – 80 ^{o} E; 48 –65 ^{o} N) and Canadian Prairie (49 – 53 ^{o} N; 90 – 110 ^{o} W) are the potential test areas.

3.5 Land Surface (submitted by E. Njoku, with contributions from T. Jackson, T. Koike)

Soil moisture is the principal retrievable Aqua AMSR land surface parameter. Surface temperature and vegetation water content are also retrieved by the algorithm, and are output with the level 2 soil moisture product as diagnostic parameters. The level 3 product is derived by compositing the level 2 parameters daily into global maps, separating ascending and descending passes so that diurnal effects can be evaluated. Soil moisture is not retrievable where significant fractions of snow cover, frozen ground, dense vegetation, precipitation, open water, or mountainous terrain occur within the sensor footprint (as determined by a classification algorithm and ancillary information). The algorithm products are generated on an earth-fixed grid with ~25-km nominal grid spacing. The spatial resolution of the products is ~60 km (determined by the 6.9 GHz footprint resolution). The products are summarized in Table 3.5.1, and are described in detail in the Aqua AMSR-E land surface parameters Algorithm Theoretical Basis Document (ATBD) http://eospso.gsfc.nasa.gov/atbd/amsrtables.html.

Table 3.5.1: AMSR-E Land-Surface Product Parameters

Product Level, Type	Parameter	*Spatial Resolution	+Grid Spacing	Temporal Resolution
2, S	Soil Moisture	56 km	25 km	swath
2, R	Vegetation Water Content	56 km	25 km	swath
2, R	Surface Temperature	56 km	25 km	swath
3, S	Soil Moisture	56 km	25 km	daily
3, R	Vegetation Water Content	56 km	25 km	daily
3, R	Surface Temperature	56 km	25 km	daily
3, S	Gridded Brightness Temps.	12, 56 km	25 km	daily

(S = Standard; R = Research)
* Average 6.9 GHz footprint dimension.
+ Nominal grid spacing (EASE-grid, global cylindrical projection)

Validation of soil moisture is emphasized since it is a standard land surface product. The main validation approach for soil moisture is to conduct a series of instrumented field experiments with comprehensive airborne and in-situ surface sampling. Validation of surface temperature and vegetation water content, which are not standard products, will be done by intercomparisons with similar parameters retrieved by AIRS and MODIS.

Understanding the spatial and temporal variability of soil moisture is a priority research focus of NASA's Land Surface Hydrology Program (LSHP). The AMSR instrument will be launched also on NASDA's ADEOS-II satellite approximately one year after the launch of AMSR-E on EOS-Aqua. For these reasons Aqua AMSR-E soil moisture validation is being coordinated with research investigations of the NASA LSHP and ADEOS-II AMSR validation activities.

This document includes contributions from E. Njoku (Aqua AMSR-E Science team member), T. Jackson (EOS-IDS investigator), and T. Koike (ADEOS-II AMSR validation leader), and reflects discussions that took place amongst a broad segment of the hydrology research community at the SGP01+ Soil Moisture Experiment Planning Workshop, and the GEWEX/BAHC Soil Moisture Workshop, in Oklahoma, May 15-18, 2000.

3.5.1 Validation Criteria and Method

The algorithm to be used at launch for retrieving soil moisture from the Aqua AMSR-E is described in the above-referenced ATBD. Soil moisture will also be retrieved from the ADEOS-II AMSR, using initially four different algorithms, including the Aqua AMSR-E algorithm. Joint Aqua/ADEOS-II validation activities will provide an opportunity to evaluate not just the soil moisture retrieval accuracy but also the relative merits of the different algorithm approaches.

The validation objectives include: (1) assessment and refinement of soil moisture algorithm performance, (2) verification of soil moisture estimation accuracy, (3) investigation of the effects of vegetation, surface temperature, topography, and soil texture in affecting the soil moisture accuracy, and (4) determination of the regions globally where useful soil moisture can be derived. The key objective of the validation is to assess whether and under what conditions the AMSR-derived soil moisture meets the simulation-estimated accuracy goal of 0.06 g-cm^{-3} at a 60-km spatial scale. Soil moisture research and applications using the data are not primary goals of the validation program.

Since there is little experience with large-scale soil moisture estimation from space, the expected accuracies of AMSR-derived land surface parameters have been determined by model simulations. With an assumed instrument noise of 0.5 K, and allowance for modeling error, the retrieval accuracies are estimated as: 0.06 g-cm^{-3}, 0.15 kg-m^{-2}, and 2.5 C for soil moisture, vegetation water content, and surface temperature, respectively for vegetation water content less than 1.5 kg-m^{-2}. (The soil moisture retrieval accuracy decreases as a function of increasing vegetation cover due to attenuation by the vegetation canopy.) These accuracies are adequate for current hydrology and climate science requirements for space-derived soil moisture data. However, as hydrologic models improve, and experience is gained in understanding large-scale hydrologic processes, increased accuracy and spatial resolution will be desirable (0.04 g-cm^{-3} at 10-30 km) that will require a dedicated soil moisture observing mission with lower frequency channels and better spatial resolution than AMSR provides. Aspects contributing to the difficulty of retrieving and validating the AMSR soil moisture product include:

- Uncertainties associated with radiative transfer model parameters (such as soil roughness, vegetation scattering and opacity, and soil texture) which propagate into the soil moisture retrieval uncertainties.
- AMSR footprints contain mixtures of different surface types. Retrievals represent spatial averages over the ~60-km 6.9-GHz footprints. Nonlinearities in the radiative transfer processes may give rise to differences between retrieved and true area-averaged quantities.
- Retrieved parameters represent averages over the vertical microwave sampling depth. This depth varies with frequency and the amount of moisture in the soil and/or vegetation. Different sampling depths at different AMSR frequencies may give rise to errors in the retrievals and comparisons between retrievals and in-situ samples, especially where the moisture and temperature profiles are nonuniform.
- Retrieval errors increase with vegetation cover. A vegetation water content transition threshold for reliability of the retrievals is estimated from simulations as ~1.5 kg-m^{-2}. Experience with AMSR data during the validation phase may help define this threshhold better.

The methods to be followed in addressing the above issues include the following components:

Algorithm calibration tests will be conducted throughout the AMSR mission to estimate, monitor, and correct bias offsets between AMSR-observed and model-computed brightness temperatures. Offsets may be due to radiometer absolute calibration errors or to errors in parameters of the radiative transfer (RT) model. Algorithm calibration will permit adjustment of

the brightness temperatures computed by the RT model (used in the retrieval algorithm) to the AMSR-observed values.

Long-term measurement networks, operated within the U.S. and in other countries, are a source of in-situ soil moisture data for point comparisons with the AMSR observations over continuous seasonal and annual cycles. These networks also provide standard automated meteorological data that will be useful in correcting and interpreting the AMSR soil moisture information.

Field experiments will provide short-term (~1 month) intensive measurements of soil moisture and other surface and atmospheric characteristics at the AMSR footprint scale, using automated and manual in-situ sampling and airborne radiometers to generate calibrated spatial soil moisture fields.

Hydrologic modeling will be performed to generate soil moisture products at larger (basin-wide and continental) scales using assimilated data independent of AMSR data. The resulting soil moisture fields will be compared with AMSR-derived soil moisture over diurnal and seasonal cycles. The model-derived soil moisture fields will be of lower accuracy than field experiment data, but will extend the comparisons to larger space and time domains.

Satellite data intercomparisons will be performed using data from sensors on the same satellite (AIRS, MODIS) and from microwave sensors on other satellites (SSM/I, TMI, ADEOS II AMSR, Radars). These intercomparisons provide consistency checks for the soil moisture. They will also provide independent information on surface temperature, vegetation cover, brightness temperature, and radar backscatter that can be used to determine the accuracy of the AMSR brightness temperatures, and the effects of temperature, vegetation, topography, and roughness on the AMSR soil moisture retrievals.

Other measurements not specifically included in this plan, such as truck-based measurements and augmentations to the operational network stations, could broaden the information available on the temporal variability of microwave brightness temperature, soil moisture, and vegetation biomass over varied ecosystems and seasonal cycles. Funding for such measurements, which would be of great value to the validation program, are being sought from other sources.

3.5.2 Algorithm Calibration

The accuracy of the AMSR retrievals will be affected by calibration offsets between AMSR-observed and radiative transfer model-computed brightness temperatures. Calibration of the models to the satellite data is necessary to eliminate retrieval bias errors. Algorithm calibration includes estimating radiometric calibration errors and tuning the parameterization of the microwave models (i.e. coefficients for surface roughness, vegetation opacity, and vegetation albedo). These parameters have in the past been estimated using ground-based and airborne data, but have not been validated at the satellite footprint scale. Tests of the algorithm calibration procedure have been initiated using existing satellite data (SMMR, SSM/I, TMI) and data from well-instrumented field experiments such as SGP97 and SGP99, as well as data from monitoring sites that have limited in-situ data but are homogeneous and have known surface characteristics.

The calibration monitoring sites are selected for geographic diversity and for homogeneity over the footprint scale, so that they can be characterized by a reduced number of parameters. Operational meteorological data (primarily surface air data and forecast model output) will be acquired over these regions. Desert sites (with minimal soil moisture and vegetation, and little seasonal variability) will be used to calibrate topographic and roughness effects. Dry and humid forests (dense vegetation) will be used to calibrate the opacity and single scattering albedo coefficients. Grasslands and savannas (low vegetation but with seasonal variability) will be used to adjust the vegetation opacity coefficients to provide the correct time-varying vegetation signal.

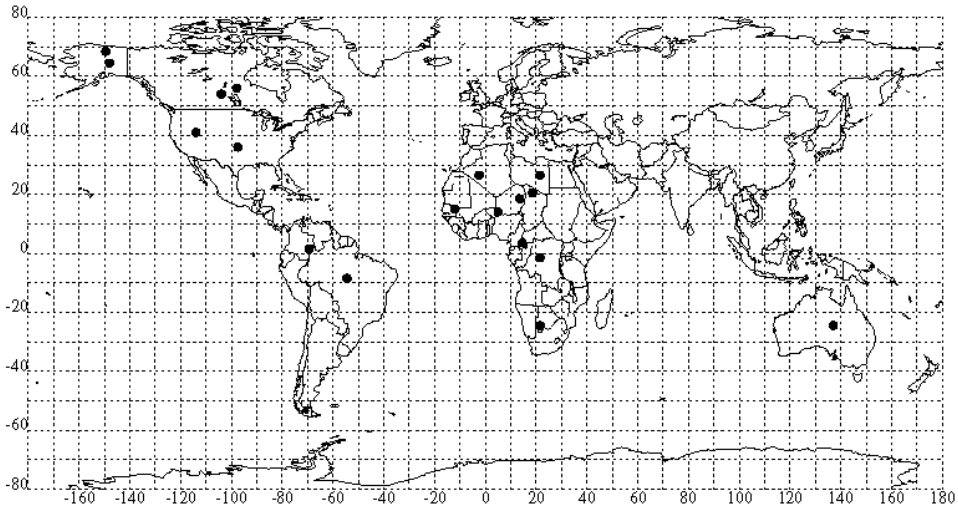

Figure 3.5.1: Locations of AMSR-E land calibration monitoring sites.

Sites have been selected in each category that span the continents and northern and southern hemispheres. In this manner, by choosing sites of extreme (but near-constant) vegetation conditions, and intermediate (but time-varying conditions) the brightness temperature calibration offsets and radiative transfer model coefficients can be fine-tuned (the ATBD document provides more details on the algorithm model equations and coefficient estimation). These offsets and coefficients are global constants in the algorithm. Local variability due to specific vegetation types and roughness are corrected in the algorithm using ancillary databases (where available).

The above procedure is analogous to the standard method for estimation of brightness temperature and model calibration offsets over the ocean (in that case using regions of low winds and incorporating ancillary information on sea surface temperature and humidity). Statistics acquired continuously at the calibration sites during the mission will be used to determine and remove long-term algorithm calibration drifts. The locations and summary descriptions of the monitoring sites are given in Figure 3.5.1 and Table 3.5.2. AMSR brightness temperature statistics will be compiled at all the sites, but algorithm coefficient estimation will be done only at those sites where meteorological data are available.

3.5.3 Operational Networks

Operational measurement networks within the U.S. and in other countries are a source of in-situ soil moisture data for long-term point comparisons with the AMSR observations. Some of these data are subject to restrictions (availability and cost) imposed by the sponsoring agencies, and are of varying quality and usefulness. The key measurement networks in the U.S. are the Department of Energy (DOE) Atmospheric Radiation Measurement (ARM) program, the Oklahoma Mesonet, the U.S. Department of Agriculture (USDA) Soil Climate Analysis Network (SCAN), the USDA Agricultural Research Service (ARS) Micronet, and the Illinois State Water Survey. Data from operational measurements in the former Soviet Union, Mongolia, and China have also recently become available. Additional measurement programs in Mongolia and Tibet are being initiated as part of the Global Energy and Water Cycle (GEWEX) Asian Monsoon Experiment (GAME) and the NASDA AMSR validation program.

The operational network measurements are point data, and thus are not representative of footprint-averaged soil moisture. They will not provide accurate point by point validation of the AMSR footprint-averaged soil moisture. However, since they are made routinely and continuously over long time periods they can be used to validate the temporal soil moisture changes observed in the AMSR data. Temporal plots and statistics of the in-situ versus AMSR data will be made over seasonal and annual cycles, and analyzed as a function of local land

cover, soil texture, and topographic conditions. Figure 3.5.2 shows operational networks in the SGP region (Oklahoma).

Table 3.5.2: Description of calibration sites

#	Ecosystem	Name	Region	Lat-Lon	Attributes
1	Desert	Simpson Desert	Central Australia	23.5-25.5 S 136-138 E	Low Relief, S. Hemisphere
2	Desert	Kalahari Desert	S.W. Botswana	23-26 S 20-23 E	Low Relief, S. Hemisphere
3	Desert	Western Desert	W. Egypt	25-28 N 25-28 E	Low Relief, N. Hemisphere
4	Desert	Sebkha Mekerrhane	S. Central Algeria	25-28 N 1-4 W	Moderate Relief, N. Hemisphere
5	Desert	Tibesti Mountains	N.W Chad	19-22 N 17-20 E	High Relief, N. Hemisphere
6	Sahel	Bilma	E. Niger	17-20 N 12-15 E	Northern Sahel
7	Sahel	Tahoua	S.W. Niger	13-15 N 4-6 E	Central Sahel
8	Sahel	Kayes	Mali/Senegal	14-16 N 11-13 W	Western Sahel
9	Tropical Forest	Boumba	S.E. Cameroon	2-5 N 13-16 E	Africa, N. Hemisphere
10	Tropical Forest	Salonga	Central Zaire	0-3 S 20-23 E	Africa, S. Hemisphere
11	Tropical Forest	Mitu	Colombia/ Brazil	0-3 N 68-71 W	S. America N. Hemisphere
12	Tropical Forest	Curua	Central Brazil	7-10 S 53-56 W	S. America, S. Hemisphere
13	Boreal Forest	Boreas SSA	Saskatchewan, Canada	53.5-54.5 N 103.5-104.5 W	Southern BOREAS Experiment Site
14	Boreal Forest	Boreas NSA	Manitoba, Canada	55.5-56.5 N 97.5-98.5 W	Northern BOREAS Experiment Site
15	Boreal Forest	Bonanza Creek	Central Alaska, U.S.	64-65 N 147.5-148.5 W	Ecological Forest Experimental Site
16	Tundra	Toolic Lake	N. Central Alaska, U.S.	68-69 N 149-150 W	LTER Site
17	Salt Lake Basin	Great Salt Lake	N.W. Utah, U.S.	38-44 N 111-117 W	Desert Hydrologic Basin
18	Plains Grassland	Southern Great Plains	Oklahoma/ Kansas, U.S.	34-38 N 96-99 W	Sub-humid Hydrologic Basin

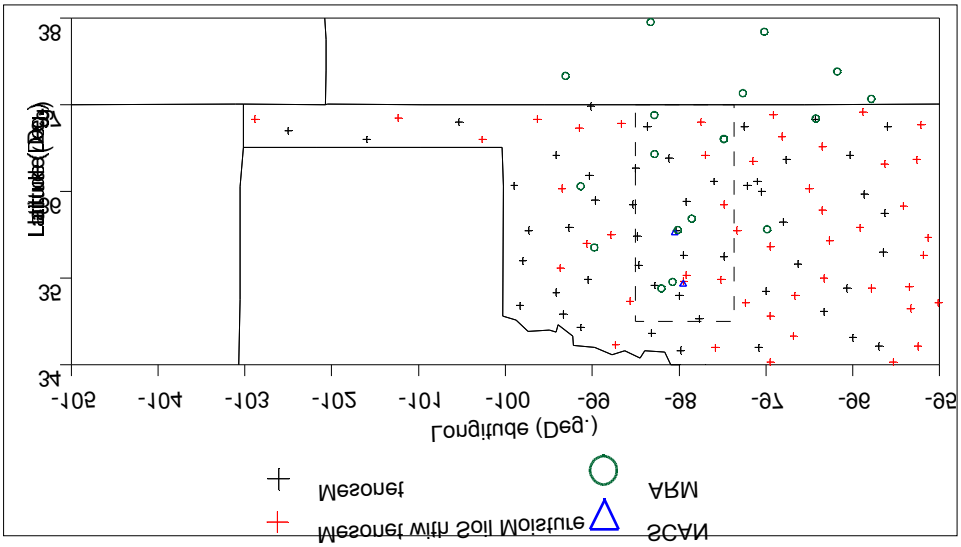

Figure 3.5.2: Operational networks in the SGP (Oklahoma) region

DOE ARM

The DOE ARM program operates a large number, and various types, of instruments within the U.S. Southern Great Plains (SGP) region. The Southern Great Plains is one of the ARM Cloud and Radiation Testbeds (CART). The SGP ARM/CART site layout is based upon a heavily instrumented central facility (CF) surrounded by 22 extended facilities (EF) with fewer instruments, 4 boundary facilities (BF), and 3 intermediate facilities (IF). Soil moisture and meteorological data are collected at the CF and EF sites. Radiosonde observations are made at the CF on weekdays at 530, 1130, 2030, and 2330 (UTC). During intensive observing periods the frequency is increased, weekends are included, and observations are also made at BF sites.

Oklahoma Mesonet

The Oklahoma Mesonet is an automated environmental observing system distributed over the state of Oklahoma. There are 114 stations providing observations every 5 minutes. Data are collected and transmitted to a central point every 15 minutes where they are quality controlled, distributed and archived. Each station consists of a 10 m tower providing measurements of air temperature (1.5 m), relative humidity (1.5 m), wind speed and direction (10 m), barometric pressure, rainfall, solar radiation, and soil temperature (10 cm for both sod and bare soil). About half the stations provide supplemental measurements of air temperature (9 m), wind speed and direction (2 m), leaf wetness, soil moisture (5, 25, 60 and 75 cm under sod), and soil temperature (5 and 30 cm under sod and 5 cm under bare soil). Data files from the Mesonet are copyrighted and must be purchased.

USDA SCAN

The USDA has initiated a nationwide soil moisture and soil temperature analysis network called SCAN. Data are provided to the public on the Internet in real time. Each system provides hourly observations of air temperature, barometric pressure, wind speed, precipitation, relative humidity, solar radiation, soil temperature at 5, 10, 20, 50 and 100 cm, and soil moisture at 5, 10, 20, 50 and 100 cm. There are SCAN sites of interest to AMSR validation operating in the SGP region (Oklahoma), Georgia and, possibly in future, Iowa.

USDA ARS Micronet

The USDA ARS Grazinglands Research Laboratory at El Reno, Oklahoma operates a meteorological network within the Little Washita watershed called the ARS Micronet. There are 42 ARS Micronet stations. The data consist of accumulated rainfall, relative humidity, air temperature at 1.5 m, solar radiation, and soil temperature at 5, 10, 15 and 30 cm below ground surface. Climate data are provided in 5-minute increments and the soil temperature data are provided in 15-minute increments. In addition, ARS also operates an experimental Soil Heat and Water Measurement System. This includes heat dissipation sensors at selected Micronet sites. These sensors provide soil water matric potential data. The data consist of matric potential values at 5, 10, 15, 20, 25, and 60 cm below the ground surface, at 1-hour increments.

Illinois State Water Survey

The Illinois State Water Survey has conducted soil moisture measurements since 1981 at 19 stations distributed over the state. The measurements are made using the neutron-probe technique at depths of 0-10, 10-30, and 20-200 cm. Measurement frequency is about every two weeks during the growing season and once per month during the rest of the year.

FSU, Mongolia, China

Data from operational measurements in the former Soviet Union, Mongolia, and China have recently become available through the Global Soil Moisture Data Bank, a web-based archive compiled by investigators at Rutgers University and their colleagues. The data are in-situ gravimetric measurements from mostly grassland and agricultural sites measured in the top 10-cm of soil. Due to the considerable effort required to compile and quality-control these data most of the data are not current, and are useful primarily for retrospective analyses. Data from Mongolian sites in closer to real time will be available through the ADEOS-II AMSR validation program.

3.5.4 Field Experiments

The AMSR soil moisture field experiments are designed to take advantage of short-term (~1 month) intensive sampling of soil moisture and other surface and atmospheric characteristics using automated and manual in-situ measurements and airborne radiometers. The data can be analyzed to provide validation products at the AMSR footprint scale. Test sites are selected for feasibility of characterizing the spatial variability of surface moisture, temperature, and vegetation over a region encompassing a few (3 to 6) AMSR footprints, and for geographic diversity of vegetation, topography, and climate. (Experiments of this type were carried out in 1997 and 1999 in the SGP region of the U.S. (SGP97 and SGP99).

Soil moisture validation experiments at U.S. sites are planned in the summers of 2001 and 2003. The sites include Oklahoma, Iowa, and Georgia for experiments in 2001 (designated SGP01+), and will include these sites and/or others in Idaho and Arizona for experiments in 2003. Selection of sites for 2003 will depend on results obtained from the SGP97, SGP99, and SGP01+ experiments (see below) and are intended to provide sites with more topographic variability and contrast between semi-arid and vegetated conditions.

ADEOS-II AMSR soil moisture validation experiments are planned at sites in Asia as NASDA-funded validation activities. Sites have been identified and are being instrumented in Thailand, Tibet, and Mongolia for experiments in 2001 and 2002 (ADEOS-II AMSR Validation Plan).

Approach

The approach for the U.S. field experiments is to use airborne radiometers and in-situ sampling to generate daily soil moisture maps over a region spanning a few AMSR footprints.

These can be compared with the AMSR soil moisture retrievals over a range of soil moisture conditions during the one-month experiment duration. The airborne soil moisture mapping will be done using (1) the NOAA Environmental Technology Laboratory (ETL) Polarimetric Scanning Radiometer (PSR) which has the same frequencies, polarizations, and viewing angle as the AMSR, and (2) the Jet Propulsion Laboratory (JPL) Passive/Active L/S-band sensor (PALS) which has L- and S-band radiometer and radar channels. The PSR will be flown on the NASA P3 aircraft at high-altitude (~7 km) to map a 100 x 300 km region at ~2-km spatial resolution. The PALS will be flown on the NCAR C-130 aircraft that will underfly the P-3 at ~1-km altitude over a limited region (10 x 50 km), to provide field-resolution (~0.4 km) soil moisture maps. Within the regions mapped by the PSR and PALS several fields with vegetation covers representative of the larger region will be intensively sampled to obtain soil moisture and temperature profiles, soil textures and bulk densities, and surface roughness and vegetation characteristics. Other microwave radiometers will also be flown in these experiments to take advantage of available accommodations on the P-3 and C-130 aircraft. These include the ESTAR (L-band), and ACMR and STEP-C (C-band) instruments. Funding support for these will come from the NASA Land Surface Hydrology Program. Table 3.5.3 shows the complement of airborne sensors for the field experiments.

The in-situ measurements will be averaged for each field and applied, using established L-band brightness temperature versus soil moisture relationships, to generate PALS soil moisture maps. Results from SGP99 show that this can be done to better than 3% volumetric soil moisture accuracy. The in-situ and PALS data will be used to calibrate the wide coverage PSR-generated soil moisture maps, which will in turn provide comparisons with the AMSR data at the AMSR footprint scale. The PSR maps will also provide insight into the effects of heterogeneity within the AMSR footprint. The accuracy of the soil moisture data maps at the different scales will be estimated using statistical techniques, and is estimated from previous experiments as ~3-4% volumetric. This approach is being tested using the SGP99 data set. (A comprehensive set of in-situ and airborne radiometer measurements was acquired in SGP99 over a wide dynamic range of soil wetness conditions – http://hydrolab.arsusda.gov/sgp99). The experimental procedure will be evaluated and refined for the subsequent experiments in 2001 and 2003.

Factors to be considered in implementing this procedure include: variability of soil texture, vegetation, and topography at different scales; logistical difficulties of coordinating in-situ and airborne radiometer measurements with the AMSR overpass times; reliability of equipment; availability of human resources for field sampling; and uncertainty of meteorological conditions (precipitation and drying) such that a good soil moisture dynamic range can be observed. Sufficient measurements must be made to assess the effects of vegetation, temperature, texture, and topography on the soil moisture accuracy. Available soils, vegetation, and topographic maps, as well as Landsat and MODIS images, will be used for these purposes.

While the core Aqua/ADEOS-II soil moisture validation team members (E. Njoku, T. Jackson, V. Lakshmi, T. Koike, I. Kaihotsu) have overall responsibility for the validation planning, a much larger group of investigators will be involved in collecting, processing, and analyzing the data. Following procedures implemented successfully for SGP97 and SGP99, validation funds will be used to support government agency, university faculty, and student personnel in the data acquisition, processing and analysis. All experiment data will be placed in a public archive (currently the GSFC DAAC) for availability to other researchers funded by NASA's EOS and Land Surface Hydrology programs.

SGP01+

Test sites in Oklahoma (SGP), Iowa, and Georgia will be used for the SGP01+ experiment in July 2001. These sites collectively include more varied vegetation, topographic, and climatic conditions than observed in SGP99. The sites are centered at USDA/ARS field locations, providing good opportunities in terms of facilities, personnel, measurements and logistics.

Table 3.5.3: Airborne microwave sensors

Sensor	Developer	Mode of Operation	Other Features
Polarimetric Scanning Radiometer (PSR/C)	NOAA ETL (A. Gasiewski)	C-band (and higher) – Scanner (P-3)	Option 1: C band V & H Option 2: 10.7, 18.7, 37.0, and 89.0 GHz V and H
Step Frequency Microwave Radiometer (Step-C)	U. Massachusetts (C. Swift)	C-band – Single beam (C-130)	V & H, multiple C band frequencies
Airborne C band Microwave Radiometer (ACMR)	NASA GSFC (E. Kim)	C-band – Single beam (P-3)	V & H
Electronically Scanned Thinned Array Radiometer (ESTAR)	U. Mass (C. Swift) NASA GSFC (D. LeVine)	L-band – Synthetic Aperture Imager (P-3)	H
Passive/Active L/S-band Sensor (PALS)	JPL (W. Wilson)	L- and S-band radiometer-radar – Dual-beam (C-130)	V & H (radiometer) VV, HH, HV (radar)

Overflights of the sites by the P-3 and C-130 aircraft will be scheduled as close to 1:30am as possible to coincide with AMSR overpasses. The nighttime passes should correspond to more uniform soil moisture and temperature profile conditions than daytime (1:30pm) passes, resulting in better comparisons between in-situ (0-2.5cm and 0-5cm) and AMSR (0-1cm) observations. Validation activities will include in-situ sampling, ground-based and airborne remote sensing, and statistical and hydrologic modeling. A detailed experiment plan, schedule, and budget have been developed for SGP01+ following a special planning workshop held in Oklahoma City, May 25, 2000.

The SGP site is similar to that used in SGP97 and SGP99, for continuity in observations over a well-characterized region. A wider region (~100 km) will be mapped by the PSR in SGP01+ to ensure that sufficient AMSR footprint coverage is obtained. The SGP region has major east-west precipitation gradients that result in a large range of seasonal soil moisture. The vegetation cover is mostly pasture, winter wheat, and small crops (alfalfa). The region includes several major observation networks and research sites (Oklahoma Mesonet, ARM-CART, ARS Micronet).

Walnut Creek, near Ames, Iowa is a region of large corn and soybean fields and has higher vegetation biomass than typically found in the SGP site. In late July the corn should be near peak biomass and the soybean cover should be significant. Story Co. which surrounds the site is the focus of a NASA Agriculture NRA investigation.

The Little River Watershed, centered at the USDA/ARS Southeast Watershed Research Center in Tifton, GA is an additional vegetated site. There is considerable forest, and the dominant crop types are peanuts and cotton. There is an NRCS SCAN site in the watershed, and the state of Georgia has an extensive meteorological network.

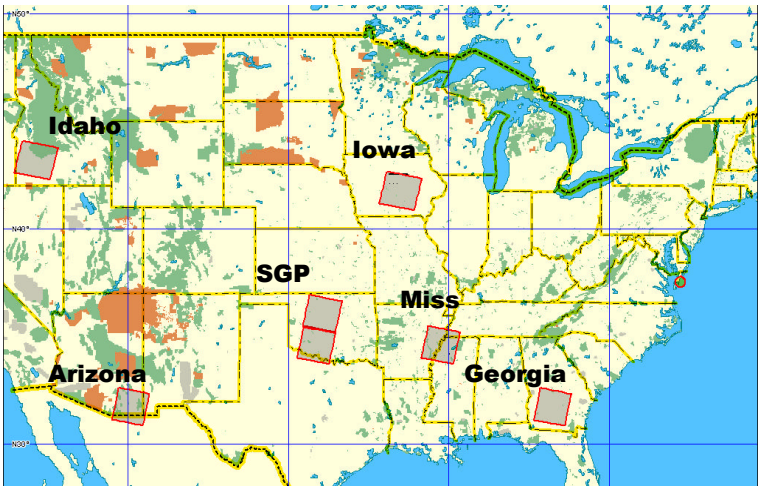

Figure 3.5.3: Locations of target field experiment sites for SGP01+ and SGP03+.

SGP03+

Experience with SGP97, SGP99, and earlier experiments has shown that planned experiment objectives are unlikely to be 100% achieved. This is due to unpredictable weather conditions, equipment breakdowns, and other unforeseen logistical difficulties. It also typically takes a year or so to fully process and analyze the acquired data and determine whether the research objectives have been achieved. For this reason, and to expand the range of land cover and topographic heterogeneity, a second experiment is planned for July 2003. This will also provide an opportunity to conduct a second experiment with two years prior experience in understanding the characteristics of the AMSR data. Depending on the outcome of the SGP01+ experiment, and the progress in achieving the soil moisture validation objectives at the SGP01+ field sites, the same sites may be revisited in July 2003, or alternative sites may be considered. These alternatives include sites in Arizona, Mississippi, and Idaho, with increased diversity including semi-arid, topographically varied, and large river basin areas.

Mongolia, Tibet, Thailand

Experiments at Asian field sites in Mongolia, Tibet, and Thailand are planned as part of the ADEOS-II AMSR validation activities. Details of these experiments can be found in the ADEOS-II Validation Plan. Data from these experiments are expected to be made available by NASDA for joint AMSR team validation. Exchanges between U.S and Japanese team members of data acquired in the SGP99 and Tibetan Plateau experiments has already occurred, and such exchanges are expected to continue. The approach for the Asian field sites is to use long-term measurements from automated stations and gravimetric sampling during periodic intensive field campaigns to acquire soil hydrology and surface meteorological data. The Mongolian Plateau experiment will cover a region 160 x 160 km in southern Ulaanbaatar where the terrain is generally flat with grass and bare surface conditions. Automated measurements include soil moisture, temperature air temperature, and precipitation. Intensive sampling to be carried out includes the above, plus plant water content and LAI, surface roughness, and soil bulk density and texture.

3.5.5 Modeling and Data Assimilation

Airborne radiometers provide one means for deriving satellite-footprint-scale soil moisture over a limited region and time period. Another method for producing soil moisture fields, over larger areas and longer time periods, is hydrologic modeling with data assimilation. The data to be assimilated can include atmospheric forcing and surface in-situ measurements. The models used can be land-surface hydrologic models or more sophisticated surface-atmosphere coupled models. The models can operate at various time and space scales, and with varying schemes for data assimilation. Key parameters at the model grid scale, such as precipitation and surface net radiation, depend on the input data quality and parameterizations of the models, and their errors can be difficult to assess. Thus, model output fields will be used mainly for consistency checking of the spatial and and temporal patterns of AMSR-derived soil moisture rather than for quantitative validation of the soil moisture accuracy.

Due to funding and other resource limitations the generation of specific model output fields for AMSR validation is not included in this plan. However, some model products currently being developed by the GSFC Data Assimilation Office (DAO) and the operational forecast centers (NCEP and ECMWF) will be useful for AMSR validation. These products are available through public databases and by contact with investigators from the above institutions (K. Mitchell, personal communication). Additional resources and validation investigations using data assimilation are being sought through the Aqua Validation NASA Research Announcement (NRA).

3.5.6 Satellite Data Intercomparison

Satellite data intercomparisons will be performed: (1) to assess brightness temperature (TB) calibration levels over land, (2) to intercompare geophysical products between AMSR, AIRS, and MODIS, and (3) to evaluate effects of heterogeneity within the AMSR footprint.

Brightness temperatures from ADEOS-II AMSR (at 6.9, 10.7, 18.7, and 36.5 GHz), TRMM Microwave Imager (TMI) (at 10.7, 19.35, and 37 GHz), and DMSP Special Sensor Microwave Imager (SSM/I) (at 19.35 and 37 GHz) will be registered to the Aqua AMSR grid and compared with the Aqua AMSR 6.9, 10.7, 18.7, and 36.5 GHz brightness temperatures. This will be done over the calibration regions shown in Figure 3.5.1 and also at the field experiment sites shown in Figure 3.5.3. Statistics will be compiled of the means and standard deviations of the TB differences as functions of time during the mission. Although the launch dates, sampling times, spatial resolutions, frequencies, and incidence angles are somewhat different between the sensors the statistics compiled over time will indicate relative sensor calibration offsets and drifts, as well as the relative instrument sensitivities.

Geophysical validation will be carried out at the AMSR footprint scale by intercomparisons between products from the Aqua AMSR, AIRS, and MODIS instruments. Specifically, using infrared (IR) land surface temperature (LST) from AIRS and MODIS, and leaf area index (LAI) from MODIS. The IR LST products will be averaged and co-registered to the AMSR footprint resolution and locations and compared with the AMSR LST. Differences will be interpreted in terms of terrain, soil moisture, and landcover characteristics. The LAI product will be averaged to the AMSR footprints and compared against the AMSR-derived vegetation water content. Relationships will be developed between LAI and vegetation water content for different vegetation types, and these relationships will be evaluated against published relationships derived at local scales for similar vegetation classes. Over limited regions, principally at the AMSR validation experiment sites (Figure 3.5.3) MODIS high-resolution landcover data will be accumulated for each AMSR footprint and used to interpret the effects of vegetation heterogeneity on AMSR soil moisture retrievals.

Data from synthetic aperture radars (SARs) such as Radarsat and ERS (if operating during the AMSR mission) can be analyzed jointly with AMSR data as case studies. Such studies may provide additional insights into effects of surface heterogeneity and microwave surface signatures at different scales. The use of SAR data is not emphasized in this plan, however, since the quantitative interpretation of vegetation, roughness, and soil moisture effects in SAR data itself requires research and careful study.

3.5.7 Validation Time Line

The field experiment schedule is shown below. The U.S. experiments at the SGP and other sites take place in July every other year, starting with SGP99 which was held in July 1999. The experiment in 2005 is a backup, and is currently undefined. It may not be supported if the experiments in 2001 and 2003 can be conducted as planned (all sensors and aircraft operating) and the range of meteorological and surface conditions (precipitation, drying, biomass range) permit a sufficiently comprehensive validation of the AMSR soil moisture. Each of these experiments consists of a 1-month field deployment followed by a 6-month to 1-year data analysis period and validation workshops or conference sessions to discuss and present results. The Experiments in Asia (Thailand, Tibet, Mongolia) are supported as part of the ADEOS-II AMSR validation plan and are shown here for information only. U.S. investigators may participate in these experiments by traveling to selected sites and participating in the data collection and analysis. However, no deployment of U.S. airborne sensors or aircraft are planned to these sites.

Field Experiment Schedule

	1999	2000	2001	2002	2003	2004	2005
AMSR-E Launch		▽					
AMSR-A Launch			▽				
SGP (99)	□═══	═══⇩ ⇩					
Thailand			◆ ◆ ◆ ◆	◆ ◆ ◆ ◆			
Tibet			▭	▭			
Mongolia			▭	▭			
SGP/US (01, 03, 05)			□═══	⇩ ⇩	□═══	⇩ ⇩	═══□ ⇩

4 IMPLEMENTATION OF VALIDATION RESULTS IN DATA PRODUCTION

4.1 Approach

AMSR-E's primary heritage is SSM/I. SSM/I is an externally calibrated instrument and over the thirteen years that it has been flying it proved to be a very stable instrument. After the initial on-orbit calibration, where the ground calibration (instrument characterization) is verified, all data should be ready to be processed routinely. A second instrument, the TRMM Microwave Imager, is currently expected to last until the end of 2001. Should TMI still be operating at the time of the AMSR-E launch, it will offer an opportunity for direct calibration when the two sensors intersect their orbits. Since TMI will be routinely compared to SSM/I, this opportunity will insure that the AMSR-E instrument calibration is commensurate with the SSM/I sensors and would give additional confidence to the radiance measurements.

Once the radiance measurements are verified, geophysical algorithm verification must begin. Experience tells us that 2-4 months are typically needed to insure that a variety of artifacts typically found in new data sets are understood and properly handled by the algorithms. These situations vary from the mundane quality control issues to the subtle conditions such as satellite maneuvers when the data appears valid but in fact require geometric corrections or are altogether unusable. Where AMSR-E algorithms utilize channels not available on SSM/I, an initial period is also required to build up the required statistics from ground based networks. Geophysical parameters that have been scrubbed of any physically implausible solutions should realistically be expected approximately six months after launch.

After the initial checkout of the instrument, the AMSR-E team will concentrate on comparing results to the routine observations gathered as part of the validation program. This process will insure that the products contain no systematic biases and will help define some of the uncertainties within the geophysical products. Systematic deviations between satellite derived and ground based products should be corrected within the first year. From an overall implementation strategy, it therefore makes sense to consider doing routine product generation 6 months after launch, with an initial reprocessing one year after launch.

The routine collection of validation data, as well as the data collected during focused experiments is intended to refine assumption within the geophysical algorithms. It should therefore be expected that the AMSR-E products would continue to improve throughout the lifetime of the AMSR-E. To make these improvements available to the research community, the AMSR-E products therefore need to be regenerated periodically to incorporate the new understanding offered by the routine and special validation campaigns. We recommend that the AMSR-E team convene annually for the purpose of examining if the scientific advances in the previous year warrant that the data be reprocessed or not.

4.2 Role of EOSDIS

EOSDIS has contracted the AMSR-E Science Investigator-led Processing System (SIPS) to process the higher level (2 and up) standard products. The AMSR-E SIPS is composed of Remote Sensing Systems (RSS) and the Global Hydrology Resource Center (GHRC) group managed by M. Goodman, co-located with the AMSR-E Team leader, at MSFC. Once the standard products are processed they will be sent to NSIDC. NSIDC DAAC will archive and distribute the AMSR-E standard products. They will also archive the Level 1A data. These data will be processed and delivered to the US by NASDA, in Japan.

4.3 Archival of Validation Data

The validation data will be archived by different DAACs. The following is a proposal that has not yet been approved by EOSDIS.

a) The sea ice and snow validation data to be archived at NSIDC. NSIDC is a well known facility, with vast experience in sea ice and snow data sets.

b) The GSFC DAAC to archive the rainfall and soil moisture validation data sets

In the next year, as specific AMSR-E validation data will be collected this proposal will be discussed and decided upon.

References:

Alishouse, J.C., S. Synder, J. Vongsathorn, and R.R. Ferraro, Determination of oceanic total precipitable water from the SSM/I, *IEEE Trans. Geoscience and Remote Sensing*, *28*, 811-816, 1990.

Armstrong, R.L. and Brodzik, M.J. 1999. A twenty year record of global snow cover fluctuations derived from passive microwave remote sensing data, 5th Conference on Polar Meteorology and Oceanography, American Meteorological Society, Dallas, TX: 113-117.

Armstrong, R.L. and Brodzik, M.J. 1995. An earth-gridded SSM/I data set for cryospheric studies and global change monitoring. Advances in Space Research, 16(10): 155-163.

Armstrong, R.L. and Brodzik, M.J. 1998. A comparison of Northern Hemisphere snow extent derived from passive microwave and visible remote sensing data. IGARSS-98, Proceedings: 1255-1257.

Armstrong, R.L. and M.J. Brodzik, 2000. Validation of passive microwave snow algorithms, proceedings IAHS Remote Sensing and Hydrology 2000 Symposium, Sante Fe, NM, April 3-7, 2000 (in press).

Armstrong, R.L., A. Chang, A. Rango and E. Josberger, 1993. Snow depths and grain size relationships with relevance for passive microwave studies, Annals of Glaciology, no.17:171-176.

Barber, D. G. and J. Yackel, The physical, radiative, and microwave scattering characteristics of melt ponds on sea ice, Int. J. Remote Sensing, 20, 2069-2090, 2000.

Brubaker, K.L., M. Jasinski, A. Chang and E. Josberger, 2000: Interpolating sparse surface measurements for calibration and validation of satellite derived snow water equivalent in Russia Siberia, proceedings IAHS Remote Sensing and Hydrology 2000 Symposium, Sante Fe, NM, 2-7 April, 2000 (in press).

Carroll, S.S., G.N. Day, N. Cressie and T.R. Carroll, 1995: Spatial modeling of snow water equivalent using airborne and ground based snow data. Enviornmetrics, 6, 127-139.

Cavalieri, D. J., J. Crawford, M. R. Drinkwater, D. Eppler, L. D. Farmer, R. R. Jentz and C. C. Wackerman, Aircraft active and passive microwave validation of sea ice concentration from the DMSP SSM/I, J. Geophys. Res., 96, 21,989-22,008, 1991.

Cavalieri, D. J., NASA Sea Ice Validation Program for the Defense Meteorological Satellite Program Special Sensor Microwave Imager, *J. Geophys. Res.*, 96, 21, 969-21,970, 1991.

Cavalieri, D. J., The validation of geophysical parameters using multisensor data, Chapter 11 in Microwave Remote Sensing of Sea Ice, edited by F. D. Carsey, American Geophysical Union Monograph 68, 233-242, 1992.

Chang, A.T.C., J.L. Foster and D.K. Hall, 1996: Effects of forest on the snow parameters derived from microwave measurements during the BOREAS winter field experiment. Hydrological Processes, 10, 1565-1574.

Chang, A.T.C., J.L. Foster, D.K. Hall, B.E. Goodison, A.E. Walker and J.R. Metcalfe, 1997: Snow parameters derived from microwave measurements during the BOREAS winter field experiment. JGR, 102, 29663-29671.

Comiso, J. C. and C. W. Sullivan, Satellite microwave and in-situ observations of the Weddell Sea Ice Cover and its Marginal Ice Zone, J. Geophys. Res., 91(C8), 9663-9681, 1986.

Comiso, J. C., D. J. Cavalieri, C. P. Parkinson, and P. Gloersen, Passive Microwave Algorithms for Sea Ice Concentration - A Comparison of Two Techniques, Remote Sensing of the Environment, 60 (3), 354-384, 1997.

Comiso, J. C., P. Wadhams, W. Krabill, R. Swift, J. Crawford, and W. Tucker, Top/Bottom multisensor remote sensing of Arctic sea ice, *J. Geophys. Res.*, 96(C2), 2693-2711, 1991.

Comiso, J. C., T. C. Grenfell, D. L. Bell, M. A. Lange,and S. F. Ackley, Passive Microwave In Situ Observations of Winter Weddell Sea Ice, J. Geophy. Res., 94, 10891-10905, 1989.

Comiso, J.C, T.C. Grenfell, M. Lange, A. Lohanick, R.Moore, and P. Wadhams,"Microwave remote sensing of the Southern Ocean Ice Cover," Chapter 12,Microwave Remote Sensing of Sea Ice, (ed. by Frank Carsey), American Geophysical Union, Washington, D.C., 243-259, 1992.

Comiso, J.C., Sea ice geophysical parameters in the Arctic and the Sea of Okhotsk using multichannel passive microwave data, Journal of Japanese Remote Sensing, 16(2), 32-46,

1996.
Grenfell, T. C., J. C. Comiso, M. A. Lang, H. Eicken, and M. R. Wensnahan, Passive microwave observations of the Weddell Sea during austral winter and early spring, J. Geophys. Res., 99, 9,995-10,010, 1994
Haggerty, C.D. and Armstrong, R.L. 1996: Snow Trends within the former Soviet Union. EOS, Transactions American Geophysical Union, Vol. 77, No. 46:F191
Liu, A. K. and D. J. Cavalieri, Sea ice drift from wavelet analysis of DMSP SSM/I Data, *Int. J. Remote Sensing*, 19, 1415-1423, 1998.
Liu, A. K., Y. Zhao, and S. Y. Wu, Arctic sea ice drift from wavelet analysis of NSCAT and special sensor microwave imager data, J. Geophys, Res., 104, 11,529-11,538, 1999.
Markus, T. and D. J. Cavalieri, A revision of the NASA Team sea ice algorithm, Transactions on Geoscience and Remote Sensing, submitted, 1999.
Markus, T. and D. J. Cavalieri, An enhanced NASA Team sea ice algorithm, IEEE Trans. Geosci. and Remote Sensing, 38, 1387-1398, 2000.
Markus, T. and D. J. Cavalieri, Snow depth distribution over sea ice in the Southern Ocean from satellite passive microwave data, American Geophysical Union, Antarctic Research Series, in press, 1997.
Markus, T. and D. J. Cavalieri, Snow depth distribution over sea ice in the Southern Ocean from satellite passive microwave data, Antarctic Sea Ice: Physical Processes, Interactions and Variability, Antarctic Research Series, Volume 74, pp 19-39, American Geophysical Union, Washington, DC, 1998.
Martinec, J., A. Rango and E. Major, 1983: The Snowmelt-Runoff Model (SRM) User's Manual. NASA Ref. Publ. 1100, 11 8pp.
Massom, R.A., J.C. Comiso, A.P. Worby, V. Lytle, and L. Stock, Satellite and in situ observations of regional classes of sea ice cover in the East Antarctic pack in winter, Remote Sensing of the Env., 68(1), 61-76, 1999.
Mognard, N. M. & Josberger, E.G. 2000: Application of a Passive Microwave Snow Depth Algorithm that includes snow metamorphism, proceedings IAHS Remote Sensing and Hydrology 2000 Symposium, Sante Fe, NM, 2-7 April, 2000 (in press).
NASA 1982: Plan of Research for Snowpack Properties Remote Sensing (PRSPRS), The Snowpack Properties Working Group, Goddard Space Flight Center, Greenbelt, Maryland.
National Snow and Ice Data Center(NSIDC), NSIDC, DMSP SSM/I Brightness Temperatures and Sea Ice Concentration Grids for the Polar Regions on CD-ROM User's Guide, National Snow and Ice Data Center, Special Report - 1, Cooperative Institute for Research in Environmental Sciences, University of Colorado, Boulder, CO, January 1992.
Peixoto, J.P. and A.H. Oort, *Physics of Climate.* American Institute of Physics, New York, 1992.
Rango, A., J. Martinec, A. Chang, J. Foster and V. Van Katwijk, 1989: Average areal water equivalent of snow on a mountainous basin using microwave and visible data. IEEE Trans. on Geoscience and Remote Sensing, 27, 740-745.
Steffen K. and A. Schweiger, NASA Team algorithm for sea ice concentration retrieval from the Defense Meteorological Satellite Program (DMSP) Special Sensor Microwave/Imager (SSM/I): comparison with Landsat imagery, *J. Geophys. Res*., 96, 21, 971-21,987, 1991.
Tao, W.-K. and J. Simpson, The Goddard Cumulus Ensemble Model. Part I: Model description, Terrestrial, Atmospheric and Oceanic Sciences, 4, 19-54, 1993.
Wentz F.J., C.L. Gentemann, D.K. Smith, D.B. Chelton, Satellite Measurements of Sea-Surface Temperature Through Clouds, *Science*, 288(5467), p. 847, 2000.
Wentz, F.J., A well-calibrated ocean algorithm for SSM/I, *J. Geophys. Res.,* 102(C4), p. 8703, 1997.
Wentz, F.J., L. A. Mattox, and S. Peteherych, New algorithms for microwave measurements of ocean winds: Applications to SeaSat and the Special Sensor Microwave Imager, *J. Geophys. Res., 91,* 2289-2307, 1986.
Wentz, F.J., Measurement of Oceanic Wind Vector Using Satellite Microwave Radiometers, *IEEE Transactions on Geoscience and Remote Sensing*, 30 (5), 960-972, 1992.
Wiesmann, A. and Maetzler, C. 1999. Microwave Emission Model of Layered Snowpacks, (Remote Sensing of Environment, in press).

Acronyms

4DDA	four-dimensional data assimilation
ADEOS-II	ADvanced Earth Observation Satellite
AIRS	Atmospheric InfraRed Sounder
AIJEX	
AMeDAS	Automatic Meteorological Data Acquisition System
AMPR	Airborne Microwave Precipitation Radiometer
AMSR-E	Advanced Microwave Scanning Radiometer for EOS
AMSU	Advanced Microwave Sounding Unit
ARM	Atmospheric Radiation Measurement
ARM-CART	ARM-Clouds And Radiation Testbed
ARS	
asc	ascending
ATBD	Algorithm Theoretical Basis Document
ATM	Airborne Topographic Mapper
ATSR	Along Track Scanning Radiometer
AVHRR	Advanced Very High Resolution Radiometer
BOREAS	BOReal. Ecosystem-Atmosphere Study
BSRN	Baseline Surface Radiation Network
CAMEX	Convection And Moisture EXperiment
CRM	Cloud Resolving Model
CZCS	Coastal Zone Color Scanner
DMSP	Defense Meteorological Satellite Program
DOE	Department of Energy
dsc	descending
EASE-grid	Equal-Area projections grid
ECMWF	European Centre for Medium-Range Weather Forcasts
ESDIS	EOS Science Data Information system
EOC	Earth Observation Center
EOS	Earth Observing System
EOSDIS	EOS Data and Information System
ERS	European Research Satellite
ESMR	Electrically Scanning Microwave Radiometer
ETL	Environmental Technology Laboratory
FIRE	First ISCCP Regional Experiment
ftp	file transfer protocol
g	gram
GAC	Global Area Coverage
GAME	GEWEX ASIAN Monsoon Experiment
GCIP	GEWEX Continental-scale International Project
GCM	Global Circulation Model
GEWEX	Global Energy and Water cycle EXperiment
GHz	Giga Hertz
GLOBEC	GLOBal ocean ECosystem dynamics
GLI	GLobal Imager
GOES	Geostationary
GPCP	Global Precipitation Climatology Project
GSFC	Goddard Space Flight Center
GT	Ground Truth
GTS	Global Telecommunications System
IANZONE	International ANtarctic ZONal Experiment
IFOV	Instantaneous Field of View
IGBP	International Geosphere- Biosphere Programme
IMS	Interactive Multisensor Snow and Ice Mapping System
IR	infra red

ISCCP	International Satellite Cloud Climatology Program
ITA	integrated team algorithm
JCET	Joint Center for Earth Science Technology.
JERS	Japanese Earth Resources Satellite
JPL	Jet Propulsion Laboratory
K	degrees Kelvin
Km	kilometer
KWAJEX	KWAJalein EXperiment
L	columnar liquid water
LAI	Leaf-Area-Index
Landsat	LAND SATtelite
LBA	Large-scale Biosphere-atmosphere experiment in Amazonia
LTER	Long Term Ecological Research
m_e	soil moisture
MAS	MODIS Airborne Simulator
MCSST	Multi-Channel SST
MHz	Mega Hertz
MIR	Millimeter Imaging Radiometer
MIZ	Marginal Ice Zone
MIZEX	Marginal Ice Zone EXperiment
MODIS	MODerate-resolution Imaging Spectraradiometer
mm	millimiter
MTPE	Mission to Planet Earth
m/s	meter per second
MSS	Multi-Spectral System
NASA	National Aeronautics and Space Administration
NASDA	National Space Development Agency of Japan
NCAR	National Center for Atmospheric Research
NCDC	National Climatic Data Center
NCEP	National Center for Environmental Prediction (NOAA)
NDBC	National Data Buoy Center
NDVI	Normalized Difference Vegetation Index
NESDIS	National Environmental Satellite, Data, and Information Service
NEXRAD	NEXt generation RADar
NMC	National Meteorological Center
NOAA	National Oceanic and Atmospheric Administration
NOHRSC	National Operational Hydrologic Remote Sensing Center
NSCAT	NASA SCATterometer
NSF	National Science Foundation
NSIDC	National Snow and Ice Data Center
NWP	numerical weather prediction
NWS	National Weather Service
OLS	Optical Line Scanner
OPPS	Operational Product Processing System
pdf	probability density function
PMEL	Pacific Marine Environmental Laboratory
PODAAC	POlar Distributed Active Archive Center
PSR	Polarimetric Scanning Radiometer
PV	Physical Validation
QC	Quality Control
RADARSAT	Canadian Synthetic Aperture Radar Satellite
RAOB	RAdiosonde OBservations
RCE	Regional Continental-scale Experiment
rms	root mean square
rpm	rotations per minute
RTM	Radiative Transfer Model

SAR	Synthetic Aperture Radar
SCF	Scientific Computing Facility
SGP	Southern Great Plains
SISEX	Shuttle Imaging Spectrometer EXperiment
SHEBA	Surface HEat Budget of the Arctic Ocean
SLFMR	Scanning Low-Frequency Microwave Radiometer
SMMR	Scanning Multichannel Microwave Radiometer
SMOS	Soil Moisture and Ocean Salinity
SSM/I	Special Sensor Microwave/Imager
SST	Sea surface temperature
SWE	Snow Water Equivalent
TAO	Tropical Atmosphere-Ocean
T_e	surface temperature
T_s	Sea Surface Temperature
Tb	brightness temperature
TL	Team Leader
TLSCF	Team Leader Science Computing Facility
TMI	TRMM Microwave Imager
TOGA	Tropical Ocean Global Atmosphere
TRMM	Tropical Rainfall Microwave Mission
USGS	United States Geological Survey
V	columnar water vapor
VIS/IR	Visible/InfraRed
W	wind speed
w_e	vegetation water content
WCRP	World Climate Research Program
WMO	World Meteorological Organization
WSR-88D	Weather Surveillance Radar- 1988 Doppler